THE MICROBIAL ECOLOGY OF DEEP-SEA HYDROTHERMAL VENTS: DETERMINING THE STRUCTURE AND FUNCTION IN MICROBIAL BIOFILMS

By

ASHLEY ELAINE GROSCHE

A dissertation submitted to the

School of Graduate Studies

Rutgers, The State University of New Jersey

In partial fulfillment of the requirements

For the degree of

Doctor of Philosophy

Graduate Program in Microbial Biology

Written under the direction of

Professor Costantino Vetriani

And approved by

_____

_____

_____

_____

New Brunswick, New Jersey

May, 2018

ABSTRACT OF THE DISSERTATION

The Microbial Ecology of Deep-Sea Hydrothermal Vents: Determining the Structure and Function in Microbial Biofilms

By ASHLEY ELAINE GROSCHE

Dissertation Director:

Dr. Costantino Vetriani

Deep-sea hydrothermal vents are a global phenomenon driven by reservoirs of geothermal energy that chemically transform seawater through the enrichment of minerals from the interacting basement crust. The chemical enrichment resulting from seawater-rock interactions at high temperature fuels microbial metabolism and enables life to flourish at a depth of the ocean typically characterized by low biomass. These systems are among the most biologically productive in the world, and rely on chemosynthesis, rather than photosynthesis, for primary production.

The aims of this dissertation are to determine the microbial biogeography of biofilm communities at a basalt-hosted deep-sea hydrothermal vent system, constrain the functional diversity as it relates to habitat composition, and compare the phenotypic profiles of pure-culture representatives with genotypes using comparative genomics in order to verify gene function, and explore novel adaptations that may play a role in the ecological success of these taxa at vent ecosystems. To determine the microbial biogeography at deep-sea vents, biofilms were analyzed from across three distinct

"bioregimes" or habitat zones, each characterized by colonization patterns of macrofauna and local fluid chemistry, which was concurrently measured during sampling. This study revealed that age, colonization substrate, and bioregime are major drivers of variation between communities, and that populations abundant during the early stages of colonization and late stages of biofilm maturity shared many of the same species, but could be distinguished at the OTU-level, revealing differential populations of pioneer and secondary colonizers. Metatranscriptomic analysis of a biofilm from the *Riftia* bioregime and hydrothermal fluids was also performed to discern functional adaptations in sessile communities. Gene transcripts related to central metabolism (*e.g.,* carbon fixation, sulfur and nitrogen metabolism) and environmental adaptations (*e.g.,* motility and chemotaxis, oxidative detoxification) were identified.

Subsequent studies investigated the metabolism and physiology of a bacterial isolate from the East Pacific Rise hydrothermal vent system. *Cetia pacifica* strain TB-6^T represents a novel genus with the *Nautiliales,* an order within the Epsilonproteobacteria whose validly described genera are found exclusively in association with deep-sea vents. *C. pacifica* is an obligate anaerobe, hydrogen-oxidizing, sulfur- and nitrate-reducing thermophile that utilizes the reductive citric acid cycle (rTCA) to fix carbon dioxide. Since phenotypic redundancy is exhibited by *Cetia* and other genera within the *Nautiliaceae* family, further investigation focused on a comparative genomic analysis of the *Nautiliaceae* to discern if genotypic redundancy was present as well. Central metabolism (C, H, N, S, P) was conserved within the family. However, a set of accessory genes was also identified, including an alginate biosynthesis pathway previously found in only two other bacterial genera (*Pseudomonas* and *Azotobacter*). Overall, the work

outlined in this dissertation contributes to our understanding of microbial abundance, distribution, and function at deep-sea hydrothermal vents.

Acknowledgements

I would like to thank the members of my dissertation committee, Dr. Costantino Vetriani, Dr. Donato Giovannelli, Dr. Gerben Zylstra, and Dr. Lee Kerkhof for their support and guidance in the completion of this dissertation work. I am indebted to my PhD advisor, Dr. Costantino Vetriani, for his encouragement, availability, good advisement, for his sincere interest in the success of my career, and most valuable, his time. I want to extend my deepest gratitude to Dr. Ines Rauschenbach, Dr. Tamar Barkay, Dr. Diane Davis, and Dr. Lisa Keddis for awakening my love and passion for teaching. My lab mates have made this entire journey possible, so thank you beyond measure to Sushmita Patwardhan, Francesco Smedile, and all other members past and present of the Deep-Sea Microbiology Laboratory. I could not have asked for better lab mates. I want to thank Dr. Judy Grassle for advising me from my undergraduate work through completion of the thesis. Many thanks to Dr. Kay Bidle and Dr. Jozef Nissimov for their guidance with the carbon fixation work. Thank you to Patty Gillen for her wit, humor, and steadfast ability to get gas mixes delivered before all of the experiments failed. I want to thank Linda McHenry, Donna Napoli, Lillian Lee, and Lucy Lettini for their administrative assistance and willingness to sneak me access to the coffee machine during off hours. I want to thank Kathy Maguire, Jessie Maguire, Tamara Crawford, Audrey Andrews, and Beth Nugent for their kindness, patience, and administrative assistance. I want to thank Johnny Lin, Chris Camastra, and Chuck Belmonte for their

unwavering IT support. I want to thank Char Fuller, Kevin Wyman, Lora McGuinness, and Frank Natale for their invaluable guidance in the laboratory. I would like to thank Dr. Gerben Zylstra for always having my best interests at heart, especially for his recommendation for the Jilin University exchange program in China and for the Facilis short course in Milan, Italy. I want to thank and acknowledge the crew of the R/V *Atlantis* and crew and pilots of the DSV *Alvin*, for their skilled operations at sea. I want to acknowledge the many funding sources that made this research possible: National Science Foundation grants to Costa Vetriani. I would also like to thank my family, especially my mom, Nick, Aunt Cat, and Uncle Brian for always encouraging me to go out and learn, and for accepting me as the weird child I was and continue to be. And of course, I would like to thank Ananya Agarwal, Nicole Lloyd, Fatima Foflonker, and Aakansha Roberts for their friendship, encouragement, and support through this journey. Finally, I would like to thank Framp for all he has done to make me the person I am today, for passing on to me his love of learning, discovery, and the ocean.

Dedication

I dedicate this thesis to the pursuit and cultivation of joie de vivre.

Table of Contents

Pages

List of Tables

List of Figures

Preface

Chapter 2 is in preparation for publication as "Microbial communities in biofilms at deep-sea hydrothermal vents: mapping the microbial landscape across space, time, and fluid dynamics" by Ashley Grosche, Francesco Smedile, Donato Giovannelli, Nadine Le Bris and Costantino Vetriani, to be submitted to the International Society for Microbial Ecology (ISME) Journal. Data analysis and figure generation were performed by A.G. working in tandem with co-authors, except for chemistry measurements, which were performed solely by N.L.B.

Chapter 3 has been published as "*Cetia pacifica* gen. nov., sp. nov., a chemolithoautotrophic, thermophilic, nitrate-ammonifying bacterium from a deep-sea hydrothermal vent." Ashley Grosche was responsible for the characterization of *Cetia pacifica*, including phylogenetic analysis, metabolic tests, culture preparation for microscopy and chemotaxonomic analyses, and manuscript preparation. All figures were generated by A.G.

Chapter 4 is in preparation for publication as "A comparative genomic analysis of *Cetia pacifica* and the *Nautiliaceae*" by Ashley Grosche, Francesco Smedile, and Costantino Vetriani to be submitted to Frontiers in Microbiology. Ashley Grosche was responsible for closing the *Cetia pacifica* genome, bioinformatic analysis of the *Nautiliaceae* genomes, and manuscript preparation. All figures were generated by A.G.

Chapter 1

Introduction

Tectonic Plate Dynamics and Formation of Deep-Sea Hydrothermal Vents

Like the seams on a baseball, tectonic plate boundaries run across the surface of oceanic crust. Along with the uppermost mantle, the oceanic crust forms the rigid outer-layer known as the lithosphere, which floats on top of a hot (~1300°C), highly viscous layer in the Earth's mantle called the asthenosphere. Approximately twenty slab-like pieces of the lithosphere, called tectonic plates (**Fig 1.1,** top), move slowly over the asthenosphere, shifting the Earth's continents in an oscillating pattern of convergence and divergence that is detailed in the theory of continental drift (Wilson, 1963). The tectonic plates interact at plate boundaries in mechanisms that result in the creation and destruction of oceanic crust, and the formation of geological features. In regions of rifting, the formation of spreading centers causes the separation of tectonic plates and the formation of mid-oceanic ridges and ocean basins while at subduction zones, tectonic plates sink and are destroyed in a cyclical process known as the Wilson Cycle (Russo *et al.*, 1996). The cycle is initiated from deep in the mantle, as a plume of hot mafic or ultramafic magma rises toward the surface at a divergent plate boundary. Heat rises to the surface in pockets, forming a convection current that remains concentrated at the rifting site in the center of a new ocean basin, causing a widening and the creation of newly-formed oceanic crust. The upwelling of magma continues, and as new oceanic crust is formed, the two plates diverge, resulting in a geological feature referred to as a spreading center.

The mid-ocean ridges encircling the Earth are found at depths typically between 2,000-5,000 meters, and are characterized by total darkness, high pressure, and temperatures close to freezing (~2°C). The formation of new crust occurs at rates which vary by location, and can occur between <20 mm yr^{-1} at ultra-slow spreading centers, up to 170 mm yr^{-1} at ultra-fast spreading centers, such as the southern portion of the East Pacific Rise (Ramirez-Llodra *et al.*, 2007).

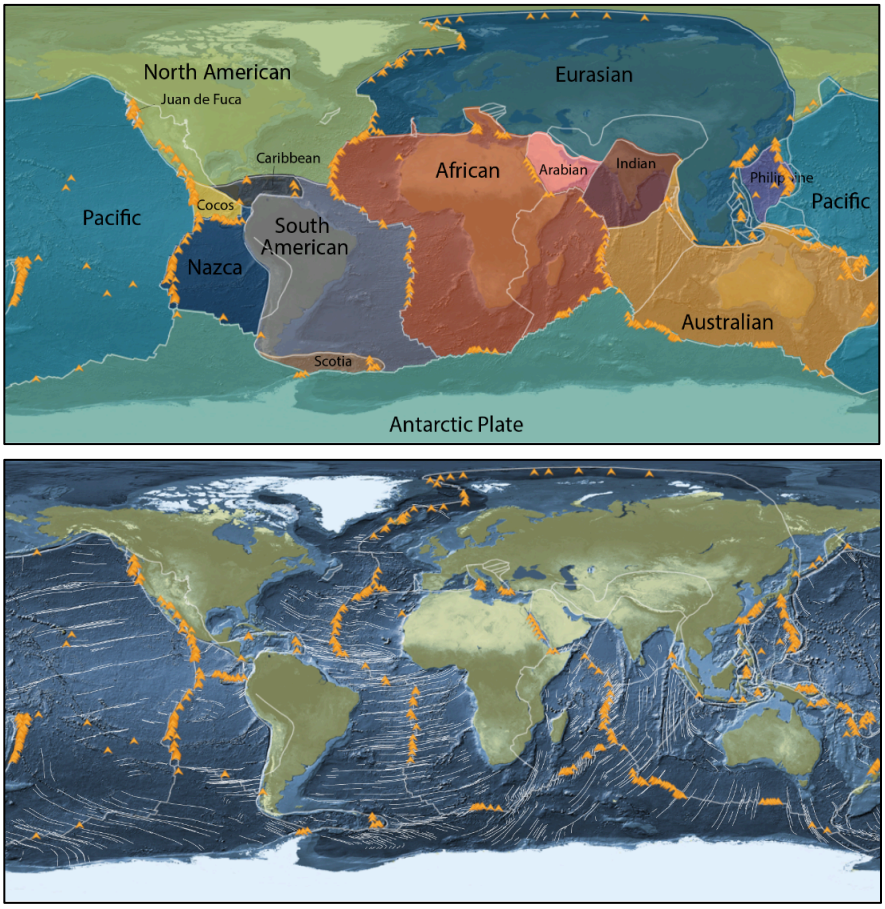

Fig 1.1 The global map of Earth with overlays of continental plates (top) and hydrothermal vent activity denoted by yellow arrows (bottom) often occurring at tectonic plate boundaries. Data gathered from (Beaulieu, 2010) and (Zahirovic *et al*., 2016) using the interactive mapping feature of the Woods Hole Oceanographic Institution "Dive and Discover" web tool (https://divediscover.whoi.edu/).

Hydrothermal activity is often associated with mid-ocean ridges as a consequence of seawater-fluid circulation through a geothermally-heated crustal basement (**Fig 1.2,** bottom). This occurs when cold seawater, dense from salinity and temperature, sinks through the porous ocean crust towards a pocket of upwelling magma. The geothermal energy from the hot magma catalyzes a chemical transformation in the seawater with its approach to the chamber, causing super-heating, depletion of oxygen, and enrichment in dissolved reduced gases (*e.g.*, CH_4, H_2S). The fluid is subject to acidification (pH of 2-3) and dissolution of numerous polymetallics (*e.g.*, Fe^{2+}, Mn^{2+}, Cu^{+}, Zn^{2+}), trace amounts of precious metals (Ag^{+}, Au^{+}, Pt^{+}) and heavy metals (Cd^{2+}, Hg^{2+}, Pb^{2+}, and As^{3+}) for an end-member fluid profile that is variable depending on the geochemical properties of the vent system (**Table 1.1**). Buoyancy imparted by super-heating propels the hydrothermal fluids upwards to be discharged into the water column (**Fig 1.2**). Focused-flow venting is characterized by fluid emission through "black smoker" chimney-like polymetallic sulfide structures. Spewing out of the sulfide chimneys, super-heated fluid billows out in black clouds from the immediate precipitation of metals into the ~2°C water column. Fluids can also be diverted through fractures in the seafloor, allowing for fluid cooling due to seawater mixing and subsurface precipitation of minerals prior to emission. Diffuse-flow venting is often associated with biological activity, and can account for up to 50% of total venting activity (Ramirez-Llodra *et al.*, 2007).

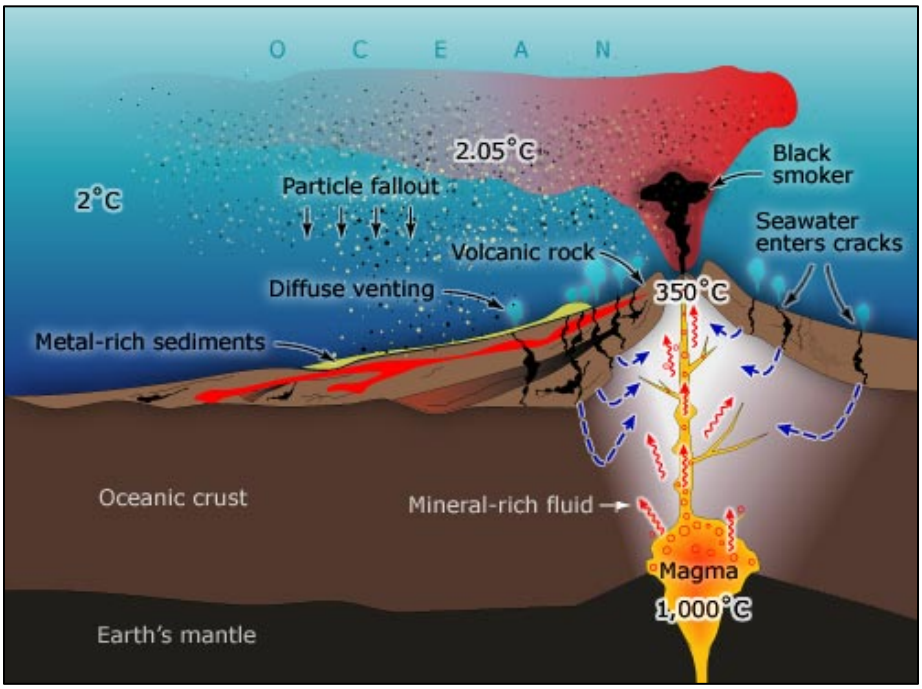

Fig 1.2 Deep-sea hydrothermal vents are driven by circulation of seawater and fluids through the ocean crust and water column (Wright *et al.,* 2006). © GNS Science

Primary Production at Deep-Sea Hydrothermal Vents

The rampant biological production rate and capacity are evident when observing the successional pattern at a post-eruptive sites, which begin as barren fields of freshly cooled basalt and succeed to fully recovered complex communities in a matter of years (Shank *et al.*, 1998). Deep-sea vents exist in total darkness and receive little particulate organic carbon (POC) input from the water column, yet primary production at deep-sea vents is projected to be 10^{13}g of biomass per year, approximately 0.02% of primary production in the ocean (McCollom *et al.*, 1997). Global primary production relies predominantly on photosynthesis, a process that derives energy from light to synthesize organic molecules from CO_2. Chemolithotrophic microorganisms circumvent the necessity for light by deriving energy from reduced chemical species via the process of chemosynthesis.

	Back-Arc	Mid-Ocean Ridge	Sediment-Hosted	Seawater
Temperature (°C)	278-334	≤ 400	100-315	2
pH (25°C)	< 1-5.0	2.8-4.5	5.1-5.9	8
Ba**	5.8-10	1.6-18.6	> 12	0.14
Ca*	6.5-89	4.0-109	160-257	10.2
Cd**	-	0-0.910	< 0.01-0.046	-
CH_4*	.005-.06	.007-2.9	-	-
Cl*	255-790	30.5-1245	412-668	545
Co**	-	0.02-1.43	< 0.005	-
CO_2*	14.4-200	3.6-39.9	-	2.36
Cu**	.003-34	0-150	< 0.02-0.652	-
Fe**	13-2500	7-18,700	0-180	-
H_2*	0.035-0.5	.0005-38	-	-
H_2S*	1.3-13.1	0-19.5	1.1-5.98	-
K*	10.5-79	1.2-58.7	13.5-49.2	10.1
Mg*	0	0	0	53
Mn**	12.0-7100	59-3300	10-236	-
Na*	210-590	10.6-983	315-560	464
NH_3*	-	< 0.065	5.6-15.6	-
Ni**	-	-	-	-
Pb**	0.036-3.9	0.183-0.1630	< 0.02-0.652	-
SO_4*	0	0	0	28
Zn**	7.6-3000	0-780	0.1-40	-

** denotes mmol/kg*
*** denotes µmol/kg*

Table 1.1 The typical chemical profiles of vent fluids from a back-arc, mid-ocean ridge, and sediment-hosted hydrothermal vent system compared to seawater from the surrounding water column. Data has been subsetted from data by references (Tivey, 2007)

Thermochemical disequilibria are generated by the mixing of hot, reduced fluids with cold, oxygenated seawater (containing O_2, NO_3^-, Fe^{3+}, SO_4^{2-}, and CO_2) from which chemolithoautotrophic microorganisms liberate energy to fuel metabolic processes (**Fig 1.3**). Primary production at deep-sea vents relies entirely on the fixation of inorganic carbon into biomass by populations of chemolithoautotrophic microorganisms. This process is coupled to a wide variety of energetically favorable redox reactions (**Table 1.2**), which may reflect the broad range of geochemical niches available for microorganisms to exploit. Electron donors that have been verified in pure-culture studies of vent isolates include methane, hydrogen gas, thiosulfate, elemental sulfur, hydrogen

sulfide gas, and ferrous iron.

Energy Metabolisms	e⁻ Donor	e⁻ Acceptor	Redox Reaction	Identified	Cultured
Methanotrophy	CH_4	O_2	$CH_4 + 2O_2 = CO_2 + 2H_2O$	Yes	Yes
Methanotrophy/sulfate reduction	CH_4	SO_4^{2-}	$CH_4 + SO_4^{2-} = HCO_3^- + HS^- + H_2O$	Yes	Not Yet
Methanotrophy/denitrification	CH_4	NO_3^-	$CH_4 + 2NO_3^- = HCO_3^- + 3OH^- + N_2$	No	No
H_2 oxidation/methanogenesis	H_2	CO_2	$H_2 + 1/4CO_2 = 1/4CH_4 + 1/2H_2O$	Yes	Yes
H_2 oxidation/sulfate reduction	H_2	SO_4^{2-}	$H_2 + 1/4SO_4^{2-} + 1/2H^+ = 1/4H_2S + H_2O$	Yes	Yes
H_2 oxidation/sulfur reduction	H_2	S°	$H_2 + S° = H_2S$	Yes	Yes
S oxidation	H_2S	O_2	$H_2S + 2O_2 = SO_4^{2-} + 2H^+$	Yes	Yes
S oxidation	S°	O_2	$S° + H_2O + 31/5O_2 = SO_4^{2-} + 2H^+$	Yes	Yes
S oxidation	$S_2O_3^{2-}$	O_2	$S_2O_3^- + 10OH^- + O_2 + 4H^+ = 2SO_4^{2-} + 7H_2O$	Yes	Yes
S oxidation/denitrification	$S_2O_3^{2-}$	NO_3^-	$S_2O_3^- + 6OH^- + 4/5NO_3^- + 4/5H^+ = 2SO_4^{--} + 17/5H_2O + 2/5N_2$	Yes	Yes
S oxidation/denitrification	S°	NO_3^-	$S° + 32/5H_2O + 6/5NO_3^- = SO_4^{2-} + 34/5H^+ + 3/5N_2 + 6OH^-$	Yes	Yes
S oxidation/denitrification	H_2S	NO_3^-	$H_2S + 36/5H_2O + 16/5NO_3^- = 2SO_4^{2-} + 84/5H^+ + 8/5N_2 + 16OH^-$	Yes	Yes
H_2 oxidation	H_2	O_2	$H_2 + 1/2O_2 = H_2O$	Yes	Yes
H_2 oxidation/Fe reduction	H_2	Fe(III)	$H_2 + 2Fe^{3+} = 2Fe^{2+} + 2H^+$	Yes	Yes
Fe oxidation	Fe(II)	O_2	$Fe^{2+} + 1/4O_2 + H^+ = Fe^{3+} + 1/2H_2O$	Yes	Yes
Fe oxidation/denitrification	Fe(II)	NO_3^-	$Fe^{2+} + 1/5NO_3^- + 2/5H_2O + 1/5H^+ = 1/10N_2 + Fe^{3+} + OH^-$	Not Yet	Not Yet*
Mn reduction	H_2	MnO_2	$H_2 + MnO_2 + 2H^+ = Mn^{2+} + 2H_2O$	Not Yet	Not Yet
Nitrification	NO_2^-	O_2	$NO_2^- + 1/2O_2 + 2OH^- + 2H^+ = NO_3^- + 2H_2O$	Not Yet	Not Yet*
Nitrification	NH_3	O_2	$NH_3 + 3OH^- + O_2 = NO_2^- + 3H_2O$	Not Yet	Not Yet*
H_2 oxidation/denitrification	H_2	NO_3^-	$H_2 + 2/5NO_3^- + 2/5H_2O = 1/5N_2 + 8/5H^+ + 2OH^-$	Yes	Yes

Table 1.2 The electron donor-acceptor couples experimentally verified or proposed at deep-sea hydrothermal vents (Fisher *et al.*, 2007).

The oxidation of these compounds can be coupled to the reduction of oxygen via aerobic respiration, or to the reduction of sulfate, nitrate, elemental sulfur, or ferric iron via

anaerobic respiration (Fisher *et al.*, 2007).

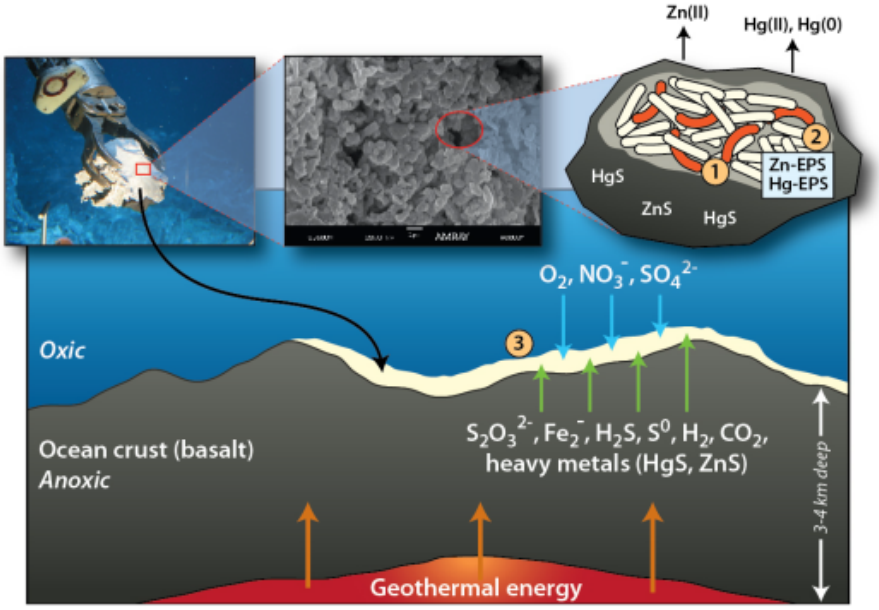

Fig 1.3 The colonization of chemolithoautotrophic microorganisms at the interface between the oxygenated water column and the reduced hydrothermal fluids (Sievert *et al.*, 2012).

Chemosynthetic Microbial Biofilms

Microorganisms colonize exposed surfaces at deep-sea vents, visibly covering portions of sulfide structures, forming patches on basaltic surfaces near diffuse-flow vents, and adhering in epibiotic association with vent macrofauna. Biofilm are formed when cells embedded in a microbially-produced matrix attach to a surface. Pure-culture studies of predominantly pathogenic biofilms have classified biofilm development into five key stages (**Fig. 1.4**).

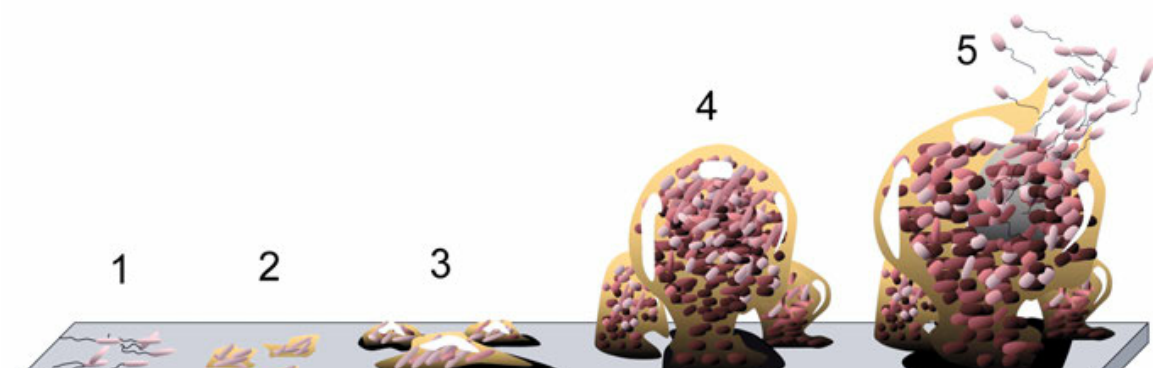

Fig. 1.4 Outline depicting the five stages of biofilm development (O'Toole *et al.*, 2000)

Formation begins with (1) initial attachment, which progresses into (2) irreversible attachment. The biofilm proceeds to (3) maturation, during which microcolonies merge together, followed by (4) restructuring of architecture to allow for nutrient accession to inner members. The final stage of biofilm development is the reversion of sessile microbes back to the planktonic lifestyle (5) and their dispersal into the surrounding habitat. Each stage of biofilm development requires poorly-understood density-dependent intercellular signaling, and in past studies has been shown to display a profile of gene transcription that is significantly different from that of bacterial planktonic counterparts (Watnick *et al.*, 2000).

Chemosynthetic microbial biofilms are a key component in nutrient cycling at deep-sea hydrothermal vents due to their unique role during the colonization of a newly formed vent sites. The microorganisms present at post-eruptive sites are thought to condition surfaces for settlement by metazoans, effectively facilitating the next order of succession (Alain *et al.*, 2004). The formation of biofilms allows microorganisms to adhere closely to nutrient and energy sources in an environment typically characterized by high turbulence, and biofilm infrastructure provides a protective barrier that shields inhabitants from adverse conditions, like dispersal into the nutrient-depleted water

column, or exposure to reactive oxygen and metal species generated during fluid-seawater mixing. The matrix is formed from extracellular polymeric substances (EPS) excreted by microorganisms, and interwoven by a network of channels for nutrient delivery to the residents. EPS are biosynthetic polymers that can be composed of polysaccharides, proteins, nucleic acids and phospholipids. Typically, biofilm matrices are composed of 40-95% polysaccharides. Characteristics such as molecular weight, conformation, and monosaccharide ratios can be influenced by environmental constraints on cellular growth (Nichols *et al.*, 2005). The switch in physiological states of free-swimming to sessile mode can be induced by unfavorable conditions including nutrient limitation, pH change, temperature, salinity, and exposure to antibiotics or oxygen (Pysz *et al.*, 2004). Since biofilms can provide a favorable lifestyle alternative to planktonic life (Watnick *et al.*, 2000), the ability to form biofilms at deep-sea vents may offer significant benefits to its members.

The Ecology of Epsilonproteobacteria at Deep-Sea Vents

The Epsilonproteobacteria are the predominant taxa associated with newly formed biofilms at deep-sea hydrothermal vents. This class is ecologically significant at deep-sea hydrothermal vents and members have been found in association with colonization devices, in symbiosis with vent macrofauna, in water column plumes, and in the subsurface population. Within the overall class, Epsilonproteobacteria exhibit global ubiquity, found in both terrestrial, marine, and host-associated systems, which is enabled by metabolic versatility and reflects selective pressure for environmental adaptation (Campbell *et al.*, 2006). The class is currently split into two orders, The Nautiliales and

the Campylobacterales. The Nautiliales are uniquely associated with deep-sea hydrothermal vent systems, and represent a basal radiation within the 16S rRNA gene-based phylogeny of the class (**Fig 1.5**). Members of the Nautiliales are chemolithoautotrophs that fix carbon dioxide via the reductive TCA (rTCA) cycle and conserve energy coupling hydrogen oxidation with elemental sulfur reduction (Nakagawa *et al.*, 2014). The metabolism of Epsilonproteobacteria isolated from deep-sea vents has

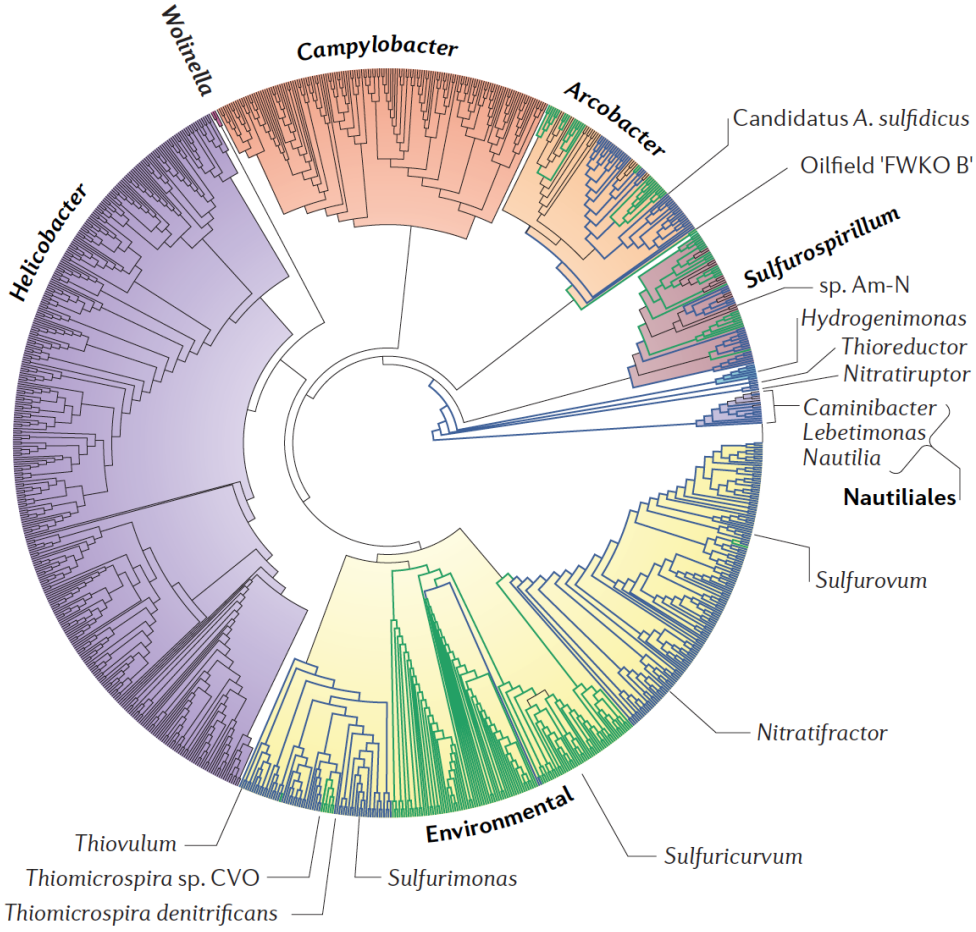

Fig. 1.5 16S rRNA phylogenetic tree of the Epsilonproteobacteria reconstructed using the Neighbor Joining method. Branches are colored to according to marine (blue) or terrestrial (green) habitats (Campbell *et al.*, 2006)

	Isolation site	Optimum T (°C)	Electron donor(s)	Electron acceptor(s)	End product of nitrate respiration	Carbon source	Reference
Epsilonproteobacteria							
Sulfurovum lithotrophicum	MOT, Iheya, sediments	28–30	$S_2O_3^=$, S^0	NO_3^-, O_2	N_2	CO_2	Inagaki et al. (2004)
Sulfurimonas paralvinellae	MOT, Iheya, *Paralvinella*	30	H_2, $S_2O_3^=$, S^0	NO_3^-, O_2	N_2	CO_2	Takai et al. (2006b)
Sulfurimonas autotrophica	MOT, Hatoma Knoll, sediments	25	$S_2O_3^=$, S^0, H_2S	O_2		CO_2	Inagaki et al. (2003)
Thioreductor micantisoli	MOT, Iheya, sediments	32	H_2	NO_3^-, S^0	NH_4^+	CO_2	Nakagawa et al. (2005a)
Nautilia lithotrophica	EPR, 13°N, *Alvinella*	53	H_2, Formate	S^0		CO_2, Formate	Miroshnichenko et al. (2002)
Nautilia nitratireducens	EPR, 9°N, chimney	55	H_2, Formate, acetate, complex organic substrates	NO_3^-, S^0, $S_2O_3^=$, $SeO_4^=$	NH_4^+	CO_2, Formate	Pérez-Rodríguez et al. (2009)
Nautilia profundicola	EPR, 9°N, *Alvinella*	40	H_2, Formate	S^0		CO_2, Formate	Smith et al. (2008)
Nautili abyssi	EPR, 13°N, chimney	60	H_2	S^0		CO_2, Yeast Extract, Peptone	Alain et al. (2009)
Hydrogenimonas thermophila	CIR, Kairei Field, colonizer	55	H_2	NO_3^-, S^0, O_2	NH_4^+	CO_2	Takai et al. (2004c)
Nitratiruptor tergarcus	MOT, Iheya, chimney	55	H_2	NO_3^-, S^0, O_2	N_2	CO_2	Nakagawa et al. (2005b)
Nitratifractor salsuginis	MOT, Iheya, chimney	37	H_2	NO_3^-, O_2	N_2	CO_2	Nakagawa et al. (2005)
Caminibacter profundus	MAR, Rainbow, vent cap	55	H_2	NO_3^-, S^0, O_2	NH_4^+	CO_2	Miroshnichenko et al. (2004)
Caminibacter mediatlanticus	MAR, Rainbow, chimney	55	H_2	NO_3^-, S^0	NH_4^+	CO_2	Voordeckers et al. (2005)
Caminibacter hydrogeniphilus	EPR, 13°N, *Alvinella*	60	H_2	NO_3^-, S^0	NH_4^+	CO_2, complex organic substrates	Alain et al. (2002)
Lebetimonas acidiphila	Mariana Arc, colonizer	50	H_2	S^0		CO_2	Takai et al. (2005)

Table 1.3 The metabolic profiles of Epsilonproteobacteria isolated from deep-sea hydrothermal vents (Sievert *et al.*, 2012)

been verified in pure-culture studies, and appears to diversify along a thermal gradient (**Table 1.3**).

Genomic Mining of Vent-Associated Epsilonproteobacteria

With the advent of next-generation sequencing and increase in accessibility of the technology, the number of available genomes of deep-sea hydrothermal vent-associated microorganisms has experienced a slow but steady rise. Genomes are now available from representative Epsilonproteobacteria (vent-associated and non-vent relatives) including the genera *Helicobacter*, *Campylobacter*, *Wolinella*, *Sulfurimonas*, *Sulfurovum*, *Arcobacter*, *Nitratiruptor*, *Caminibacter, Nautilia*, *Sulfuricurvum*, *Sulfurospirillum*, and *Lebetimonas*. As part of an initiative by the Deep-Sea Microbiology Lab, eighteen vent-associated genomes were sequenced, including the genome of novel genus *Cetia pacifica* strain TB-6. The expansion of the genome database allows for a more comprehensive view of genomic potential within the Epsilonproteobacteria, and reduces the skew of available data from the disproportionally large quantity of epsilonproteobacterial pathogens (*e.g.*, *Helicobacter* and *Campylobacter*) in the database. The *Nautiliaceae* family within the Epsilonproteobacteria is comprised of four genera, *Cetia*, *Caminibacter*, *Nautilia*, and *Lebetimonas*, which together have twelve available genomes for comparative analysis (**Fig. 1.6**). The abundance of genomic data from this family has allowed for the reconstruction of central metabolism, identification of genus-specific accessory genes, and paints a broad picture of environmental adaptation within a deep-

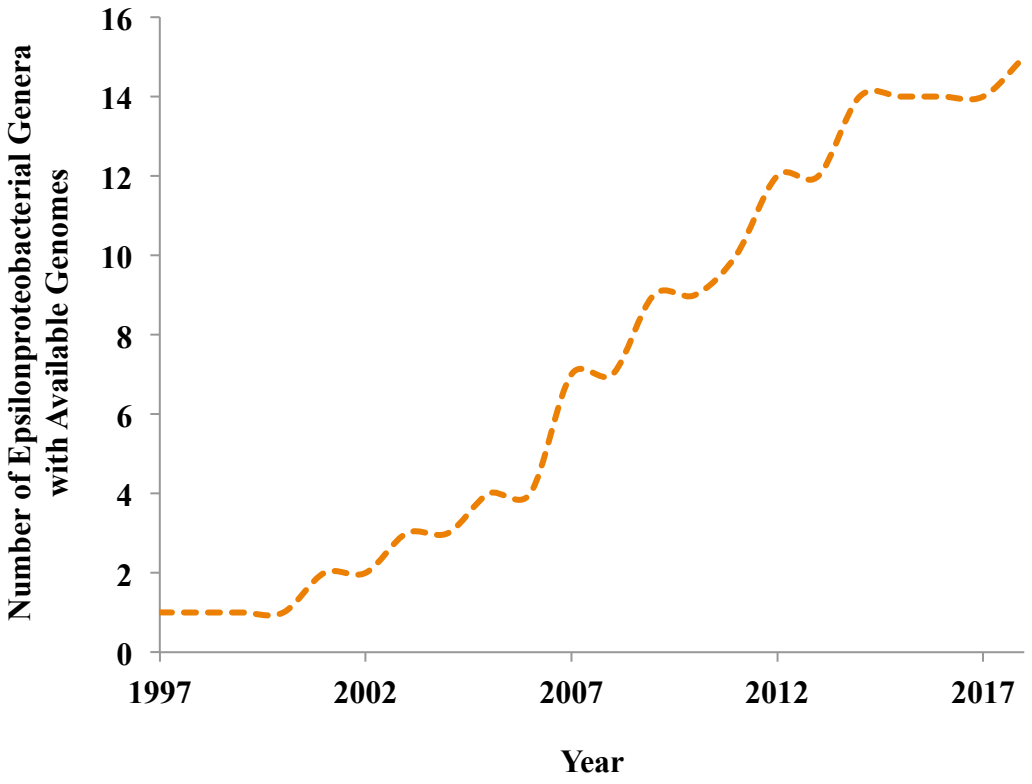

Fig. 1.6 The total epsilonproteobacterial genera over time with available sequenced genomes over the past decade

sea endemic taxonomic group.

Study Scope and Objectives

The attachment and development in chemosynthetic biofilms, the influence of local redox chemistry, and the long-term observation of patterns of microbial succession in biofilms are all crucial components governing the microbial food web in the deep-sea that have been scarcely investigated across a broad range of habitat constraints. This study investigates biofilm structure and function as it relates to community composition, which is selected for by the geochemical constraints of the surrounding environment. Despite environmental variables, it was predicted that a common pattern of low diversity in newly-formed biofilms and increased diversity in established biofilms would be

observed, which may reflect a rise in microbial diversity as secondary colonization occurs. In order to link cell physiology with structure, function, and development of the biofilm, using the outlined polyphasic approach, the specific objectives of this study are to:

Determine the structure and composition of biofilm communities at various stages of development when exposed to varying thermal, geochemical and biological regimes. This will confirm that biofilms in early developmental stages are dominated by chemosynthetic Epsilonproteobacteria. As the biofilm matures, it is predicted that microbial diversity will increase as secondary colonizers, which may include heterotrophic microorganisms such as Gammaproteobacteria and Deltaproteobacteria, join the biofilm.

Define which genes are expressed by these organisms during attachment to substrates and during development of the biofilm. It is predicted that transcripts involved in cellular adhesion (*e.g.* chemotaxis, flagellar proteins, adhesins and pili), transcripts related to regulating the formation and secretion of extracellular polymeric substance (EPS) used in the biofilm matrix (*e.g.* secretion proteins, EPS production) and density-specific quorum-sensing molecules will be expressed in the initial stages of biofilm development.

Measure redox chemistry within the biofilm. Microorganisms at the deep-sea vents are regularly exposed to a variety of reducing and oxidizing agents. It is expected that genes involved in energy yielding redox reactions (*e.g.*, oxidases for hydrogen and/or sulfide

and terminal reductases for sulfur and/or nitrate and/or oxygen respiration) will be simultaneously expressed by the biofilm communities exposed to multiple terminal electron donors/acceptors determined by geochemical parameters of each sampling site. I hypothesize that the biofilm communities exposed to higher temperature regimes (>25°C) will express genes involved in anaerobic respiration as opposed to the communities exposed to increasing lower temperature regimes, which will predominantly express genes involved in (micro)aerobic respiration.

Determine the phenotypic profiles recorded in pure-culture isolates are reflected in the genomes. Past studies have demonstrated that the *Nautiliaceae*, a family of vent-endemic genera, display phenotypic redundancy during laboratory studies. It was predicted that the core metabolic pathways of these species will be conserved among the family, but genus-specific accessory genes to better adapt each clade for sub-niche specialization will also be present.

Chapter 2

Microbial communities in biofilms at deep-sea hydrothermal vents: mapping the microbial biogeography across space, time, and fluid dynamics

Introduction

Variations in ridge-crest dynamics, including the chemical evolution of crust, metal speciation, bathymetry and zone refinement of ore deposits dictate the fluid pathway, flow, geochemistry, and longevity of venting, which ultimately governs the biogeography of vent-associated fauna (Van Dover, 2000). During fluid-seawater mixing in the water column and subsurface, hot, reduced fluids enriched in polymetallic sulfides, anhydrite, and gases blend with cold, oxygenated seawater, generating steep, and often unstable, thermochemical gradients (Jannasch, 1985). The chemical disequilibrium within these gradients fuels microbial metabolism, enabling life to exist and flourish at deep-sea hydrothermal vents, while also exerting selective pressure and growth constraints on the biological community. This is ultimately reflected in the spatially

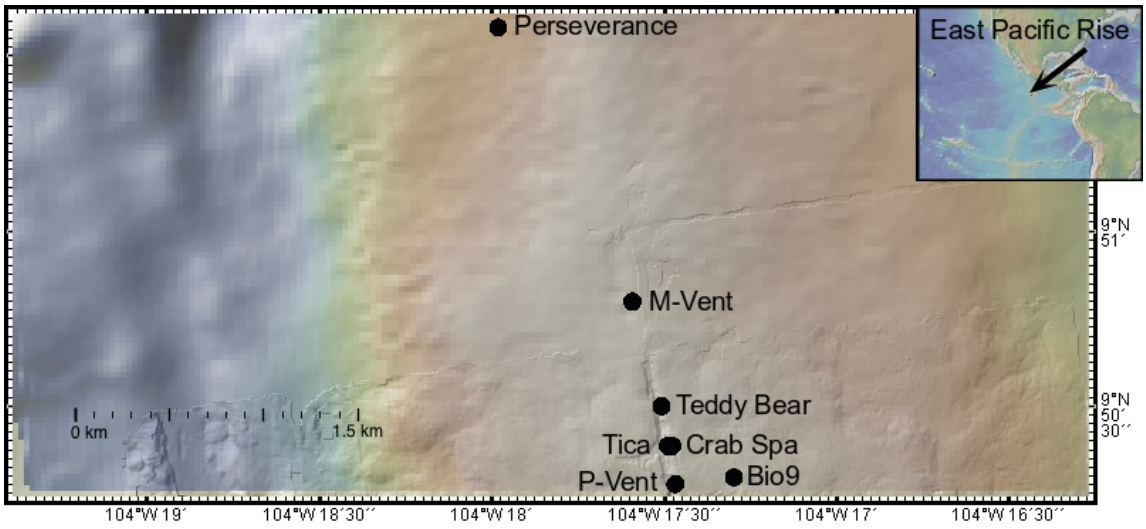

Fig. 2.1 Map of the East Pacific Rise (9°N, 140°W) sampling sites (•).

heterogeneous species distribution of the resident macrofauna (Lutz *et al.*, 2008).

The East Pacific Rise (EPR) is host to hydrothermal vent communities that exhibit a typical faunal zonation pattern well-documented since the discovery of deep-sea vents (**Fig. 2.1**) (Childress *et al.*, 1992; Galkin, 2016; Hessler *et al.*, 1985; Johnson *et al.*, 1988; Lenihan *et al.*, 2008; Tunnicliffe, 1988). Structured along physiochemical gradients, vent species partition according to the ecological needs of each macrofaunal species, which stem from a combination of growth constraints of the metazoan, microbial requirements, and often, interplay between both (**Fig. 2.2**). The oligothermal zones of low-temperature (~3-5°C), diffuse-flow venting are host to mussel beds of *Bathymodiolus thermophilus*, whose thermophilic gill-dwelling endosymbionts derive energy from the oxidation of H_2S supplied in the hydrothermal fluids. Equipped to filter-feed on suspended organic particles, the vent mussel is not strictly reliant on symbiotrophy, which might explain its tolerance of a broad range of conditions relative to other vent macrofauna (Hessler *et al.*, 1985). The euthermal zone of the EPR, characterized by visibly shimmering fluids and temperatures of up to 25°C, selects for the growth of *Riftia pachyptila* and its close relative, *Tevnia jerichonana*. These tubeworm species require exposure to H_2S, CO_2 and O_2 and support chemolithoautotrophic endosymbionts that supply nutrients to the worms (Felbeck, 1981; Gardebrecht *et al.*, 2012). Higher temperature venting zones of > 20°C are marked by the growth of tubeworms *Alvinella pompejana* and *Alvinella caudata* (Galkin, 2016), species endemic to the EPR found in dense bushes colonizing the walls of actively-venting high-temperature chimneys. The dorsal epithelium of the worms is coated by a consortium of episymbiotic "fleece" consisting of predominately filamentous, exopolysaccharide (EPS)-secreting Epsilonproteobacteria that enable the survival of

Alvinella worms threefold; the epibionts provide a layer of EPS which is hypothesized to insulate the worm against high-temperature fluids, while also detoxifying hydrogen sulfide, and providing organic end-products via carbon fixation to be foraged by neighboring alvinellids (Campbell *et al.*, 2003; Cary *et al.*, 1997; Desbruyères *et al.*, 1998; Haddad *et al.*, 1995).

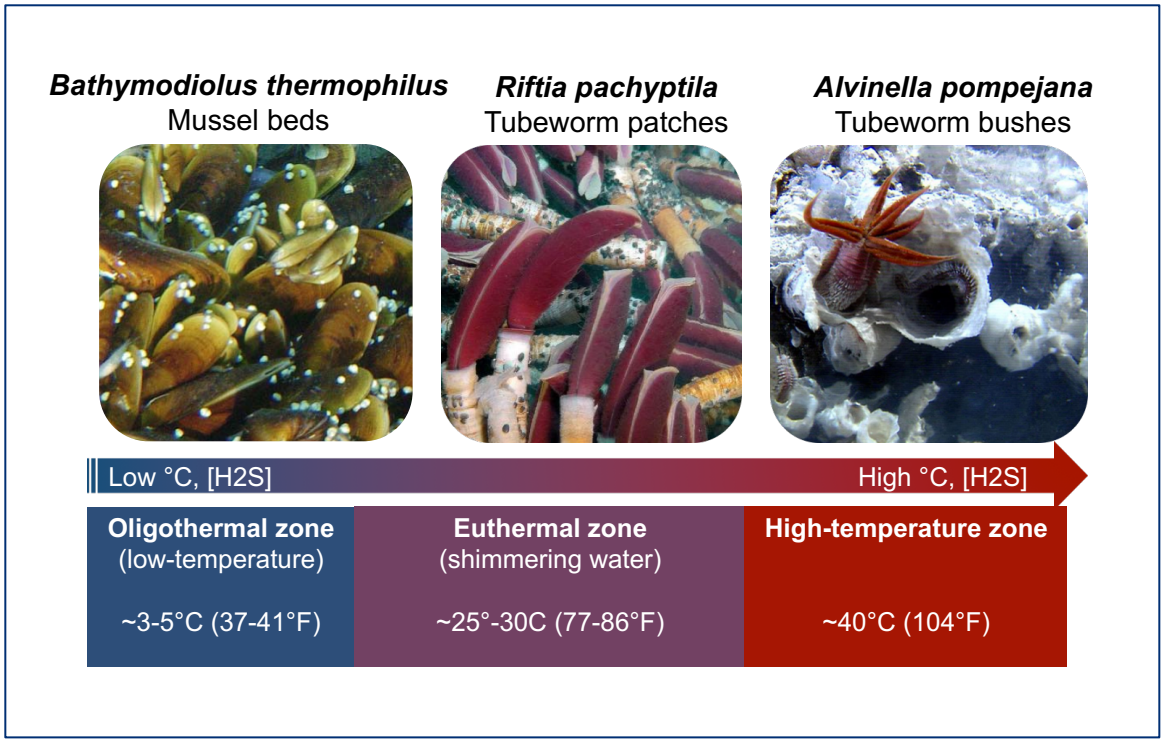

Fig. 2.2 The partitioning of macrofaunal species according to metabolic and physiologic requirements into bioregimes of *Bathymodiolus thermophilus* mussel beds, *Riftia pachyptila* tubeworm patches, and *Alvinella pompejana* bushes

While the biogeography of metazoans at deep-sea hydrothermal vents has been described in detail (Childress *et al.*, 1992; Galkin, 2016; Gollner *et al.*, 2015; Johnson *et al.*, 1988; Shank *et al.*, 1998), related patterns of surface-associated microbial biofilms hosted across macrofauna-defined boundaries have not yet been established. Biofilms are a keystone component of the deep-sea vent ecosystem and are integral in the early colonization and conditioning of vent surfaces, succession of higher trophic levels, and

maintenance of a steady-state community. Chemosynthetic microbial biofilms colonize freshly-exposed surfaces at newly-formed vent sites, serving as the pioneer colonizers and the foundation of the food chain at deep-sea vents. Functioning in a similar capacity at post-eruptive sites, these biofilms are the first order of succession, signaling the "rebirth" of the ecosystem (Gulmann *et al.*, 2015; O'Brien *et al.*, 2015; Shank *et al.*, 1998). Upon maturation of a vent site, epibiotic microbial biofilms remain essential in many macrofaunal species for nutrient acquisition. The sessile lifestyle benefits the microbe, the host, and the ecosystem as a whole, allowing microbes to adhere closely to sources of energy and nutrients in a high-turbulence environment, while fueling higher trophic levels with available carbon.

Although epibiotic biofilms are an important ecological component of deep-sea hydrothermal vents, past studies have focused more on the abiotic constraints of local fluid chemistry on free-living microbial communities, endosymbionts, or biofilm communities formed on *in situ* experimental colonizers. From these studies, researchers have established that the Epsilonproteobacteria are an ecologically significant group at deep-sea vent environments (Campbell *et al.*, 2006; Nakagawa *et al.*, 2008; Nakagawa *et al.*, 2005b). Newly-formed, chemosynthetic biofilms from diffuse-flow microbial communities have been shown to be dominated almost entirely by Epsilonproteobacteria (Alain *et al.*, 2004; Gulmann *et al.*, 2015; Nakagawa *et al.*, 2005b; O'Brien *et al.*, 2015), which may have implications for their role in the conditioning of surfaces for the settlement of metazoans. While most abundant in young biofilms, populations of Epsilonproteobacteria have also been observed in hydrothermal plumes (Dick *et al.*, 2013; Sunamura *et al.*, 2004), diffuse-flow fluids (Huber *et al.*, 2003; Huber *et al.*, 2007),

on active sulfide structures (Nakagawa *et al.*, 2005a; Sylvan *et al.*, 2012; Voordeckers *et al.*, 2008), comprising filamentous mats (Jannasch *et al.*, 1981) and in symbiotic association with macrofauna (Cavanaugh *et al.*, 1981; Distel *et al.*, 1988; Haddad *et al.*, 1995; López‐García *et al.*, 2002; Polz *et al.*, 1995). Their widespread abundance and metabolic versatility imply that Epsilonproteobacteria play an integral role as pioneer organisms and primary producers at deep-sea hydrothermal vents (Campbell *et al.*, 2004; Campbell *et al.*, 2006; Grzymski *et al.*, 2008; Pérez-Rodríguez *et al.*, 2015; Vetriani *et al.*, 2014). Identifying the habitat-specific distribution of Epsilonproteobacterial is therefore central to understanding shifts in the microbial structure and function within the metabolically active fraction of biofilms.

The primary aim of this study is to elucidate the biogeographical patterns of active microbial biofilm communities at deep-sea hydrothermal vents, and discover how these communities are shaped by biological, spatial, temporal and geochemical constraints. The microbial diversity data from biofilms collected at the EPR (9°50 N) has been integrated with measurements of time, temperature, sulfide, geographical location, and characterization of biological regime by observation of macrofaunal colonization. Through comparative analyses, we have mapped the taxonomic variation within microbial biofilm communities across the characteristic habitats at deep-sea hydrothermal vents.

Materials and methods

Habitat biogeochemical characterization

During sample deployment, monitoring, and recovery, co-registered measurements were taken of temperature, dissolved H_2S, and Eh using an autonomous potentiostat (SPOT, NKE electronics) according to standard procedures (Contreira-Pereira *et al.*, 2013).

Sampling of microbial biomass from deep-sea hydrothermal vents

Microbial biofilms were collected at the East Pacific Rise (9°N, 104°W) during R/V *Atlantis* cruises AT26-10 (December–January 2014) and AT26–23 (November 2014) using the remotely operated vehicle *Jason* and deep-submergence vehicle *Alvin* (**Table 2.1**). Newly formed biofilms obtained for this study were collected using experimental microbial colonization devices (denoted "colonizer" under "Type" column in Table 3.1) constructed from stainless steel mesh and incubated at each bioregime (**Fig 2.2, 2.3**). Native biofilms (denoted "scraping," "sulfide," or "basalt" in Table 3.1) were sampled via scrapings of invertebrates, basalts and sulfides. Samples were taken at Crab Spa (9°50.39' N, 104°17.48' W: 2503-m depth), P-vent (9°50.28' N, 104°17.47' W:

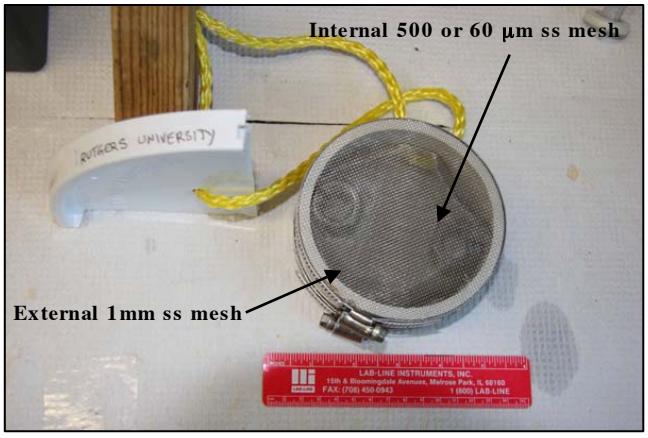

Fig. 2.3 The experimental microbial colonizer is wrapped with stainless steel (ss) mesh. The flow of hydrothermal fluids through the device allows colonizing microorganisms to attach to the mesh (Photo courtesy of Dr. Vetriani).

2506-m depth), Teddy Bear (9°50.50' N, 104°17.51' W: 2514-m depth), Bio9 (9°50.30' N, 104°17.30' W: 2503-m depth), Tica (9°50.39' N, 104°17.49' W: 2511-m depth), Perseverance (9°50.95' N, 104°17.59' W: 2507-m depth), and M-vent (9°50.97' N, 104°17.53' W: 2500-m depth) (**Table 2.1).** Macrofauna-associated biofilms were obtained from scrapings coating the surfaces of tubeworms *Riftia pachyptila* recovered from P-vent, tubeworms *Alvinella pompejana* recovered from Bio9, and mussels *Bathymodiolus thermophilus* recovered from Crab Spa. The total number of biofilms (n=20) collected from each regime was n=4 from the *Alvinella* bioregime (ALV), n=6 from the *Riftia* bioregime (RIF), n=4 biofilms from the *Bathymodiolus* mussel bioregime (MUS), n=3 from substrates with no visible macrofaunal colonization (NM) and n=3 from water column seawater samples (SW). Hydrothermal fluids were collected using a large volume pump (approximately 400 l sample $^{-1}$) and were passed through a 0.45 μm glass fiber pre-filter and a 0.2 μm polysulfone filter (LVP). Filters were quartered and distributed for multiple analyses. Filters and biofilms were immediately preserved in RNA later solution and frozen at -80°C until analyses. Sample LVP2B (SW3) was contaminated by seawater during pumping. Bottom seawater samples were collected in titanium samplers and were filtered shipboard on 0.2 μm Supor Gelman filters (Ann Arbor, MI).

Sample ID	Type	Bioregime	Temperature (°C)	H_2S (μM)	pH	Vent Site
ALV1	Colonizer	Alvinella	29.2	155.3	7.5	Bio9
ALV2	Colonizer	Alvinella	75.2	412.9	7.5	M-vent
ALV3	Colonizer	Alvinella	29.2	155.3	7.5	Bio9
ALV4	Scraping	Alvinella	29.2	155.3	7.5	Bio9
RIF1	Basalt	Riftia	15.4	86.8	6.4	Crab Spa
RIF2	Colonizer	Riftia	14.5	62.6	6.3	Tica
RIF3	Colonizer	Riftia	15.4	14.4	6.8	Crab Spa
RIF4	Scraping	Riftia	6.6	4.9	7.2	P-vent
RIF5	Scraping	Riftia	6.6	22.9	7.0	P-vent
RIF6	Colonizer	Riftia	14.5	81.0	6.2	Tica
MUS1	Basalt	Mussels	5.7	23.8	6.7	Crab Spa
MUS2	Colonizer	Mussels	8.0	12.3	6.7	Perseverance
MUS3	Scraping	Mussels	5.7	23.8	6.7	Crab Spa
MUS4	Scraping	Mussels	5.7	23.8	6.7	Crab Spa
NM1	Colonizer	Bare basalt	4.7	5.1	7.2	Teddybear
NM2	Basalt	Bare basalt	6.1	7.8	7.0	Teddybear
NM3	Sulfide	Bare sulfide	6.6	nd	nd	P-vent
SW1	Major bottle	Water column	1.9	0.0	7.9	Off-axis water column
SW2	Major bottle	Water column	1.9	0.0	7.9	Off-axis water column
SW3	Hydrothermal fluid	Water column/Subsurface	n/a	n/a	n/a	Crab Spa
LVP2	Hydrothermal fluid	Subsurface	n/a	n/a	n/a	Crab Spa
LVP2B	Hydrothermal fluid	Water column/Subsurface	n/a	n/a	n/a	Crab Spa
LVP3	Hydrothermal fluid	Subsurface	n/a	n/a	n/a	Crab Spa
LVP4	Hydrothermal fluid	Subsurface	n/a	n/a	n/a	Crab Spa
LVP5	Hydrothermal fluid	Subsurface	n/a	n/a	n/a	Teddybear
LVP8	Hydrothermal fluid	Subsurface	n/a	n/a	n/a	Teddybear
LVP10	Hydrothermal fluid	Subsurface	n/a	n/a	n/a	Tica
LVP11	Hydrothermal fluid	Subsurface	n/a	n/a	n/a	Tica

Table 2.1 Summary of environmental data associated with the study samples. Temperature, sulfide concentration, and pH were extrapolated from geochemical data for statistical analyses.

rRNA Extraction and cDNA Synthesis

All biofilm samples were resuspended in RNA later (Ambion) and stored at - 80°C. Total RNA was extracted from the biofilm samples by centrifuging biomass in RNA later and resuspending in Solution I (50 mM glucose, 10 mM EDTA, 25 mM tris-HCl pH 8.0) and 75 µL of 0.5 M EDTA. The samples were subjected to three freeze/thaw cycles, after which 100 µL of lysozyme solution (4 mg/mL lysozyme in Solution I) was added, and samples were set to shake for 15 minutes. Afterwards, 50 µL 10% SDS was added to each sample. Samples were extracted twice with 800 µL phenol pH 4.3 and once using 800 µL phenol-chloroform-isoamyl alcohol (25:24:1) pH 6.7. RNA was precipitated by adding 0.1 volumes of 3.0 M Na-acetate and 1 mL of 100% ice-cold ethanol at -20°C overnight. The samples were centrifuged at 4°C for 30 minutes, supernatant was removed, and samples were washed with 1 mL 80% ethanol. After the 15 minute centrifugation, supernatant was removed and samples were left to dry at room temperature. Samples were resuspended in 50 µL ddH_20. DNase-treated RNA was reversed transcribed to single-stranded cDNA using SuperScript III First-Strand Synthesis System with SuperScript III Reverse Transcriptase primed with random hexamers (Invitrogen, Carlsbad, CA, USA). Samples were subsequently stored at -20°C until further analyses.

Synthesis of cDNA and Metatranscriptomic Analyses

Total RNA was extracted from biomass collected from the large volume pump (LVP4) filter collected at the Crab Spa diffuse flow vent and from the corresponding

biofilm (CV88). Following collection, both samples were stored in RNA later (Ambion). Six mL lysis buffer (1.6 mL 0.5M EDTA, 1.0 mL 1 M tris (pH 8.3), 5.13 g sucrose) were added to the filter and to the biofilm biomass while thawing on ice. Samples were subject to three freeze/thaw cycles using liquid nitrogen and a water bath pre-heated to 40°C. 120 µL lysozyme solution (120 µL lysis buffer with 6 mg lysozyme dissolved in) was added to the filter and the mixture was incubated at 37°C rotating for 45 minutes. 300 µL of proteinase K solution (3 mg proteinase K dissolved in 300uL ddH_20) and 200 µL SDS were added to each filter, and samples were incubated at 55°C rotating for 2 hours. Lysate was transferred to 50 mL polypropylene centrifuge tubes. Samples were extracted twice using an equal volume of phenol pH 4.3 and once using an equal volume of chloroform-isoamyl alcohol (24:1). Samples were washed once with 70% ethanol and 2x with sterile TE buffer. The samples were then concentrated using an Amicon Ultra-15 Centrifugal Device. DNase-treated RNA (1 µg reactions) was amplified by *in vitro* transcription using the MessageAmp II aRNA Amplification Kit (Ambion). The aRNA generated was poly-A tailed and precipitated according to the kit instructions using NH_4OAc and ethanol. RNA (0.2–5 µg) was resuspended in 5 µL DEPC-treated water and reversed transcribed to double-stranded cDNA using SuperScript Double-Stranded cDNA Synthesis Kit (Invitrogen, Carlsbad, CA, USA). cDNA was quantified with a Qubit® fluorometer using a dsDNA BR Assay kit (Q32850, ThermoFisher), and quality was assessed using High Sensitivity D1000 ScreenTape (5067-5584, Agilent) and reagents (5067-5585, Agilent) on an Agilent 2200 TapeStation. Sequencing libraries were prepared using an Ovation Ultralow DR Multiplex System (0331-32, NuGEN) with some modifications to the manufacturer's protocol. Briefly, cDNA was sheared in a total

volume of 130 µl in a microTUBE AFA Fiber Snap-Cap (520045, Covaris) using a Covaris M220 focused-ultrasonicator with the following settings: Peak Incident Power = 50; Duty Factor = 2.0; Cycles per burst = 200; Treatment Time = 160 s. Sheared DNA was cleaned up using a MinElute Reaction Cleanup kit (28204, QIAGEN). End Repair, Ligation and Amplification steps were performed according to manufacturer's protocol, but ligation and amplified library purification steps were performed with a QIAquick PCR Purification kit (28104, QIAGEN). Amplified libraries were size-selected on a BluePippin (Sage Sciences) using a 1.5% agarose gel cassette (BDF1510, Sage Sciences) with a size range of 300 – 500 bp. The size-selected libraries were cleaned up using a MinElute Reaction Cleanup kit, assessed for quality on an Agilent 2200 TapeStation using D1000 ScreenTape and reagents, and quantified with a KAPA Library Quantification Kit (KK4824, KAPA). Libraries were multiplexed and sequenced on an Illumina NextSeq 500 sequencer using a High Output v1 NextSeq kit (FC-404-1004, Illumina). Raw, paired-end reads were quality-trimmed with Trimmomatic v0.32 (-phred33 LEADING:0 TRAILING:5 SLIDINGWINDOW:4:15 MINLEN:36) and stitched together with Pandaseq (-A rdp_mle -C min_phred:10 -o 20).

16S rRNA Gene Amplification, Tag-Encoded Amplicon Sequencing and Annotation

The variable 4 (V4) region of the 16S rRNA transcripts was amplified from approximately 2 µg of cDNA of each biofilm communities using prokaryotic universal primers (515f 5'-GTG CCA GCM GCC GCG GTA A-3' and 806r 5'-GGA CTA CVS GGG TAT CTA AT-3', (Caporaso *et al.*, 2011). DNase-treated RNA was used as a template in PCR reactions using the same set of primers to ensure that there was no

carryover of genomic DNA. cDNAs were subjected to amplicon sequencing using the Ion Torrent PGM platform at the Molecular Research LP facilities (Shallowater, TX, USA).

Fluid samples were sequenced separately using bacterial primers 27F and 518R, and archaeal primers 349F and 806R via the 454 sequencing platform. Sequences were denoised and demultiplexed, and were subsequently processed using the Quantitative Insights Into Microbial Ecology bioinformatics pipeline (QIIME version 1.9.1; (Caporaso *et al.*, 2010)). Community level diversity across the biological regimes was analyzed by comparing the number of operational taxonomic units (OTUs), with an OTU defined at the 97% similarity level for both bacteria and archaea (Kunin *et al.*, 2010). OTUs with less than 5 sequences were discarded. At random, a sequence from each OTU was selected as a representative sequence and was subsequently assigned taxonomy using the Basic Local Alignment Search Tool (BLAST) against a subset of the SILVA database (Altschul *et al.*, 1990; Pruesse *et al.*, 2007). Relative abundance bar graphs of microbial taxa were prepared in R (Team, 2015) using the ggplot2 package (Wickham, 2009). Core microbiome analysis was performed by manually pooling OTU abundances of samples from each bioregime and using the compute_core_microbiome.py script (QIIME 1.9.1) to determine shared OTUs between sampling types. Venn diagrams were constructed using the Orange data mining toolbox version 3.6 (Demšar *et al.*, 2013).

Statistical Analysis

Samples were randomly rarefied to the size of the smallest library of 3,197 sequences before diversity metrics were calculated (Gihring *et al.*, 2012). Sample LVP2B was excluded due to poor sequencing depth. Community diversity indices (alpha

diversity) were determined using observed OTUs within each sample by the alpha _diversity.py script (QIIME 1.9.1) including the Chao (Chao, 1984), Shannon-Wiener diversity (Shannon, 1948), Simpson diversity (Simpson, 1949) and ACE richness (Chao *et al.*, 1993) indices. Weighted UniFrac matrices were obtained through beta_diversity_through_plots.py (Lozupone *et al.*, 2005). Analysis of similarity (ANOSIM) (Clarke, 1993) was used to determine statistical differences between samples (beta diversity) using the QIIME compare_categories.py script (All scripts are available at http://qiime.org/scripts/). Geochemical data were normalized and tested for normality distribution using Kolmogorov-Smirnov test within SigmaStat software for Windows, version 3.1 (Fox *et al.*, 1994). The weighted Unifrac distance matrix and sample mapping file were imported in R to perform nonmetric multi-dimensional scaling (nMDS) and cluster analysis using Ward clustering with vector overlays of environmental data in Vegan (Oksanen, 2011).

Results

Habitat biogeochemical characterization

The chemical characteristics of the sampling sites were typical of fluid-seawater mixing zones, including near-neutral pH, depleted oxygen, and elevated temperature and sulfide levels. Analyses of fluids showed M-vent and Bio9 had the highest temperature and sulfide concentrations of the sampling sites, with average recorded temperatures of 75°C and 29°C and sulfide concentrations of 413 μM and 155 μM, respectively (**Table 2.1**). Diffuse-flow vent site Crab Spa was closely monitored during the duration of the cruise, and maintained an average temperature of ~25°C, although samples experienced 5-16°C and 14-24 μM sulfide. Tica had a similar temperature profile at 14.5°C, but the

sulfide concentration was elevated (62.6 μM). The P-vent sulfide biofilm (NM3) was collected at the interphase between the external wall of an active black smoker and seawater (T: 6.6°C). Teddybear was a site characterized by diffuse-flow venting from a fissure on the ocean floor, low temperature (~4-6°C) and sulfide concentration (~5-8 μM), and by the widespread growth of filamentous bacteria on the surrounding basalt. The temperature of off-axis seawater was 1.9 °C and hydrogen sulfide was undetectable.

Comparative Alpha Diversity Analysis of the Biofilm Communities

Biofilm and seawater samples (n=20) yielded a total of 1,277,361 sequences (mean of 63,868 sequences/sample and average read length of 246bp) that passed all quality checks, including denoising and chimera removal. Reads were distributed across 11,218 operational taxonomic units (OTUs), defined at 97% sequence similarity, with five or more sequences needed to qualify as an OTU. Fluid samples (n=8) had a total of 99,642 sequences (mean of 12,455 sequences/sample and average length of 437bp), distributed across 3,308 OTUs. Hydrothermal fluids had the highest average diversity index (Shannon-Wiener index) among the sample types of H= 8.36 ±0.33. Compared with fluids, newly formed biofilms on experimental colonizers showed a decrease in diversity, with an average Shannon-Wiener index of 6.43 ±0.38. Within the newly formed biofilms, diversity increased as temperature and sulfide decreased, ranging from a Shannon-Wiener index (H) of 6.04 ±0.13 in the *Alvinella* bioregime, 6.55±0.31 in the *Riftia* bioregime, and 6.76 (n=1) in the *Bathymodiolus* bioregime. The colonizer exposed to the lowest temperature (4.7°C) located on basalt without animal colonization had the highest Shannon-Wiener index (H) of 6.88 (n=1). To establish shifts in community

composition with time, colonizer-associated microbial communities were also compared to mature biofilms derived from native substrates, including basalts, sulfides, and animal scrapings from each bioregime. Mature biofilms from the native substrates had higher diversity compared to the newly formed biofilms of the colonizers from each respective bioregime (**Table 2.2**). The increase in microbial diversity between newly formed and mature, invertebrate-associated biofilms shifted from H=6.04 to H=7.36 in the *Alvinella* bioregime, H=6.55 to H=6.85 in the *Riftia* bioregime, and H=6.76 to H=7.36 in the *Bathymodiolus* bioregime. Biofilms taken from bare basalts and sulfides, categorized in analyses as "no macrofauna," had the lowest diversity H=indices of all the biofilm samples collected, of H=3.75 in the sulfide sample and H=5.62 in the basalt sample.

						Species richness indicators			*Diversity*
Sample ID	**Type**	**Bioregime**	**Sequences**	**Total OTUs**	**Rarified OTUs**	**Chao1**	**ACE**	**Simpson's Evenness**	**Shannon-Wiener Index**
ALV1	Colonizer	Alvinella bushes	9,053	597	359	686	692	0.95	5.90
ALV2	Colonizer	Alvinella bushes	7,311	494	333	588	562	0.96	6.15
ALV3	Colonizer	Alvinella bushes	124,832	2,510	465	1062	1127	0.94	6.08
ALV4	Scraping	Alvinella bushes	36,227	1,506	570	1149	1161	0.98	7.36
RIF1	Basalt	Riftia tubeworms	288,837	4,739	763	1704	1713	0.99	8.03
RIF2	Colonizer	Riftia tubeworms	53,560	1,884	514	1031	1041	0.97	6.86
RIF3	Colonizer	Riftia tubeworms	127,215	2,876	495	1126	1144	0.94	6.25
RIF4	Scraping	Riftia tubeworms	72,569	1,739	582	1022	1064	0.98	7.23
RIF5	Scraping	Riftia tubeworms	32,096	824	395	574	580	0.96	6.47
RIF6	Colonizer	Riftia tubeworms	81,287	2,287	501	1110	1113	0.96	6.55
MUS1	Basalt	Mussel beds	16,974	899	499	858	851	0.98	7.20
MUS2	Colonizer	Mussel beds	48,332	1,456	468	837	899	0.98	6.76
MUS3	Scraping	Mussel beds	21,228	1,195	627	959	1018	0.98	7.62
MUS4	Scraping	Mussel beds	6,403	453	359	486	506	0.99	7.10
NM1	Colonizer	Bare basalt	70,073	2,086	546	1023	1181	0.97	6.88
NM2	Basalt	Bare basalt	7,216	287	248	296	291	0.93	5.62
NM3	Sulfide	Bare sulfide	75,018	1,012	299	642	704	0.72	3.75
SW1	Major bottle	Water column	121,926	2,404	523	1112	1233	0.85	5.54
SW2	Major bottle	Water column	74,007	2,092	695	1310	1483	0.98	7.52
SW3	Major bottle	Water column/Subsurface	3,197	115	113	156	130	0.94	5.13
LVP2	Hydrothermal fluid	Subsurface	15,811	1,544	797	1585	1644	0.99	7.88
LVP2B	Hydrothermal fluid	Water column/Subsurface	978	59	n/a	n/a	n/a	n/a	n/a
LVP3	Hydrothermal fluid	Subsurface	13,198	1,810	981	1656	1881	0.99	8.61
LVP4	Hydrothermal fluid	Subsurface	13,633	1,710	937	1709	1855	0.99	8.33
LVP5	Hydrothermal fluid	Subsurface	12,700	1,585	929	1395	1551	0.99	8.68
LVP8	Hydrothermal fluid	Subsurface	13,275	1,547	962	1485	1587	0.99	8.73
LVP10	Hydrothermal fluid	Subsurface	13,981	1,392	801	1292	1354	0.98	8.00
LVP11	Hydrothermal fluid	Subsurface	16,066	1,703	910	1528	1746	0.99	8.31

Table 2.2 Alpha diversity metrics for the comparative microbiome analysis of deep-sea vent bioregimes. Samples were rarefied to 3,197 sequences.

Statistical Analysis

Results from ANOSIM reported the highest R-value of 0.695 (where an R-value of 1 indicates that all similarities within groups are less than any similarity between groups) (p-value=0.001) for the factor of age, indicating significant differences between the newly formed and mature biofilms (**Table 2.3**). Biogeochemical drivers ranked in order of R-value were sulfide (R=0.574, p=0.003), pH (R=0.574, p=0.003), biological regime (R=0.393, p=0.004), temperature (R=0.394, p=0.007), and sampling site (R=0.338, p=0.015).

Diversity of the Active Microbial Biofilm Communities

Hydrothermal fluids (n=7) from Teddy Bear, Tica, and Crab Spa were dominated by Proteobacteria ($\bar{x}$=84%), of which an average of 76% were Epsilonproteobacteria. Within the class Epsilonproteobacteria, the predominant genera were *Sulfurovum* ($\bar{x}$=31%), *Sulfurimonas* ($\bar{x}$=27%), and *Arcobacter* ($\bar{x}$=13%). Biofilms collected from microbial colonizers (n=8) were compared to fluids to establish the transition in community composition between the subsurface and the seafloor. Newly formed biofilms had similar community composition across all bioregimes. Microbial colonizers placed at bioregimes of *Alvinella* bushes, *Riftia* tubeworms, and *Bathymodiolus* mussel beds

Factor	Age	Bioregime	Location	pH	H_2S	Temperature
Test groups	5	5	8	14	14	10
***R*-value**	0.695	0.393	0.338	0.574	0.574	0.394
***p*-value**	0.001	0.004	0.015	0.003	0.003	0.007

Table 2.3 Differences of microbial community composition investigated by analysis of similarities (ANOSIM)

contained 96%, 87% and 71% ($\bar{x}$= 87%) Proteobacteria respectively, showing increasing proportions of Proteobacteria with increasing temperature and sulfide concentrations in the fluids, and greater proportions of Bacteroidetes ($\bar{x}$=+8%), Fusobacteria ($\bar{x}$= +0.18%), Verrucomicrobia ($\bar{x}$= +0.28%), and Fibrobacteres ($\bar{x}$= +0.21%) in comparison with fluids.

Within the phylum Proteobacteria ($\bar{x}$= 87%), biofilms from microbial colonizers were dominated by Epsilonproteobacteria ($\bar{x}$= 97%), with small proportions present of Gammaproteobacteria ($\bar{x}$=1%) Deltaproteobacteria ($\bar{x}$=1%), and Alphaproteobacteria ($\bar{x}$=0.2%) (**Fig. 2.4**). The majority of sequences were phylogenetically affiliated with *Sulfurimonas* ($\bar{x}$=51%), *Sulfurovum* ($\bar{x}$=28%) and *Arcobacter* ($\bar{x}$=5%) (**Fig. 2.4**), showing an overall trend of increasing relative proportions of *Sulfurimonas* and decreasing proportions of *Sulfurovum* and *Arcobacter* associated with the migration of microbial communities from the subsurface (fluids) to the seafloor (microbial colonizers).

Fig. 2.4 (next page). UPGMA (Unweighted pair group method with arithmetic mean) cluster analysis of hydrothermal vent-associated microbial communities (using the Euclidean algorithm) based on weighted Unifrac distances between samples shows clustering by substrate-type, bioregime, and age. Relative abundances of dominant taxa based on the 16S rRNA gene sequences (>0.1%, with OTU filtering cutoff n≥5 reads) of microbial communities from deep-sea hydrothermal vent bioregimes displayed at the (left) phylum-level, (middle) class-level, and genus-level (right) of reads.

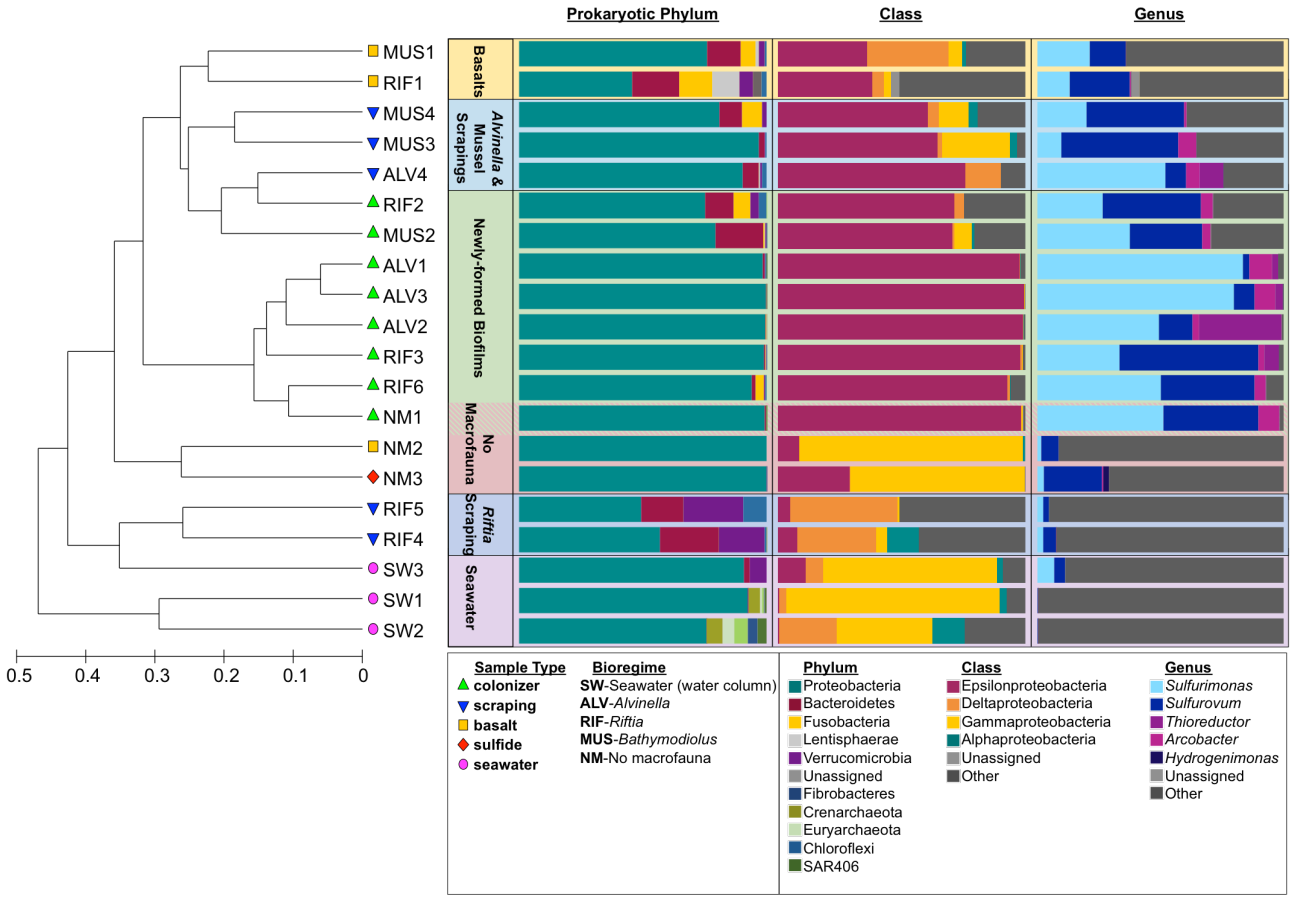
Prokaryotic Phylum
Class
Genus
MUS1
RIF1
MUS4
MUS3
ALV4
RIF2
MUS2
ALV1
ALV3
ALV2
RIF3
RIF6
NM1
NM2
NM3
RIF5
RIF4
SW3
SW1
SW2
0.5
0.4
0.3
0.2
0.1
0
Basalts
Alvinella & Mussel Scrapings
Newly-formed Biofilms
No Macrofauna
Riftia Scraping
Seawater
Sample Type
colonizer
scraping
basalt
sulfide
seawater
Bioregime
SW-Seawater (water column)
ALV-Alvinella
RIF-Riftia
MUS-Bathymodiolus
NM-No macrofauna
Phylum
Proteobacteria
Bacteroidetes
Fusobacteria
Lentisphaerae
Verrucomicrobia
Unassigned
Fibrobacteres
Crenarchaeota
Euryarchaeota
Chloroflexi
SAR406
Class
Epsilonproteobacteria
Deltaproteobacteria
Gammaproteobacteria
Alphaproteobacteria
Unassigned
Other
Genus
Sulfurimonas
Sulfurovum
Thioreductor
Arcobacter
Hydrogenimonas
Unassigned
Other

Despite congruencies at the class- and genus-level, newly formed biofilms shared a core microbiome consisting of only 5% of the total pooled OTUs, and a core of 8% of total OTUs when excluding biofilms not associated with a bioregime (NM1, NM2, and NM3).

Biofilms scraped from the surfaces of native substrates differed considerably from fluids (LVPs) and newly formed biofilms at the class level. Basalt-hosted microbial biofilms located within *Bathymodiolus* mussel beds (MUS1) and *Riftia* tubeworm patches (RIF1) grouped together during hierarchical clustering analyses (**Fig. 2.4**) and showed reduced proportions of Epsilonproteobacteria, decreasing from $\bar{x}$=78% of the total population in newly-formed biofilms to 18% on basalt within the *Riftia* bioregime (RIF2, RIF3, RIF6, RIF1), and decreasing from 55% in newly-formed biofilms to 27% on basalt within the *Bathymodiolus* bioregime (MUS2, MUS1). This corresponded with an increase in Gammaproteobacteria by and average of 1% of the total population in the *Riftia* bioregime, and an increase in Deltaproteobacteria by an average of 24% in the *Bathymodiolus* bioregime. A basalt from the *Alvinella* bioregime was not collected at the time of sampling.

Scrapings taken from metazoans were collected to determine if, in addition to age, biotic substrates would further influence community composition. Hierarchical clustering analyses grouped *Alvinella* (ALV4) and *Bathymodiolus* scraping samples together (MUS3 and MUS4) (**Fig. 2.4**), and *Riftia* scrapings (RIF4 and RIF5) in a separate cluster with seawater sample SW3. *Riftia* scrapings showed an increase in Verrucomicrobia ($\bar{x}$=+16%), Proteobacteria ($\bar{x}$=+7%) Fibrobacteres ($\bar{x}$=+3%), and Bacteroidetes ($\bar{x}$=+1%) relative to the basalt-associated microbial community from the same bioregime (RIF1). In

contrast with basalt samples, *Riftia* scrapings were abundant in Deltaproteobacteria ($\bar{x}$=20%, 17% greater than basalts) and also showed a higher proportion of Alphaproteobacteria ($\bar{x}$=+3%). Mussel scrapings contained an average of 28% more Epsilonproteobacteria, 13% more Gammaproteobacteria, 2% more Alphaproteobacteria corresponding with a 21% decrease of Deltaproteobacteria than basalts of the same bioregime.

Core microbiome analysis determined OTUs specific to each bioregime, and OTUs differentially present between newly-formed and established biofilms under the same bioregime. Samples from the *Riftia* bioregime had the highest proportion of bioregime-specific OTUs at 17%, followed by 9% of *Alvinella* OTUs, and 8% of *Bathymodiolus* OTUs. The *Alvinella* bioregime shared 99% of OTUs between newly-formed (ALV1, ALV2, ALV3) and established (ALV4) biofilms, with the addition of Flavobacteriales and Campylobacterales members, including *Crocinitomix* and *Sulfurovum* spp. (**Fig. 2.5**). The *Riftia* bioregime shared 95% of OTUs, showing the addition of *Nitratiruptor*, *Alteromonas* and *Vibrio* spp., as well as taxa associated from the Myxococcales family *Polyangiaceae* in established biofilms (RIF1, RIF4, RIF5). The vent mussel bioregime shared 89% of OTUs, and showed the addition of Campylobacterales members *Sulfurimonas* spp., Thiotrichales members *Marithrix* and *Cocleimonas* spp., and taxa from the Bacteroidales and Victivalles orders

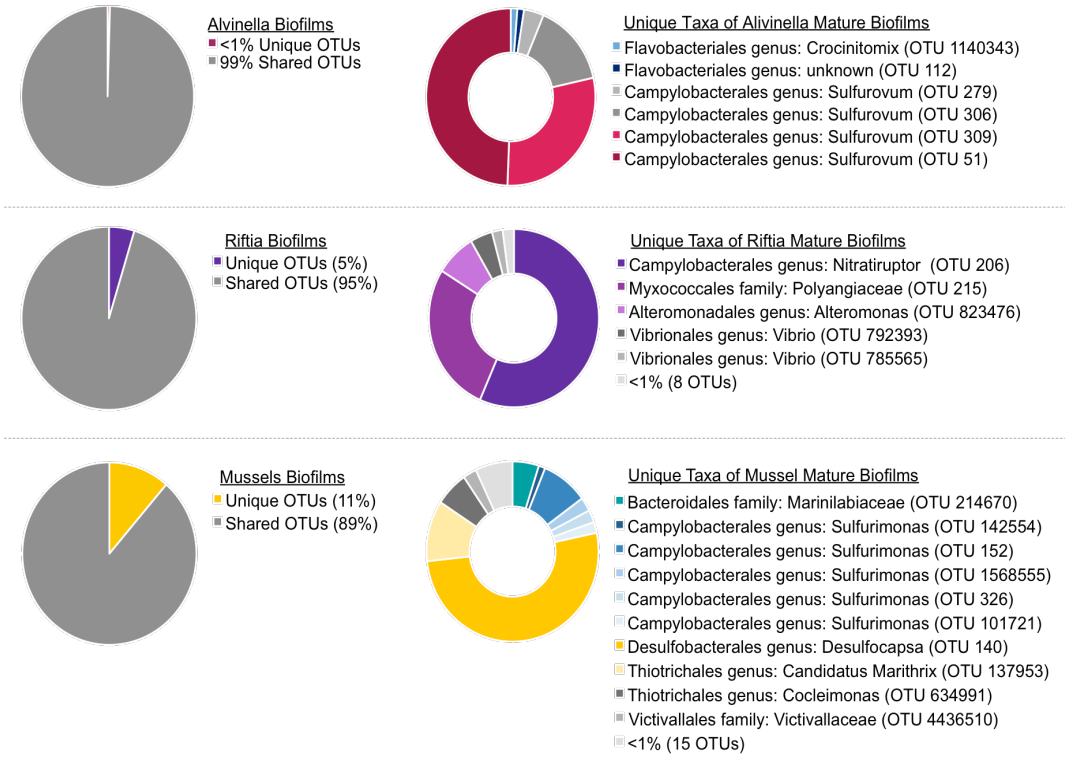

Fig. 2.5 Core microbiome analysis visualizing shared and unique OTUs between newly formed and established biofilms (left) and OTUs specific to established biofilms in each bioregime (right).

The Ubiquity and Diversity of Sulfurovum, Sulfurimonas, and Arcobacter.

Within the dominant Epsilonproteobacterial clades, a total of 1,097 *Sulfurovum*-like, 1,432 *Sulfurimonas*-like, and 390 *Arcobacter*-like OTUs were identified from biofilms samples. The core community found across all bioregimes consisted of 208 *Sulfurovum* OTUs (19%), 290 *Sulfurimonas* OTUs (20%), and 90 *Arcobacter* OTUs

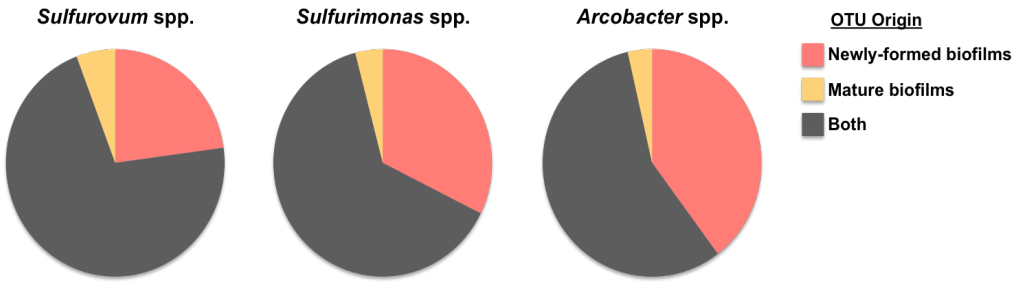

Fig. 2.6 Distribution of *Sulfurovum*-, *Sulfurimonas*- and *Arcobacter*-like OTUs in new and mature biofilms

(23%). Interegime analysis found co-occurrence of 71% *Sulfurovum*-, 64% of *Sulfurimonas*-, and 57% of *Arcobacter*-related OTUs shared between newly formed and established biofilms. Intraregime analysis revealed that the highest proportions of regime-specific (only found in a single bioregime) OTUs were found in the *Riftia* bioregime, constituting 32% of *Sulfurovum* OTUs, compared to 2% in both the *Bathymodiolus* and *Alvinella* regimes. Of the *Sulfurimonas* OTUs, 16% were found only in the *Riftia* bioregime, compared to 5% in *Alvinella,* and 2% in *Bathymodiolus*. Of the *Arcobacter* OTUs, 11% were specific to the *Riftia* bioregime, compared to 8% in the *Alvinella* bioregime and <1% in the *Bathymodiolus* bioregime.

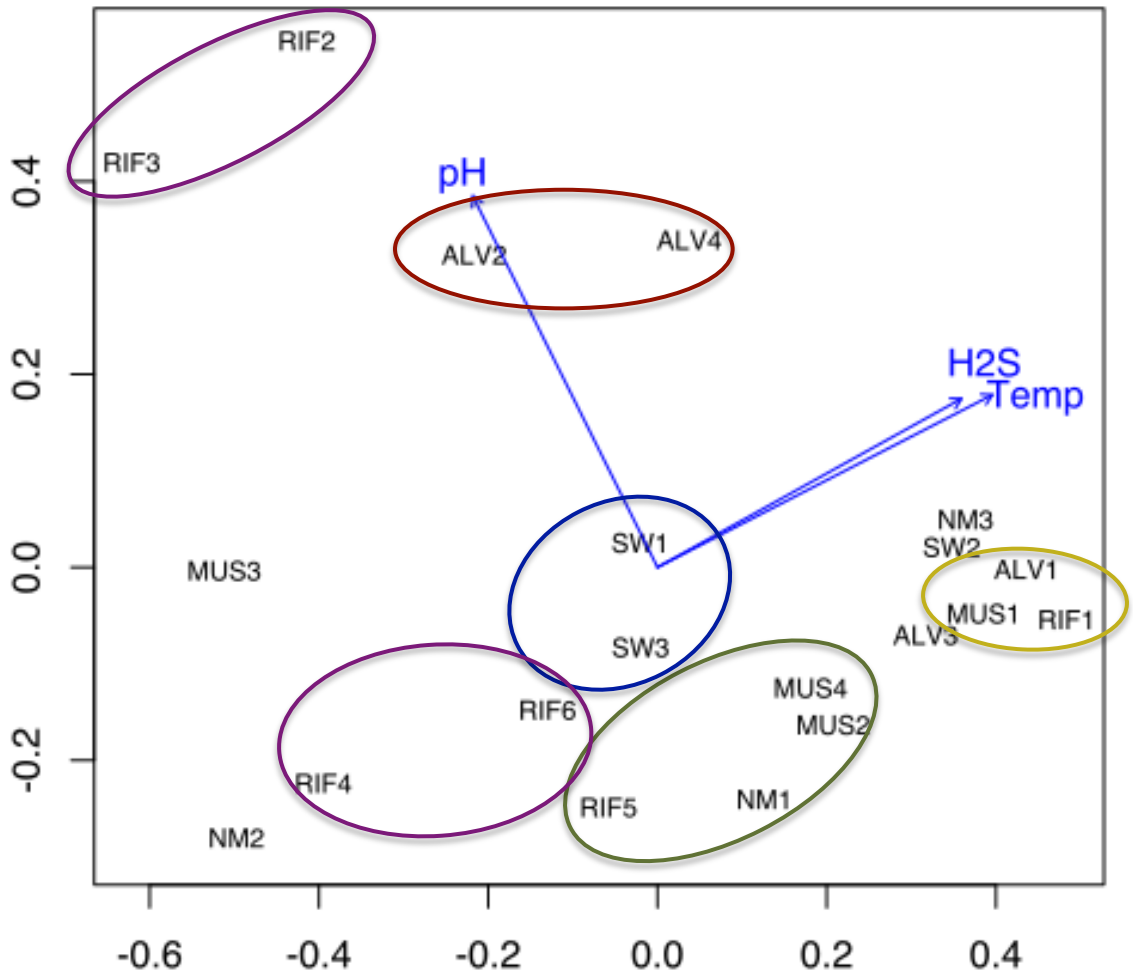

Fig. 2.7 Ordination of the microbial communities constructed using non-metric dimensional scaling (NMDS) analysis using OTU frequencies in samples. Variables with the highest contributions to the separation among groups are displayed as vectors in the biplot. Orbital overlays by color encircle *Riftia* biofilms (purple), *Alvinella* biofilms (red), colonizers, basalts (yellow), and seawater samples (blue). Stress=0.2

Detection of functional gene transcripts in chemosynthetic biofilms and corresponding hydrothermal fluids.

The metatranscriptomic analysis of hydrothermal fluids (LVP4) and the corresponding biofilm (CV88/RIF3) collected at the Crab Spa diffuse flow vent site revealed the functional diversity within the two communities. A summary of the metatranscriptomic features is shown in **Table 2.4.** The 16S rRNA transcripts were

compared to 16S rRNA genes detected in a pyrotag analysis of fluids (LVPs) and biofilms (CV88/RIF3), and the resulting taxonomic profiles were very similar (**Fig. 2.8**). Approximately 25% of the functional transcripts were affiliated with the Epsilonproteobacteria (**Fig. 2.9**). Transcripts encoding for genes in central metabolism, environmental sensing and motility as well as oxidative detoxification were detected, including the ATP-citrate lyase transcript (*aclA*) diagnostic of carbon fixation via the reductive TCA cycle, and the periplasmic nitrate reductase transcript (*napA*) used for dissimilatory nitrate reduction (**Fig. 2.10**). Overall, these findings indicate that the microbial community flushed out from the subsurface (fluids) to form biofilms is actively metabolizing carbon dioxide, reducing nitrate, and combating biologically adverse conditions such as oxidative stress.

Metatranscriptome Features	**Biofilm (CV88)**	**Fluids (LVP4)**
Total bp	942,174,098	482,071,720
Sequences	5,563,427	3,141,766
Mean sequence length (bp)	169+/- 42	153 +/- 32
Mean G+C (%)	41 +/- 9	37 +/- 8
Predicted protein features	323,523	2,167,826
Predicted rRNA features	1,040,025	14,518
Identified protein features	155,219	615,886
Identified rRNA features	604,523	6,243
Functional categories	125,713	495,184

Table 2.4 Features of the metatranscriptomes of hydrothermal fluids (LVP4) and corresponding newly formed biofilm (CV88/RIF3) from the *Riftia* bioregime

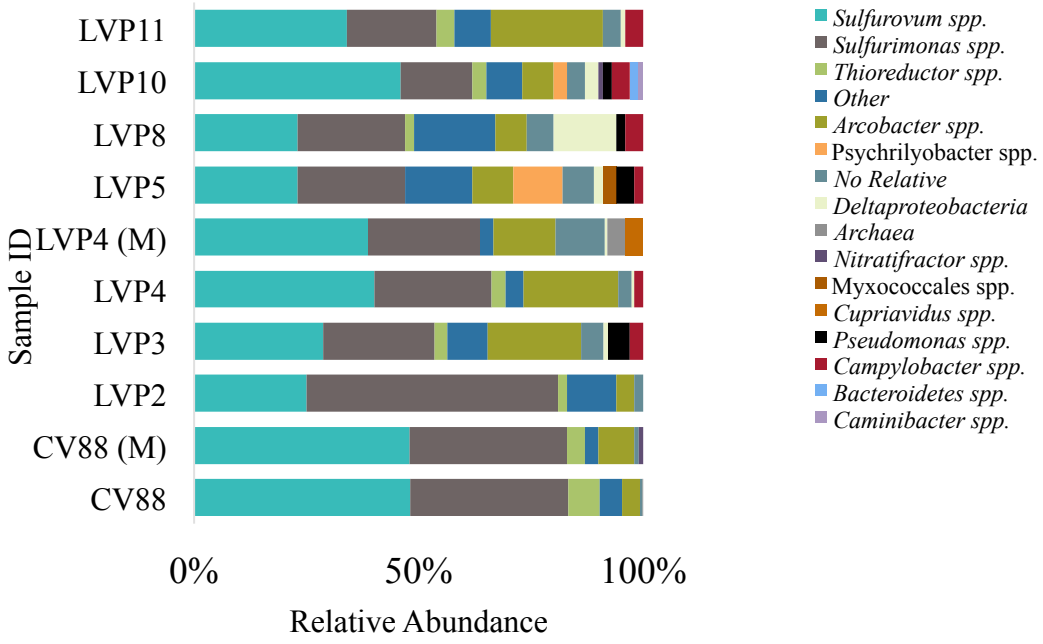

Fig. 2.8 Taxonomic composition of two metatranscriptomic datasets of hydrothermal fluid, LVP4 (M), and a newly-formed biofilm, CV88 (M), with the16S rRNA pyrotag of the active microbial communities in fluids using output from SILVAngs

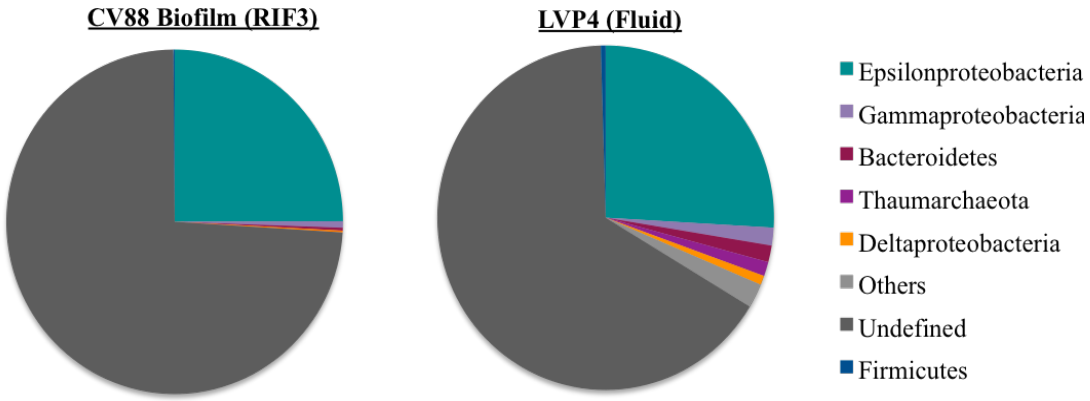

Fig 2.9 The taxonomic affiliation of functional transcripts from the metatranscriptomic analysis of hydrothermal fluids (LVP4; right) and the corresponding biofilm sample (CV88/RIF3; left)

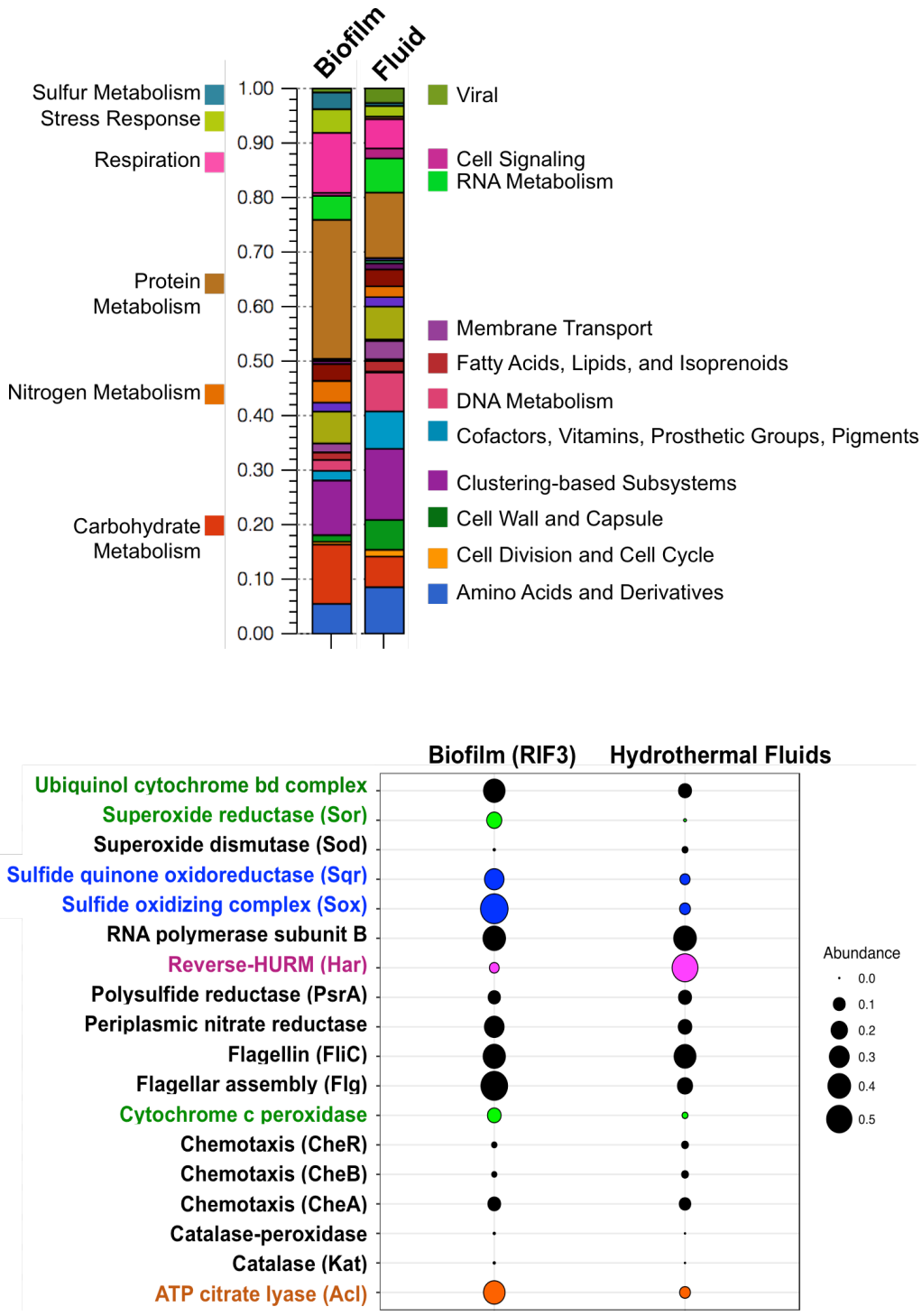

Fig 2.10 Subsystem annotation of transcripts from biofilm and fluid metatranscriptomes with labels partitioned by enrichment (top) and the relative abundance of key transcripts detected in the metatranscriptomes of fluids (LVP4) and biofilm (CV88/RIF3) (bottom)

Discussion

The ecological structure and diversity of microbial communities is intrinsically linked to the heterogeneity and stability of the ecosystems they inhabit. The aim of this study was to elucidate the biogeographical patterns of the active microbial communities at deep-sea hydrothermal vents, and discover how these communities are shaped by biogeochemical, spatial, and temporal constraints. Through 16S rRNA transcript analyses, we have established the composition of active microbial biofilm communities across a broad range of samples. Co-registered measurements of temperature, sulfide, and pH recorded at the time of sampling were used to establish the major drivers that influence the observed variation in community composition. The results obtained indicate that hydrothermal fluids differing in temperature and sulfide concentration support fairly homogeneous seafloor microbial communities in the early stages of biofilm formation. These early biofilm communities are less diverse than the subsurface (**Table 2.2**). We hypothesize that the decrease in diversity observed during the transition from the fluid-associated subsurface community to the substrate-attached biofilms at the seafloor can be attributed to the selection of a subpopulation capable to form biofilms. Taxonomic diversity appeared to increase with biofilm maturity and in association with vent macrofauna (**Table 2.2**). The generation of sufficient organic carbon through primary production by the chemosynthetic pioneer colonizers enables the recruitment of a broader range of species, such as those found on native substrates, as the biofilm matures. While previous studies have also documented the reduction in diversity and evenness from the subsurface to the seafloor-associated communities, as well as successional patterns of diversification of microbial communities on specific substrates (Gulmann *et al.*, 2015),

this study has additionally exposed patterns of species partitioning as a function of biogeochemical and temporal influence imparted by bioregime and age on the active fraction of microbial biofilms that is reflective of the archetypal macrofaunal distribution at deep-sea hydrothermal vents.

Community Structure in Newly Formed Biofilms

The data show significant differences between newly formed and mature biofilms, and that age is a primary driver in variation between microbial biofilm composition at deep-sea vents, ranking highest (R=0.695, p=0.001) using the analysis of similarities (ANOSIM). The effect of age is especially prominent when comparing young biofilms collected from contrasting bioregimes (*e.g.*, low-temperature, low-sulfide mussel beds and high-temperature, high-sulfide *Alvinella* colonies), which had greater similarity than young and mature biofilms collected within a single bioregime (**2.4, 2.7**). Regardless of bioregime, newly-formed biofilms were dominated by Epsilonproteobacteria ($\bar{x}$=85% of the total population), composed of *Sulfurimonas* ($\bar{x}$=51% of the total population), *Sulfurovum* ($\bar{x}$=28% of the total population), and *Arcobacter* ($\bar{x}$=5% of the total population) species, which have been previously reported as pioneer populations at deep-sea vents (Gulmann *et al.*, 2015; O'Brien *et al.*, 2015; Ponsard *et al.*, 2013). *Thioreductor, Caminibacter, Nitratifractor, Sulfurospirillum,* and *Campylobacter* spp. were also present in smaller proportions (<1%) and varied by bioregime. Newly-formed biofilms contained an average of 1% Gammaproteobacteria, with small proportions of SUP05, a clade that includes mesophilic, autotrophic hydrogen-oxidizers. Common at deep-sea vents, in this study, SUP05 were found exclusively in colonizer and basalt

samples, and were missing from native biofilms scraped from metazoans. SUP05 are widespread in pelagic environments, and prior studies have detected SUP05 at hydrothermal vents in plumes, areas of low-temperature diffuse flow, in symbiosis with vent fauana, and often in co-occurrence with sulfur-oxidizing Epsilonproteobacteria (Meier *et al.*, 2017). The proportionally higher abundance of *Sulfurimonas* and detection of SUP05 may be linked with energy metabolism, since *Sulfurimonas* isolates have been found to derive energy from hydrogen oxidation (Han *et al.*, 2014, 2015; Inagaki *et al.*, 2003; Mino *et al.*, 2017; Sievert *et al.*, 2008), and there is strong evidence for hydrogen oxidation capabilities in SUP05 (Anantharaman *et al.*, 2013). Available energy sources appear to drive proportional variation between *Sulfurimonas* and *Sulfurovum* species in newly formed biofilms.

Bioregime Dictates the Recruitment of Species to Mature Biofilms

Bioregime is a contributing factor towards determining community diversity as the surfaces of vent macrofauna provide a dynamic, bioactive matrix for microbes to adhere to, a nutrient-rich substrate to metabolize, and in many cases, metazoans influence the local geochemistry through the excretion of metabolic by-products (*e.g.*, the release of sulfate localized at the plume surface of *Riftia*). Microbial communities formed on native substrates (*e.i.*, the surface of animals, sulfides, and basalts) had greater diversity compared with young biofilms in general, but only when taken from intraregime zones (**Table 2.2**). This increase in diversity could correlate with biofilm maturity and/or substrate availability, via the recruitment of species from the water column, or perhaps

through the increase of seeding populations originally present in small proportions in fluids better adapted to attach to substrates or for growth under seafloor conditions.

Core microbiome analysis allowed for the identification of differential prokaryotic OTU abundance, which facilitated the identification of potential successive species as well as intraregime comparison to establish shared OTUs, indicative of bioregime interconnectedness. Our findings showed that biofilms from the *Alvinella* bioregime maintained the highest proportion of OTUs shared between young and mature populations, with the addition of Flavobacteria-related and *Sulfurovum*-related species to mature biofilms. This is likely due to the highly selective conditions of the *Alvinella* bioregime, and the conserved metabolic strategy of chemolithoautotrophic metabolism in both newly formed and mature biofilms. Previous work established that more than 80% of the *Alvinella* epibiotic community is dominated by bacteria belonging to a single monophyletic clade within the Epsilonproteobacteria with potential for chemolithoautotrophic growth (Campbell *et al.*, 2001; Campbell *et al.*, 2003; Cary *et al.*, 1997; Haddad *et al.*, 1995). Incongruent with previous findings, Epsilonproteobacteria only amounted to 64% of the epibiotic population of the *Alvinella* tubeworm from this study. Deltaproteobacteria (13%) were surprisingly abundant, and included relatives of chemoorganotrophic species *Desulfobulbus* (3% of total) and ectoparasite *Bdellovibrio* (4% of total), a novel occurrence of *Bdellovibrio*-like microorganisms in a high-temperature habitat. Given the deeply-branching position of *Bdellovibrio* and genomic remnants of thermophilic, biosynthetic pathways, a thermophilic or thermotolerant isolate of *Bdellovibrio* has been hypothesized to exist (Iizuka *et al.*, 2006). Early morphological studies using SEM/TEM images of *Alvinella* worms noted the presence of *Bdellovibrio*-

like corpuscules (Gaill *et al.*, 1987) which, along with the sequencing-based evidence provided in this study, supports the hypothesis that thermophilic *Bdellovibrio* inhabit deep-sea hydrothermal vents, and furthermore, a potential pattern of association between *Bdellovibrio* with *Alvinella* tubeworms. Further investigation may shed light on the evolution of an early deltaproteobacterial predatory ancestor.

Samples from the *Riftia* bioregime showed the addition of *Nitratiruptor*-related species, *Vibrio*-related species, *Alteromonas*-related species, as well as taxa associated from the Myxococcales family *Polyangiaceae* to established biofilms. Although *Nitratiruptor* have historically displayed chemolithoautotrophic metabolic capabilities, recent studies have confirmed heat-stable endolytic alginate lyase activity in deep-sea vent isolates (Inoue *et al.*, 2016) that may aid in a parasitic-type of colonization of the tubeworm surface. Deep-sea isolates of *Vibrio* and *Alteromonas* have both been shown to excrete sulfated heteropolysaccarides high in uronic acids, with heparin-like activity (Nakagawa *et al.*, 2005c; Nichols *et al.*, 2005; Raguénès *et al.*, 1997). In addition to the obvious advantage of attachment and the suggested benefit of detoxification via the high metal-binding capacity of EPS, the anti-coagulant-like activity found in deep-sea isolates hints at the possibility that EPS may ultimately aid in the degradation of plume tissue as well. These observations point to the need of further physiological studies correlating tubeworm health with the epibiont microbiome.

The vent mussel bioregime shared 89% of OTUs between mature and newly formed biofilms, the lowest proportion among bioregimes, likely correlating with the least amount of selective pressure applied to the system. The mussel bioregime also shares greater commonality with ambient conditions, enabling greater colonization of

seawater-derived microorganisms (18% in mature biofilms) compared to *Riftia* (15%) and *Alvinella* (13%) bioregimes. These observations suggest that, as temperature and sulfide concentration increase, habitats become more selective for species highly adapted to these conditions, and recruitment of species from the water column decreases. Mature biofilms showed the addition of *Sulfurimonas* spp., *Marithrix* and *Cocleimonas* spp., and taxa from the Bacteroidales and Victivalles orders. Notably present in the mussel-associated biofilms were sequences clustering with Epsilonproteobacteria shown to have a widespread association with bathymodiolan species in the gill of the animal. A recent study linking sequencing data and fluorescence *in situ* hybridization (FISH) assays found evidence of the proposed novel family in *B. childressi* and *B. azoricus*, but not in *B. thermophilus* (Assié *et al.*, 2016), with this study providing the first evidence of their occurrence of these OTUs in the biofilm formed on the shell of the mussel, confirming that the mussel symbiont is acquired from the environment.

Interregime zones give rise to low-complexity communities, with native biofilms taken from areas lacking metazoan colonization ranking lowest in diversity among all the biofilm samples. Biofilms acquired from areas of low venting (NM2 from Teddy Bear) and an extinct vent (NM3 from P-vent) exposed to ambient seawater shared a similar taxonomic profile dominated by the filamentous gammaproteobacterial species Candidatus *Marithrix*. These findings are in accordance with previous surveys, which have documented Thiotrichales colonization in no-flow areas of hydrothermal vents (O'Brien *et al.*, 2015). Derived from a lineage that forms a monophyletic cluster within the large sulfide-oxidizing family *Beggiatoaceae* (Teske *et al.*, 2014), Candidatus *Marithrix* is a facultative aerobic sulfide-oxidizer with a non-motile lifestyle whose

genome houses multiple copies encoding for the high-affinity carbon uptake protein Hat/HatR (Salman-Carvalho *et al.*, 2016). The adaptation to low-carbon dioxide conditions may permit this species to flourish in areas that would otherwise would have resource competition, succeeding others in zones of low-venting and inactive chimneys.

The Ubiquity and Diversity of Sulfurovum, Sulfurimonas, and Arcobacter

Epsilonproteobacteria are among the most ubiquitous primary producers at deep-sea hydrothermal vents, found in symbiotic association with vent macrofauna, adhered to vent substrates, and free-living in diffuse-flow hydrothermal fluids and plumes (Campbell *et al.*, 2006; Dick *et al.*, 2013). Their ecological success at deep-sea vents has been attributed to metabolic versatility, enabling phenotypic adjustment in response to environmental perturbation (Campbell *et al.*, 2006; Nakagawa *et al.*, 2005b). Prior time-series analyses tracking proportions of Epsilonproteobacteria have determined *Sulfurovum* to be the dominant epsilonproteobacterial species during colonization (O'Brien *et al*, 2015) and in mature biofilms on basalt (Gulmann *et al.*, 2015). Our findings show that *Sulfurimonas* was the dominant epsilonproteobacterial genus in 6 of the 8 newly formed biofilms collected from microbial colonizers, in greater proportion relative to *Sulfurovum*. Prior studies have also noted the continuity of OTUs from early colonization through approximately a year of growth on native substrates (Gulmann *et al.*, 2015). Core microbiome analyses performed during this study further resolves that the proportion of OTUs shared between young and mature biofilms varies with bioregime, with an approximate range of 89-99% total OTU commonality, and between 57%-71% conserved *Sulfurovum*, *Sulfurimonas*, and *Arcobacter*-associated OTUs.

Although *Sulfurovum* and *Sulfurimonas* dominated most biofilm samples, at the OTU level (defined at 97% sequence-similarity), partitioning of OTUs by biofilm age and bioregime was evident. It has been proposed that the high intragenus diversity of co-occurring *Sulfurovum*- and *Sulfurimonas*-related species may be a direct reflection of the high fluctuation of environmental conditions, and that environmental perturbation over time aids in the niche diversification of *Sulfurimonas* and *Sulfurovum*, enabling oscillating proportions stemming from an environment of intermediate disturbance (Gulmann *et al.*, 2015; Meier *et al.*, 2017). Intermediate disturbance theory purports that the greatest diversity often occurs at moderate levels of disturbance since resilience of the ecosystem is buffered through varied response of species to environmental fluctuations (Ives *et al.*, 2007). Organisms that occupy a functionally redundant role also help ensure ecosystem stability during species reduction resulting from environmental stress. Phenotypic divergence is often driven by habitat fragmentation, resource competition, or during times of ecological opportunity (*e.g.*, during the rebirth of a vent). It has also been observed in macrofaunal communities at deep-sea hydrothermal vents, species richness peaks in intermediate stress zones, such as fragmented habitats typically characterized by tubeworm and mussel colonization (Gollner *et al.*, 2015). Accordingly, data from this study report the greatest OTU abundances of *Sulfurimonas*, *Sulfurovum*, and *Arcobacter* were from biofilms collected in the *Riftia* bioregime. Deep-sequencing has enabled the detection of the numerous co-existing *Sulfurimonas* and *Sulfurovum* species and a pattern of microhabitat species partitioning, both indicative of adaptive radiation within their lineages (Schluter, 2000). Whether these phylotypes contribute to community

compensation potential through metabolic redundancy or plasticity has yet to be determined, although the data presented in this study suggest a combination of both.

Conclusions

Microbial diversity surveys at deep-sea vents have increasingly stated that community composition cannot be inferred solely by geochemical constraints. The results of this study are in agreement and further resolve that age and biological association of the biofilm play a greater role in community structure than previously predicted. Much like the successional pattern observed in vent macrofauna, vent microorganisms display a shift in community structure over time, and logically, just as vent macrofauna partition according to biological requirements, this study provides evidence that vent microorganisms do as well. Therefore, when assessing microbial biogeography, in addition to vent geochemistry, factors including bioregime and age should also be considered. Further research to determine mechanisms of estimating age, such as detection of community disturbance and age-dependent physical attributes of biofilms are needed. The diversity, abundance, and distribution of *Sulfurovum*, *Sulfurimonas*, and *Arcobacter* species at deep-sea vents has been constrained by the current study, however, additional investigation of functional diversity within these keystone phylotypes may offer novel insights into the biogeochemical drivers behind adaptive radiation in microbial species.

Chapter 3

Cetia pacifica gen. nov., sp. nov., a chemolithoautotrophic, thermophilic, nitrate-ammonifying bacterium from a deep-sea hydrothermal vent.

Published in: International Journal of Systematic and Evolutionary Microbiology (2015), 65, 1144–1150

Introduction

The class Epsilonproteobacteria consists of two recognized orders, Nautiliales (Miroshnichenko *et al*., 2004) and Campylobacterales (Garrity *et al*., 2005). Species of the order Nautiliales with validly published names are moderately thermophilic bacteria which originate exclusively from deep-sea hydrothermal vents and are found in association with invertebrates, chimney edifices and *in situ* colonization devices, as well as hydrothermal sediments (Nakagawa *et al*., 2005; Takai *et al*., 2005; Voordeckers *et al*., 2005; Perez-Rodrıguez *et al*., 2010). Within the order Nautiliales, the family *Nautiliaceae* consists of three genera, *Nautilia* (Miroshnichenko et al., 2002), *Caminibacter* (Alain et al., 2002) and *Lebetimonas* (Takai et al., 2005). The genus *Nautilia* has four cultured representatives, *Nautilia nitratireducens* (Perez-Rodriguez et al., 2010), *N. abyssi* (Alain et al., 2009), *N. profundicola* (Smith et al., 2008) and *N. lithotrophica* (Miroshnichenko et al., 2002). All representatives were isolated from the East Pacific Rise hydrothermal vent system. The group is composed entirely of hydrogen-oxidizing, chemolithoautotrophic bacteria, although the majority of known species of the genus *Nautilia* are also capable of utilizing formate as an electron donor and/or carbon source. All cultured strains of the genus *Nautilia* couple hydrogen/ formate oxidation to the

reduction of elemental sulfur and, in some cases, to the reduction of nitrate (e.g., *N. nitratireducens* and *N. profundicola*) (Hanson et al., 2013; Perez-Rodrıguez et al., 2010).

At the time of writing, the genus *Caminibacter* includes three species with validly published names, *Caminibacter mediatlanticus* (Voordeckers et al., 2005), *Caminibacter profundus* (Miroshnichenko et al., 2004) and *Caminibacter hydrogeniphilus* (Alain et al., 2002), which were isolated from both the East Pacific Rise and the Mid-Atlantic Ridge. Members of this taxon are solely capable of lithotrophic growth, during which they couple the oxidation of hydrogen to the reduction of nitrate, elemental sulfur and/or oxygen. *Lebetimonas*, the third genus within the family *Nautiliaceae*, contains one member, *Lebetimonas acidiphila*, whose primary distinction from species of the genera *Nautilia* and *Caminibacter* is its ability to grow at a slightly lower pH, as well as its origin of isolation, the Mariana Arc. Although members of the genera *Caminibacter*, *Nautilia* and *Lebetimonas* originate from geographically distant vent sites, they share many physiological characteristics, including optimal temperatures ranging from 40 to 60 °C, optimal salinities between 2 and 3.2 % and optimal pH from 5.2 to 7.1. Genera within the family *Nautiliaceae* also share the ability to oxidize hydrogen while using either nitrate and/or sulfur as a terminal electron acceptor.

Their similar metabolic properties and growth requirements may imply that the bacteria in these groups occupy a niche that is similar throughout various deep-sea vent sites. In this study, the isolation and characterization of a thermophilic, chemolithoautotrophic, strictly anaerobic, nitrate-ammonifying epsilonproteobacterium isolated from an active chimney at the East Pacific Rise are described. Based on 16S

rRNA gene phylogeny, physiological traits and a distinct chemotaxonomic profile, this strain represents a novel genus within the family *Nautiliaceae*.

Materials and Methods

Samples from a black smoker chimney were collected during R/V *Atlantis* cruise AT 15-15, January 2007 at the East Pacific Rise ('Bio 9' Vent, 9u 499 N, 104u 179 W, depth: 2500 m). The hydrothermal fluid temperature of emissions from the sampled sulfide structure was 378 °C. Chimney samples were collected using the manipulator arm of DSV Alvin and subsequently stored in boxes on the submersible's working platform for the remainder of the dive. At the surface, samples were transferred to the ship's laboratory and subsamples were stored at 4 °C under a dinitrogen atmosphere. Primary enrichment cultures were performed on board the ship by inoculating a slurry containing 1 g of the black smoker chimney sample resuspended in 1 ml of anaerobic artificial seawater into 10 ml of modified SME medium (Stetter et al., 1983; Vetriani et al., 2004) supplemented with 10 % (w/v) nitrate under a H_2/CO_2 gas phase (80 : 20; 200 kPa. The primary enrichments were diluted to extinction and incubated shipboard at 60 °C. After samples were transferred to the main lab, aliquots from a 1024 dilution of the primary enrichments were inoculated into fresh medium (1 : 100 dilution factor). *Cetia pacifica* was routinely grown in modified SME medium which contained (l^{-1}): NaCl, 20.0 g; $MgSO_4 \cdot 7H_2O$, 3.5 g; $MgCl_2 \cdot 6H_2O$, 2.75 g; KCl, 0.325 g; KNO_3, 1.0 g; NaBr, 50.0 mg; H_3BO_3, 15.0 mg; $SrCl_2 \cdot 6H_2O$, 7.5 mg; $(NH_4)\ 2SO_4$, 10.0 mg; KI, 0.05 mg; $Na_2WO_2.2H_2O$, 0.1 mg; $CaCl_2 \cdot 2H_2O$, 0.75 g; KH_2PO_4, 0.5 g; $NiCl_2 \cdot 6H_2O$, 2.0 mg; resazurin, 1.0 mg; trace element solution, 10 ml. The salt solution was heated to boiling

point and then cooled under a stream of N_2 for 30 min. $Na_2S \cdot 9H_2O$ (0.5 g l^{-1}) was added to reduce the medium and the pH was adjusted to 6.0 with H_2SO_4. The medium was aliquoted into portions of 10 mL per tube, which were tightly stoppered tubes (Bellco Glass) and autoclaved (200 kPa, 20 min, 121 °C). Prior to inoculation, the medium was supplemented aseptically with 0.25 ml MES buffer (20%, w/v; pH 5.5), 0.1 ml KNO_3 (10%, w/v) and 0.04 ml $Na_2S \cdot 9H_2O$ (3%, w/v; neutralized with HCl). An overpressure of 2 bars (30 psi) of H_2/CO_2 (80:20; 200 kPa) was added to each tube, and cultures were incubated overnight at 60 °C.

Pure cultures were obtained by performing ten consecutive series of dilutions to extinction. The dilution series were followed by isolation of single colonies on plates containing SME medium solidified with 1 g Phytagel l21 (Sigma). Plates were incubated in an Oxoid anaerobic jar pressurized with H_2/CO_2 (80 : 20; 200 kPa). During the isolation procedures, the cultures were incubated at 60 °C. The two pure cultures obtained using this procedure were designated strains TB-6^T and TB-8. Preliminary phylogenetic analysis of the 16S rRNA gene sequences indicated that strains TB-6^T and TB-8 were closely related (sequence identity: 99 %); TB-6^T was chosen for further characterization. Long-term stocks of isolates were prepared by adding 50 ml DSMO (Fisher Scientific) to 1 ml culture and were immediately stored at 280 °C. Direct counts of cells stained with acridine orange (0.1 % w/v) were determined by visualization on an Olympus BX 60 microscope with an oil immersion objective (UPlanFl 100/1.3). Transmission electron micrographs were obtained as previously described (Vetriani et al., 2004).

Growth rates (μ; h^{-1}) were estimated as $\mu=(\ln N_2-\ln N_1)/ (t_2-t_1)$, where N_2 and N_1 represent the cell densities (cells ml^{-1}) at times (hours of incubation) t_2 and t_1, respectively. Generation times (tg; measured in h) were calculated as $t_g-\ln(2)/\mu$. All growth experiments were performed in duplicate, in 25 ml of modified SME medium supplemented with 20 mM potassium nitrate under H_2/CO_2 (80 : 20; 200 kPa) unless stated otherwise. Strain TB-6^T was incubated at temperatures between 35 and 75 °C, at 5 °C intervals. Subsequent experiments were performed at 60 °C. Optimum salinity was established by varying the concentration of NaCl between 0 and 40 g l^{-1}, at 5 g l^{-1} intervals. The pH optimum for strain TB-6^T was determined as previously described (Vetriani et al., 2004). Further experiments were carried out at pH 5.5, 2 % NaCl and 60 °C. Antibiotic sensitivity was tested in liquid cultures containing ampicillin, chloramphenicol or kanamycin (all 100 mg ml^{-1}). All antibiotics were added aseptically before incubation at 60 °C. An ethanol control was performed in parallel to the chloramphenicol resistance tests. The presence of catalase activity was determined by resuspending concentrated cells in 70 ml of a 3 % solution of H_2O_2 at room temperature. The effect of organic substrates on the growth of TB-6^T was tested by adding the following compounds to the medium under a H_2/CO_2 gas phase (80 : 20; 200 kPa): formate, lactate, peptone, tryptone, acetate, (+)-D-glucose, Casamino acids and sucrose (final concentration of each substrate was 2 gl^{-1}). Yeast extract was also tested at concentrations of 0.1 and 1 g l^{-1} . The ability of strain TB-6^T to use alternative electron acceptors in addition to nitrate was investigated by adding thiosulfate (4 mM), sulfite (4.1 mM), arsenate (5 mM), selenate (5 mM), sulfur (3 %, w/v) and oxygen (0.5 %, v/v) to nitrate-depleted media. Genomic DNA was extracted from cells of strain TB-6^T, and

fragments of the 16S rRNA gene (1482 bp) and of the *napA* gene (1150 bp; encoding the periplasmic nitrate reductase) were amplified from the genomic DNA and sequenced as described previously (Vetriani et al., 2004).

Maximum-likelihood phylogenetic trees of the 16S rRNA gene were reconstructed using PhyML (Gouy et al., 2010) with the Jukes and Cantor nucleotide substitution model (Jukes & Cantor, 1969) with 500 bootstrap resamplings. TB-6^T was compared with its closest relatives to calculate the pairwise nucleotide similarity of the 16S rRNA gene using the EzTaxon web-based tool (http://www.ezbiocloud.net/ eztaxon). The phylogenetic tree of the periplasmic nitrate reductase was reconstructed from the amino acid sequence deduced from the napA gene using the maximum-likelihood algorithm with the CpREV substitution model and 500 bootstrap resamplings (**Fig. 2.3**).

The G+C content of the genomic DNA of strain TB-6^T was determined by the Identification Service of the DSMZ (Deutsche Sammlung von Mikroorganismen und Zelkulturen, Braunschweig, Germany) by HPLC analysis of deoxyribonucleosides as described by Mesbah *et al*., 1989. Chemotaxonomic analyses of strain TB-6^T, including cellular fatty acid composition, polar lipids and respiratory quinones, were carried out by the Identification Service of the DSMZ using 200 mg of freeze-dried cells grown to stationary phase under optimal culture conditions. The cellular fatty acids composition of strain TB-6^T was analyzed as the methyl ester derivatives using the Sherlock Microbial Identification System (MIS) (MIDI) and an Agilent model 6890N gas chromatograph (Labrenz et al., 1998). Polar lipids were identified by staining with molybdophosphoric acid to visualize lipids (Tindall, 1990). The polar lipids were classified as phosphatidylethanolamine, phosphatidylglycerol and an unidentified aminolipid.

Lipoquinones of strain TB-6T were identified using TLC followed by HPLC of the eluted products (Tindall, 1990).

Results

The cells of strain TB-6^T were rod-shaped, approximately 1–1.5 mm in length and 0.5 mm in width and appeared to divide by constriction (**Fig. 3.1a**). Platinum-shadowed electron micrographs of planktonic cells showed the presence of single or multiple polar flagella (**Fig. 3.1b**). Cells were Gram-staining negative. The presence of endospores was not observed. Growth was observed at temperatures between 45 and 70 °C, with optimal growth between 55 and 60 °C. No growth was detected at 40 or 75 °C. Growth was observed at NaCl concentrations between 0 and 35 g l^{-1} with optimal growth at 20–30 g l^{-1}. No growth was detected at 40 g l^{-1} . Growth occurred at pH values between pH 4.5 and pH 7.5, with an optimum between pH 5.5 and 6.

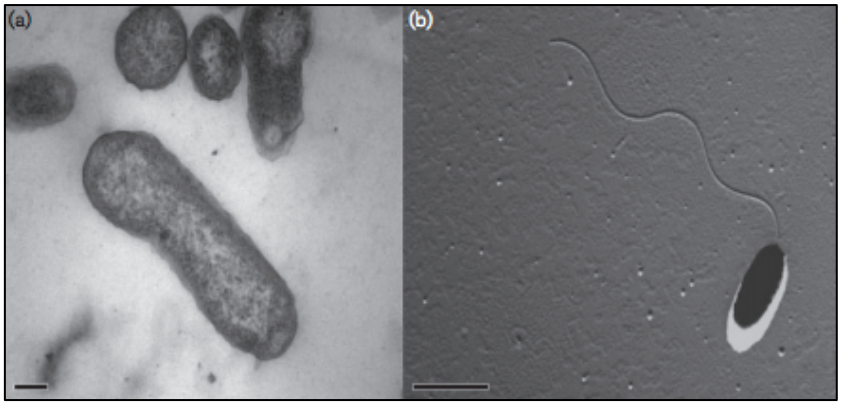

Figure 3.1 (a) Transmission electron micrograph of cells of strain TB-6^T; thin section of cells showing cell morphology. Bar=0.2 mm. (b) Transmission electron micrograph of a platinum-shadowed TB-6^T cell, showing a polar flagellum. Bar=1.0 mm.

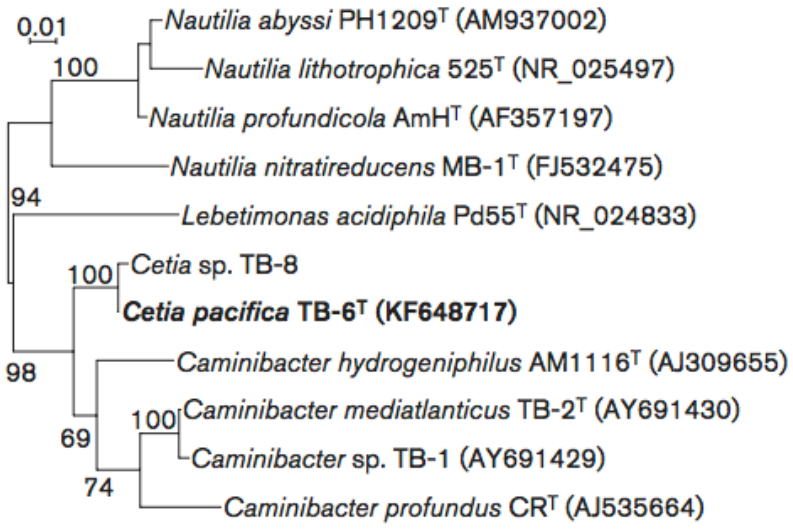

Fig. 3.2 Phylogenetic tree derived from 16S rRNA gene sequences showing the position of TB-6ᵀ within the class Epsilonproteobacteria. The phylogenetic tree was reconstructed using the Maximum-likelihood method. Bootstrap values higher than 50% are based on 500 replicates and are shown at each node. Bar= 0.01 % substitutions.

The generation time of strain TB-6^T under the determined optimal conditions (pH 5.5–6.0, 2–3 % NaCl, 55–60 °C) was 2 h. Strain TB-6^T was resistant to chloramphenicol, while growth was inhibited by kanamycin and ampicillin.

With the addition of hydrogen peroxide, strain TB-6^T formed gas bubbles, indicating catalase activity. Lactate, peptone, tryptone, acetate and yeast extract (1 g l^{-1}) inhibited growth under a H_2/CO_2 (80 : 20; 200 kPa) gas phase. Growth of strain TB-6^T was not affected by (+)-D-glucose, Casamino acids, sucrose and yeast extract (0.1 g l^{-1}). Strain TB-6^T did not grow when each of these compounds was supplemented to the culture medium under a N^2/CO^2 (80 : 20; 200 kPa) or N^2 (100 %; 200 kPa) gas phase,

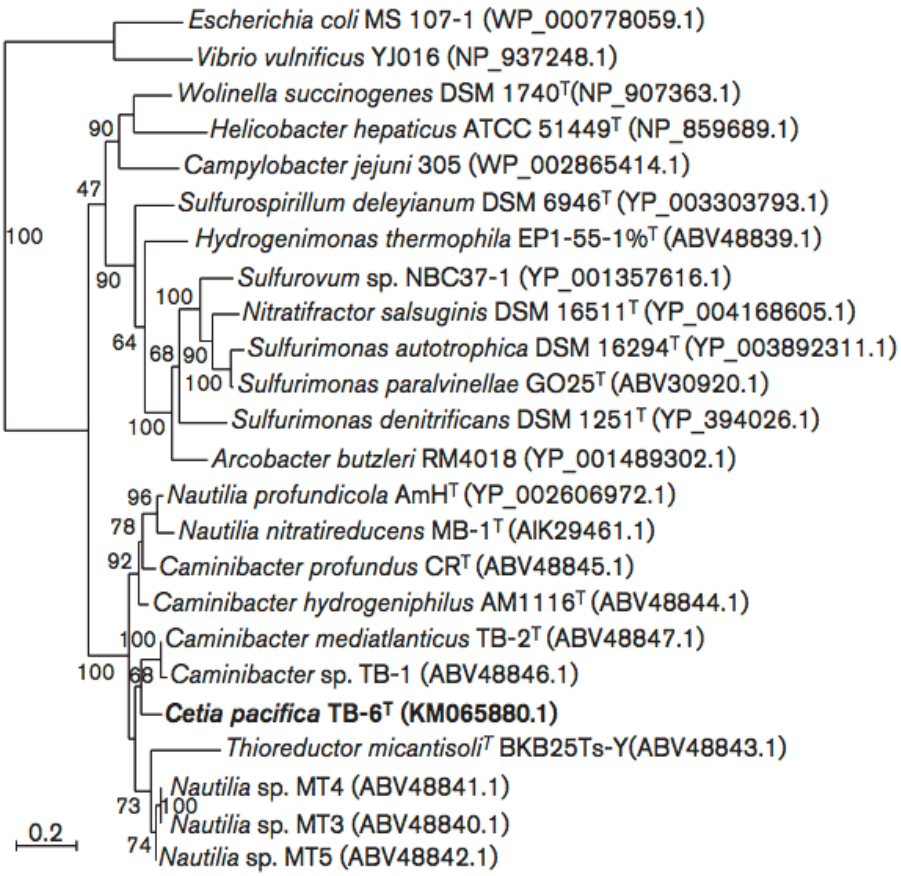

Fig. 3.3 Phylogenetic tree reconstructed from the amino acid sequences derived from a fragment of the *napA* gene (periplasmic nitrate reductase) showing the position of TB-6ᵀ and closely related species using the maximum-likelihood method. Bootstrap values based on 500 resamplings are shown as percentages at branch nodes. Bar = 0.2 % substitutions.

indicating that the organic substrates were not used as electron and/or carbon sources. However, weak growth was supported by formate under a N_2/CO_2 (80 : 20; 200 kPa) atmosphere. Growth only occurred when nitrate or sulfur was available in the growth medium with the concomitant production of ammonium (measured qualitatively by adding 100 ml of Nessler's reagent to 500 ml of culture collected during mid-exponential growth phase) and hydrogen sulfide (measured as described by Vetriani et al., 2004), respectively.

Characteristic	1	2	3	4	5	6	7	8	9
16S rRNA pairwise similarity (%) to strain TB-6^T	100	95.9	95.6	95.1	93.9	93.6	93.4	94.4	92.9
Temperature range for growth (°C)	45–70	50–70	45–70	45–65	33–65	37–68	25–65	30–55	30–68
Optimum temperature for growth (°C)	55–60	60	55	55	60	53	55	40	50
pH range for growth	4.5–7.5	5.0–7.5	4.5–7.5	6.5–7.4	5.0–8.0	6.4–7.4	4.5–8.5	6.0–9.0	4.2–7.0
Optimum pH for growth	5.5–6.0	5.5–6.0	5.5	6.9–7.1	6.0–6.5	6.8–7.0	7.0	7.0	5.2
NaCl concentration range for growth (g l^{-1})	0–35	10–40	10–40	5–50	20–40	8–50	10–35	20–50	6–50
Optimum NaCl concentration for growth (g l^{-1})	20–30	20–25	30	30	30	30	20	30	20
Doubling time under optimal conditions (h)	2.0	1.5	0.83	0.67	2	2.3	0.75	6	2
G+C content of genomic DNA (mol%)	36.8	29±1	25.6	32.1	35	34.7	36.0	33.5	34.0
Origin of isolation	EPR 9° N	EPR 13° N	MAR 36° N	MAR 36° N	EPR 1° N	EPR 13° N	EPR 9° N	EPR 13° N	Mariana Arc
Terminal electron acceptors									
Nitrate	+	+	+	+	−	−	+	+	−
Sulfur	+	+	+	+	+	+	+	+	+
Oxygen	−	ND	−	+	−	−	−	−	−
Selenate	−	ND	−	ND	ND	ND	+	−	−
Thiosulfate	−	−	−	−	−	−	+	−	−
Alternative electron donors to H_2									
Acetate	−	−	−	−	−	−	+	ND	ND
Formate	+	−	−	−	−	+	+	+	−
Yeast extract	−	−	−	−	−	−	+	ND	−
Alternative carbon source to CO_2									
Formate	−	−	−	−	−	+	+	+	−
Complex organic substrate	−	+	−	−	+	−	−	−	−

Table 3.1 Differentiating characteristics of strain TB-6^T and members of the family *Nautiliaceae* Strains: 1, *Cetia pacifica* gen. nov., sp. nov. TB-6^T (data from this study); 2, *Caminibacter hydrogeniphilus* AM1116^T (Alain *et al*., 2002); 3, *Caminibacter mediatlanticus* TB-2^T (Voordeckers *et al*., 2005); 4, *Caminibacter profundus* CR^T (Miroshnichenko *et al*., 2004); 5, *N. abyssi* PH1209^T (Alain *et al*., 2009); 6, *N. lithotrophica* 525^T (Miroshnichenko *et al*., 2002); 7, *N. nitratireducens* MB-1^T (Pérez-Rodríguez *et al*., 2010); 8, *N. profundicola* AmH^T (Smith *et al*., 2008); 9, *L. acidiphila* Pd55^T (Takai *et al*., 2005). EPR, East Pacific Rise; MAR, Mid-Atlantic Ridge; +, positive; 2, negative; ND, not determined.

Maximum-likelihood phylogenetic trees of the 16S rRNA gene, reconstructed using PhyML (Gouy et al., 2010) with the Jukes and Cantor nucleotide substitution model (Jukes & Cantor, 1969) and 500 bootstrap resamplings, indicated that strains TB-6^T and TB-8 were members of the family *Nautiliaceae* within the class Epsilonproteobacteria (**Fig. 3.2**). However, strains TB-6^T and TB-8 formed a lineage distinct from the three genera comprising the family *Nautiliaceae*: *Caminibacter*, *Nautilia* and *Lebetimonas*. The branching topology of strains TB-6^T and TB-8 was supported by a high bootstrap value (98%; **Fig. 3.2**).

When compared with its closest relatives, the pairwise nucleotide similarity of the 16S rRNA gene of strain TB-6^T, calculated using the EzTaxon web-based tool (http://www.ezbiocloud.net/eztaxon), was 95.9 % to *Caminibacter hydrogeniphilus* strain AM1116^T, 95.6 % to *Caminibacter mediatlanticus* strain TB-2^T , 95.1 % to *Caminibacter profundus* strain CR^T and 94.4 % to *N. profundicola* strain AmH^T . These values are within the range (90–96 %) indicative of genus-level differentiation (Gillis et al., 2001). The periplasmic nitrate reductase of strain TB-6^T was placed in a unique lineage distinct from the enzymes from the genera *Nautilia* and *Caminibacter* (**Fig. 3.3**).

The genomic DNA of strain TB-6^T had a 36.8 mol% G+C content, the highest value when compared with any of its closest cultured relatives, including *Caminibacter profundus* (32.1 %) *Caminibacter hydrogeniphilus* (29.1 %), *Caminibacter mediatlanticus* (25.6 %) and *N. profundicola* (33.5 %) (**Table 3.1**). The fatty acid composition of strain TB-6^T, analyzed using the version 6.1 of the MIDI Sherlock MIS software, consisted primarily of $C_{18:1}\omega7c$ (25.1 %), $C_{16:1}\omega7c$ and/or C_{15} iso 2-OH (summed feature 3; 18.04 %), $C_{14:0}$ 3OH and/or $C_{16:1}$ iso I (summed feature 2; 16.61 %),

$C_{16:0}$ (15.3 %), $C_{18:0}$ (14.9 %) and $C_{14:0}$ (4.08 %) (Table S1 available in the online Supplementary Material). In contrast to *N. profundicola* and *L. acidiphila* (Smith et al., 2008; Takai et al., 2005), small amounts of $C_{18:1}$ 2-OH (2.1 %) and $C_{16:1}$ 2-OH (1.1 %) were present in strain TB-6^T . The lipoquinones of strain TB-6^T consisted of menaquinone-7 (MK-7) and methylmenaquinone-7 (MMK-7) at 65 % and 35 % respectively.

Discussion

Strain TB-6^T exhibited several divergent characteristics from its closest relatives, *Caminibacter hydrogeniphilus*, *Caminibacter mediatlanticus* and *Caminibacter profundus*. Both the 16S rRNA gene- and the periplasmic nitrate reductase-based phylogenies placed strain TB-6^T in a separate lineage from the genera *Caminibacter* and *Nautilia*. In addition to genetic distinctions, strain TB-6^T also had the highest mol% DNA G+C content and displayed a unique fatty acid profile. The phylogenetic position of strain TB-6^T and its relatively low 16S rRNA identity with other members of the family *Nautiliaceae*, as well as its chemotaxonomic profile, are indicative of genus-level differentiation. Hence, we propose the name *Cetia* gen. nov. with the type species *Cetia pacifica* sp. nov., type strain TB-6^T .

Description of *Cetia pacifica* sp. nov. *Cetia pacifica* (pa.ci'fi.ca. L. fem. adj. *pacifica* peaceful, referring to the Pacific Ocean, indicating the type strain's origin of isolation). General morphological and chemotaxonomic characteristics are as given above for the genus. Growth occurs between 45 and 70 °C, 0 and 35 g NaCl l^{-1} and pH 4.5 and 7.5.

Under optimal growth conditions (55–60 °C, 20–30 g NaCl l^{-1} and pH 5.5–6.0) the generation time is 2 h. Growth occurs in the presence of CO_2 and hydrogen, which is oxidized with nitrate or elemental sulfur. This results in the formation of ammonium and hydrogen sulfide, respectively. No chemo-organotrophic growth occurs in the presence of acetate, (+)-D-glucose, Casamino acids, sucrose or yeast extract. The following are not utilized as electron acceptors: oxygen, arsenate, selenate, thiosulfate and sulfite. Under a H_2/CO_2 gas phase, growth is inhibited by lactate, peptone and tryptone. Resistant to chloramphenicol, sensitive to kanamycin and ampicillin. The type strain is *Cetia pacifica* TB-6^T (=DSM 27783^T =JCM 19563^T), isolated from chimney fragments sampled from an active deep-sea hydrothermal vent on the East Pacific Rise at Bio 99 site (9° 49’ N 104° 17’ W). The genomic DNA G+C content of the type strain is 36.8 mol%.

Chapter 4

Pangenomic Analysis of the *Nautiliaceae*: Links Between Vent Ecology and Metabolic Strategies Derived from the Genome of *Cetia pacifica* and Epsilonproteobacterial Relatives

Introduction

The Epsilonproteobacteria are an ecologically significant group at deep-sea hydrothermal vents and represent a basal radiation within the 16S rRNA gene-based phylogeny of the Proteobacteria. The class branches into two orders, the Campylobacterales, whose cultured representatives include the clinically significant pathogens, *Helicobacter* and *Campylobacter*, and the order Nautiliales, a small thermophilic group unique to hydrothermal vent environments. The *Nautiliaceae*, is the sole family within the order Nautiliales, is composed of four validly-described genera: *Nautilia* (Miroshnichenko *et al.*, 2002), *Caminibacter* (Alain *et al.*, 2002), *Lebetimonas* (Takai *et al.*, 2005), and *Cetia* (Grosche *et al.*, 2015). Although *Nautiliaceae* are endemic to deep-sea hydrothermal vents, they exhibit a global biogeography (**Fig. 4.1**) and representative cultures have been isolated from the East Pacific Rise (EPR), the Mid-Atlantic Ridge (MAR), the Mid-Okinawa Trough (MOT), and the Mariana Arc (MA). The *Nautiliaceae* are often detected in low abundance, in association with colonization devices placed in areas of high temperature (> 40°C) and sulfide (Nakagawa *et al.*, 2014). Frequent detection in newly formed biofilms incubated in areas of diffuse flow active venting suggests that, although the *Nautiliaceae* represent a small portion of the overall community, they may play a significant role as part of the pioneer colonizing species

during the early stages of microbial colonization of new vent sites.

Physiologic studies of the *Nautiliaceae* have revealed that they display a phenotypic redundancy within the family, including thermophily, anaerobiosis, and chemolithoautotrophy, with the shared capacity for hydrogen oxidation and sulfur and/or nitrate reduction. 16S rRNA gene phylogeny of the *Nautiliaceae* shows a topology of equidistant branching and low sequence similarity of the 16S rRNA gene between genera, which has hinted at the possibility for greater genotypic divergence than the observed phenotypic similarities in physiology and metabolism.

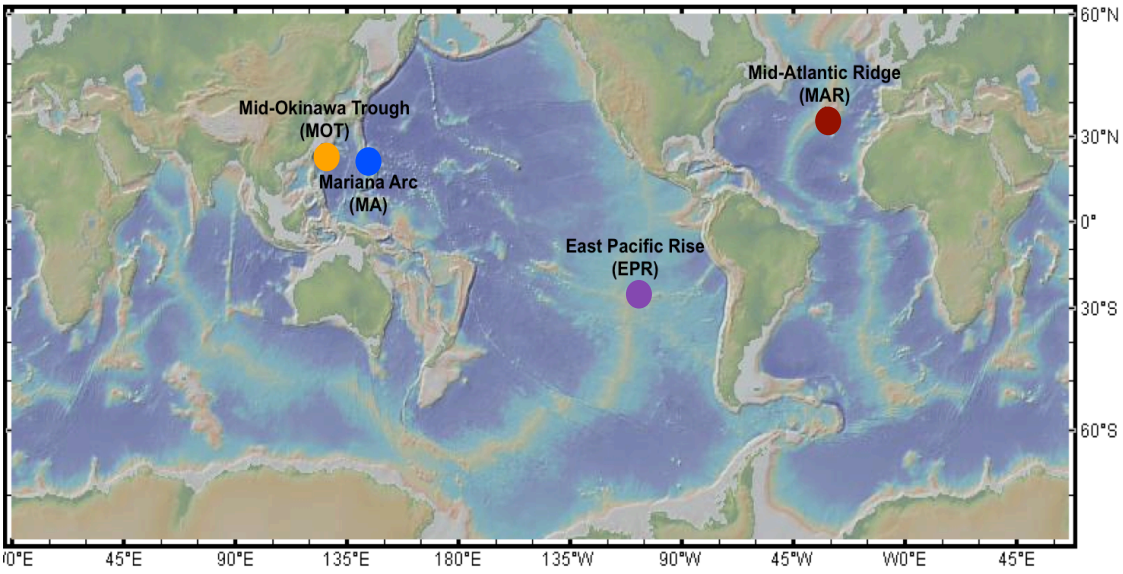

Fig. 4.1 The biogeography of *Nautiliaceae* members *Cetia pacifica*, *Caminibacter* spp., *Nautilia* spp., and *Lebetimonas* spp.

This study evaluates the core metabolism conserved within the *Nautiliaceae* and identifies intergenus accessory genes to determine if the phenotypic redundancy is also reflected at the genomic level, or alternatively, if intergenomic disparities indicative of underlying differential metabolic capabilities exist.

Materials and Methods

Bacterial Isolates

Microbial biomass was obtained from *Cetia pacifica* TB-6, *Caminibacter* sp. TB-1, and *Nautilia* sp. PV-1 through cultivation using modified SME medium (Vetriani *et al.*, 2004) and incubation under growth conditions as outlined in previous literature (Grosche *et al.*, 2015) overnight at 55°C. Cells were harvested after 24 hours of growth and DNA was extracted immediately using the phenol chloroform method described by Grosche *et al*. (2018). DNA concentration was quantified fluorometrically using the Invitrogen QuBit Fluorometer 2.0 and the Qubit dsDNA HS Assay Kit (Invitrogen Q32854). DNA was cleaned using the magnetic bead purification kit AMPure XP (Beckman Coulter A63880). In addition, the genome sequence of nine members of the *Nautiliaceae* were downloaded from the NCBI database for comparative analyses.

Genomic Library Preparation, Sequencing, and Assembly

Genome sequencing was performed by MicrobesNG (Birmingham, UK) as outlined (https://microbesng.uk/microbesng-faq/). In brief, libraries were sequenced on the Illumina MiSeq using 2x250 bp paired-end protocol. Reads were trimmed using Trimmomatic v0.36 (Bolger *et al.*, 2014) and quality checked using custom scripts and Samtools (Li *et al.*, 2009b), BedTools (Quinlan *et al.*, 2010), and BWA mem (Li *et al.*, 2009a). Kraken (Wood *et al.*, 2014) was used to identify the closest reference genome, and reads were mapped using BWA mem. *De novo* assembly of reads was performed using SPAdes (Bankevich *et al.*, 2012) and a secondary mapping step was performed using BWA mem. Variant calling was performed using VarScan (Koboldt *et al.*, 2009),

whole genome alignment using MUMmer (Delcher *et al.*, 1999), and automated annotation using Prokka (Seemann, 2014). Assembly metrics were calculated using QUAST (Gurevich *et al.*, 2013), and genome completeness was estimated using CheckM (Parks *et al.*, 2015).

Gap Closing of Draft Genomes

The draft genomes of *Cetia pacifica* TB-6, and *Nautilia* sp. PV-1 were closed using the MinIon Sequencing platform (Oxford Nanopore Technologies). Per sample, libraries were prepared using approximately 400 ng of high molecular weight DNA and the Rapid Barcoding Kit (Oxford Nanopore Technologies SQK-RBK004) and loaded into the flow cell (Oxford Nanopore Technologies FLO-MIN106) for sequencing. Samples were run on the MinIon Sequencing Device for 20-48hrs depending on estimated genome size and completeness. Base calling was performed using Albacore v2.0.2 and hybrid assembly using MinIon-generated long reads and Illumina-generated contigs was performed using Unicycler v0.4.4 (Wick *et al.*, 2017).

Genome Annotation and Analysis

The 12 genomes used for the comparative analyses were deposited in Genbank, re-annotated for private use using the RAST Annotation Pipeline (Tatusova *et al.*, 2016), and are also publically available in the NCBI Assembly database. Pairwise synteny was calculated using SyMAP v4.2 (Soderlund *et al.*, 2006) according to default settings.

CRISPRS, Prophages, and Genomics Islands

Clustered regularly interspaced short palindromic repeats (CRISPRS) were identified using CRISPRFinder (Grissa *et al.*, 2007) and compared between genomes using CRISPRcompar (Grissa *et al.*, 2008), and putative prophages were identified using PHAST and PHASTER (Arndt *et al.*, 2016; Zhou *et al.*, 2011). IslandViewer (Langille *et al.*, 2009) was used to identify genomic islands.

Average Nucleotide Analysis

To determine genome similarity between genera, Average Nucleotide Identity (ANI) was calculated. The best hits (one-way ANI) and the reciprocal best hits (two-way ANI) were considered (Rodriguez-R *et al.*, 2016).

Analysis of plasmid DNA

The presence of a single circular plasmid was resolved using Unicycler assembly (Wick *et al.*, 2017). The plasmid was evaluated using Resfinder 3.0 (Zankari *et al.*, 2012) , CARD (Jia *et al.*, 2016), and ARG-ANNOT (Gupta *et al.*, 2014) for the detection of antibiotic-resistance genes, and pathogenicity predictor PathogenFinder 1.1 (Cosentino *et al.*, 2013), and BacMet (Pal *et al.*, 2013) for identification of biocide and metal-resistance genes. The plasmid was visualized using SnapGene Viewer.

Results & Discussion

Genome features

The general genomic features of the *Nautiliaceae* are summarized in **Table 4.1**. The genome of *Cetia pacifica* is closed and contains a singular chromosome of 1.78 Mbp,

and a 92,229 bp plasmid (29.7 G+C (mol%)). The genome is constructed from 6 scaffolds of 903,785 bp, 786,133 bp, 83,706bp, 5,188 bp, 4,419 bp, and 3,174 bp. lengths. Whole genome pairwise nucleotide analysis showed clustering of *C. pacifica* with *Lebetimonas natsushimae*, which grouped separately from all other *Lebetimonas* species. All of the genomes are between 98-100% completeness as estimated by CheckM. The G+C contents of genomes are all above 26% (26.7-34.3%). The predicted coding DNA sequences (CDS) range from 1712 to 1989bp. The central metabolism of the *Nautiliaceae* was reconstructed (**Fig 4.2**).

Features	*Cetia pacifica*	*Caminibacter mediatlanticus*	*Caminibacter sp.*	*Nautilia profundicola*	*Nautilia sp.*	*Lebetimonas natsushimae*	*Lebetimonas sp.*	*Lebetimonas sp.*	*Lebetimonas sp.*	*Lebetimonas sp.*	*Lebetimonas sp.*	*Lebetimonas sp.*
Strain	**TB-6**	**TB-2**	**TB-1**	**AmH**	**PV-1**	**HS1857**	**JH292**	**JH369**	**JS032**	**JS085**	**JS138**	**JS170**
DSM number	27783	16658	n/a	18972	n/a	104102	n/a	n/a	n/a	n/a	n/a	n/a
Genome size (Mbp)	1.78	1.56	1.69	1.56	1.79	1.64	1.64	1.74	1.7	1.74	1.68	1.74
G+C (%)	34.3	26.7	26.7	33.6	34.6	30.4	31	31	31	31	32	31
Total genes	1872	1740	1767	1727	1849	1712	1955	1989	1913	1929	1882	1914
CRISPR counts	5	0	8	0	0	2	0	0	0	0	0	0
Estimated completeness (%)	100	98.67	98.78	98.17	100	99.59	98.58	98.98	98.39	98.58	99.19	99.39

Table 4.1 General genome features of the *Nautiliaceae* family members

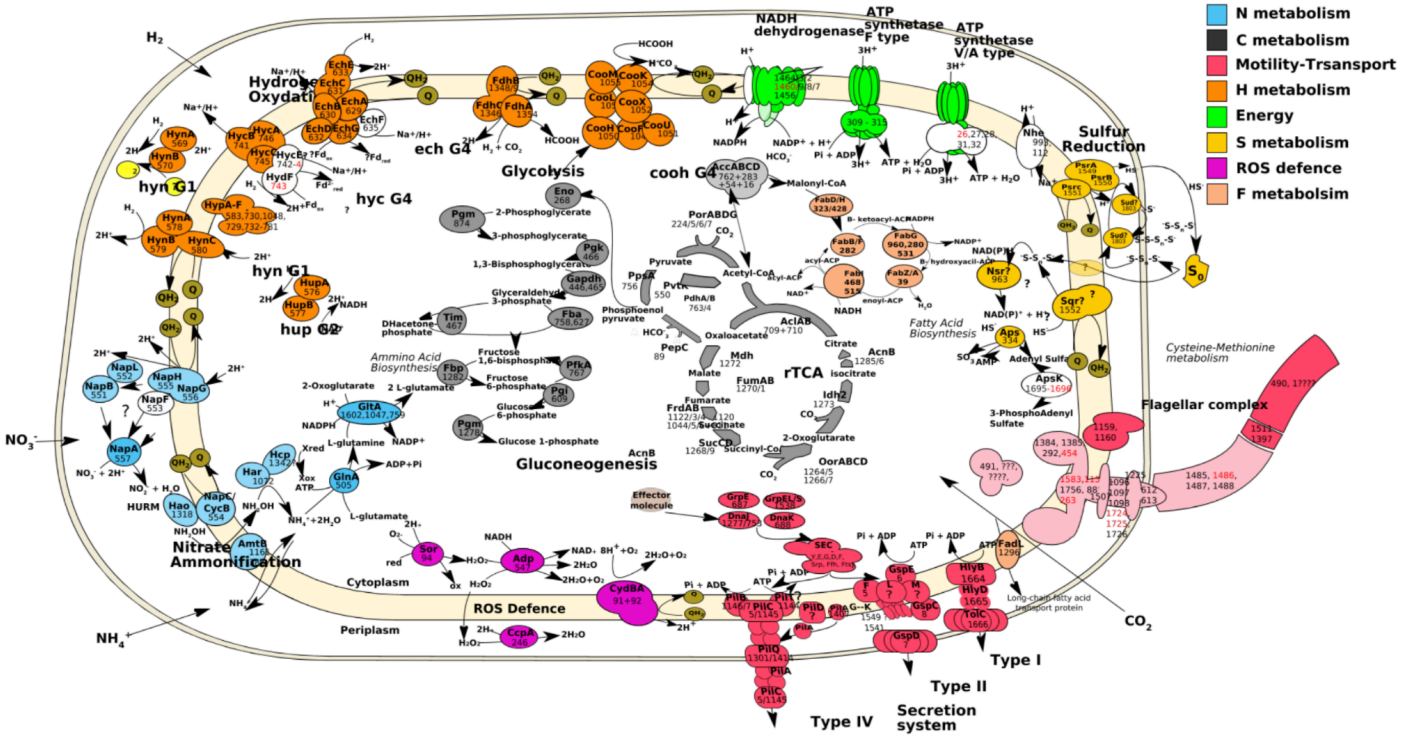

Fig. 4.2 The reconstruction of the central metabolism of *Cetia pacifica* and *Nautiliaceae* members

Whole Genome Nucleotide Analyses

The topology of 16S rRNA single-copy genes is shared with clustered whole-genome pairwise similarity, with the exception of the placement of *Lebetimonas natsushimae*, which clusters with *Cetia pacifica*, separate from the clade of all other *Lebetimonas* species. Whole-genome pairwise analysis shows intergenus similarity of *Cetia* to all other genera as most similar to *Nautilia* spp. (79-80%) with 78% sequence similarity to *Caminibacter* spp. and 77-78% sequence similarity to *Lebetimonas* spp. (**Table 4.2**). Intragenus similarity of each genus is 99% among the *Caminibacter* species, 96-99% among the *Nautilia* species, and 96-99% among the *Lebetimonas* species, except for *Lebetimonas natsushimae*, which has a considerably lower sequence similarity of 81% to other species and may be indicative of allopatric speciation within the genus.

	Lebetimonas natsushimae HS1857	*Cetia pacifica* TB-6	*Nautilia* sp. PV-1	*Nautilia profundicola* AmH	*Caminibacter mediatlanticus* TB-2	*Caminibacter* sp. TB-1	*Lebetimonas* sp. JS170	*Lebetimonas* sp. JS085	*Lebetimonas* sp. JS032	*Lebetimonas* sp. JS138	*Lebetimonas* sp. JH369	*Lebetimonas* sp. JH292
Lebetimonas natsushimae HS1857	100	78	77	77	79	78	81	81	81	81	81	81
Cetia pacifica TB-6	78	100	79	80	78	78	77	77	77	78	78	78
Nautilia sp. PV-1	77	79	100	84	76	77	78	78	78	78	78	78
Nautilia profundicola AmH	77	80	84	100	77	77	77	77	77	77	77	77
Caminibacter mediatlanticus TB-2	79	78	76	77	100	99	77	77	77	77	77	77
Caminibacter sp. TB-1	78	78	77	77	99	100	78	78	78	78	78	78
Lebetimonas sp. JS170	81	77	78	77	77	78	100	100	99	99	99	96
Lebetimonas sp. JS085	81	77	78	77	77	78	100	100	99	99	99	96
Lebetimonas sp. JS032	81	77	78	77	77	78	99	99	100	98	98	96
Lebetimonas sp. JS138	81	78	78	77	77	78	99	99	98	100	99	96
Lebetimonas sp. JH369	81	78	78	77	77	78	99	99	98	99	100	96
Lebetimonas sp. JH292	81	78	78	77	77	78	96	96	96	96	96	100

Table 4.2 Average nucleotide identity pairwise comparison of the available genomes of *Nautiliaceae* family members. The species are organized in phylogenetic order. 95% sequence similarity is indicative of species-level differentiation while 70% sequence similarity is indicative of genus-level differentiation.

Carbon Fixation

The genome of *Cetia pacifica* encodes for a complete reductive TCA cycle, which is the predominant carbon fixation pathway at deep-sea hydrothermal vents (Campbell *et al.*, 2004). Enzymes specific to the reductive cycle include the ATP-citrate (pro-S)-lyase (*aclAB*, 2-oxoglutarate synthase, and fumarate reductase (*frd*). The synthesis of 2-oxoglutarate appears to be from succinyl-CoA rather than via citrate. *Cetia* uses the gluconeogenesis pathway to synthesize pentose and hexose monosaccharides. We identified in the genome the key genes of this pathway including fructose-1,6-biphosphatase (*fbp*) and all other genes necessary for the functioning of the pathway.

Hydrogen oxidation

C. pacifica and other members of the *Nautiliaceae* gain electrons via hydrogen oxidation, and possess multiple hydrogenases including Ni-Fe hydrogenase (*hypABCDEF*,), group I Ni-Fe-hydrogenases (*hyd*), group 2 Ni-Fe-hydrogenases (*hup*), group 4 Ni-Fe hydrogenases (*hyc*) in an operon associated with a formate dehydrogenase (*fdh*), as noted in a previous comparison of *Lebetimonas* genomes, group 4 Ni-Fe hydrogenases (*coo*), group 4 Ni-Fe hydrogenases (*ech*) and an Fe-Fe hydrogenase. Since many *Nautiliaceae* rely solely on hydrogen oxidation to conserve energy, the diverse suite of hydrogenases many enable metabolic viability under a range of hydrogen concentrations in the environment.

Sulfur Reduction

Cultured members of the *Nautiliaceae* can conserve energy by reducing elemental sulfur to hydrogen sulfide (Nakagawa *et al.*, 2014). The *Cetia pacifica* genome was found

to encode the polysulfide reductase (*psrA*), and putative subunits B and C. The polysulfide reductase is an integral transmembrane protein that is thought to shuttle protons between the quinone pool and the reduction site of polysulfide, and consists of the three subunits encoded by the *psrABC* operon. Originally identified in *Wolinella succinogenes*, it was shown to couple the reduction of polysulfide with the oxidation of hydrogen or formate (Krafft *et al.*, 1995). Sequence homology to the *Wolinella* PsrA is 41%.

Sulfide quinone oxidoreductase (*sqr*) encodes a flavoprotein that has been shown to oxidize sulfide ions (S_2^-, HS^-) to zero-valent sulfur in sulfide-oxidizing bacteria. Two copies of sulfide quinone oxidoreductase are annotated in the *Cetia* genome. The duplicate copy of the *sqr* is also found in both *Caminibacter* species and *Nautilia* sp. PV-1. No copies of *sqr* were found in *Nautilia profundicola*, and all *Lebetimonas* strains analyzed contain a single copy of the gene. Multiple copies of *sqr* have been previously detected in *Caminibacter mediatlanticus*, *Nitratiruptor*, *Sulfurimonas*, and *Sulfurovum* species (Meyer *et al.*, 2014). While the role of *sqr* is not clear in strict anaerobes like *C. pacifica*, this enzyme may have a role in hydrogen sulfide detoxification (Jelen et al., 2018).

Nitrate Reduction

Cetia pacifica and *Nautiliaceae* isolates have been shown to reduce nitrate to ammonium via dissimilatory nitrate reduction in pure-culture analyses, and many isolates have shown favorable growth under nitrate-reducing conditions relative to elemental sulfur (Grosche *et al.*, 2015). Frequent detection in many of the epsilonproteobacterial

genomes and *in situ* expression of the periplasmic nitrate reductase (*napA*) in Epsilonproteobacteria-dominated biofilms is evidence that nitrate respiration is widespread at deep-sea hydrothermal vents (Vetriani *et al.*, 2014; Waite *et al.*, 2017).

Oxidative Stress Tolerance

Cytochrome b ubiquinol oxidase subunits I and II (*cydAB*) are annotated in all of the *Nautiliaceae* genomes. Co-localized on many of the genomes is an inner-membrane bound hypothetical protein that could be the third cytochrome ("cytochrome x") in the cytochrome bd complex, which catalyzes the conversion of dioxygen to water (Giuffrè *et al.*, 2014). Cytochrome bd oxidase is widespread among pathogens and is thought to promote virulence through the scavenging of oxidative and nitrosative species prevalent during host immune response to infection. This adaptation may be useful at deep-sea hydrothermal vents, where the constant mixing of reduced vent fluids with oxidized compounds in seawater generates reactive oxygen and reactive sulfur species. Additional oxidative detoxification mechanisms annotated include a bcp-type thiol peroxidase (*bcp*), tpx-type thiol peroxidase (*tpx*), Alkyl hydroperoxide reductase subunit C (*ahpC*), superoxide reductase (*sor*), and peptide methionine sulfoxide reductase (*msrAB*), a repair enzyme for proteins that have been inactivated by oxidation.

Detoxification and Adaptations to Adverse Environmental Conditions

Cetia pacifica encodes for a lead, cadmium, zinc and mercury transporting/copper-translocating P-type ATPase, multiple cobalt-zinc-cadmium resistance proteins, a periplasmic divalent cation tolerance protein involved in copper

homeostasis (*cutA*), and arsenate reductase (*arsAB*), which may confer resistance to aresenite and antimonite. The *dnaK* gene cluster (*dnaK-grpE-dnaJ-clpB*) is encoded for by the genome of *Cetia pacifica* and is conserved within the family, which may reflect an advantageous adaptation to extreme heat flux under venting conditions. The dnaK system is a group of chaperones that regulate protein folding and aggregation throughout the cells by physically shielding the exposed hydrophobic surfaces of protein transitioning from their native conformation, and may be particularly advantageous in an environment characterized by fluctuating exposure to heat stress (Calloni *et al.*, 2012). The *Nautiliaceae* also encode for a DNA reverse gyrase, which in *Lebetimonas* species is fragmented into topoisomerase and helicase domains (*rgy*) (Meyer *et al.*, 2014). The reverse gyrase is a hyperthermophilic enzyme that can introduce positive supercoiling in substrate DNA at the expense of ATP-hydrolysis (Forterre, 2002; Kikuchi *et al.*, 1984). The enzyme has only been documented in thermophilic and hyperthermophilic microorganisms and is thought to aid in preventing aggregation of denatured DNA regions and promote correct annealing, an adaptation which would be useful in turbulent environments such as deep-sea vents, where organisms experience transient exposure to geothermally-heated fluids.

Transporters

The genome of *Cetia pacifica* encodes for ABC transporters for branched-chain amino acid transport (*livFGHM*), magnesium and cobalt transporter proteins (*corA*), and a TRAP-type uncharacterized system. TRAP-type C4-dicarboxylate transport systems have been characterized in other systems to enable the uptake of C4-dicarboxylates such

as succinate, fumarate, and malate (Janausch *et al.*, 2002), zinc chelation protein (*ychJK*), and phospholipid-lipopolysaccharide ABC transporter. The phosphate ABC transport system (*pstABCS*), phosphate regulatory proteins (*phoU*), phosphate starvation-inducible proteins (*phoH*), and a probable low-affinity phosphate transporter were annotated in a gene cluster with a two-component system histidine kinase response regulator, which may be a beneficial adaptation during phosphorous limitation. Components for the twin-arginine transport pathway were also identified (*tatABC*).

Motility and Sensing

Environmental sensing and motility are ecologically advantageous, especially at deep-sea vents, which are characterized by rapidly fluctuating gradients imposed by local fluid chemistry and venting dynamics. *Cetia* encodes for the chemotaxis-regulating system (*cheAYV*W) and multiple aerotaxis genes. Among deep-sea vent isolates cultured in the laboratory, *Cetia* was observed to be among the most sensitive strains to oxygen. The multiple genes encoding for aerotaxis proteins, and motile lifestyle could enable *Cetia* to position itself to minimize its exposure to oxygenated areas at deep-sea vents.

Pathogenesis-related functions

The *Cetia pacifica* genome codes for genes related to pseudaminic acid synthesis (*pglE*). Pseudaminic acid, an isomer of legionaminic acid, has been detected in epsilonproteobacterial and gammaproteobacterial pathogens bacteria including *Helicobacter*, *Campylobacter*, and *Legionella* in the assembly of flagellin proteins (Schoenhofen *et al.*, 2006). Of the genes involved for protein glycosylation pathway, the

Nautiliaceae members encode for *pglE*, which has been shown to be essential for colonization of the gastrointestinal tract during *Campylobacter* invasion, during which proteins have been shown to be secreted through the flagellar complex into the host system. Additionally, *Cetia* encodes for the *Campylobacter* invasion protein (*ciaB*), another enzyme required for successful host colonization. The CiaB is highly conserved among the *Nautiliaceae* and other Epsilonproteobacteria members, and may be part of a widespread mechanical adaptation for the colonization of host substrates, from the human gut to the outside of a deep-sea tubeworm.

Genetic Recombination

The *Nautiliaceae* encode for a highly-conserved recombination protein (*recR*) shown in other bacterial systems to play a critical role in homologous recombination (Rocha *et al.*, 2005). *Cetia* encodes for RuvABC complex and transcription factor YebC responsible for processing recombination intermediates during genetic recombination and recombination repair, and competence proteins, which if functional, would enable the uptake of exogenous DNA for genetic recombination.

Plasmid Analysis

Cetia pacifica encodes a single putative plasmid of 92,229 bp (29.7 G+C (mol%)) (**Fig. 4.2**). Although an origin of replication could not be identified, genes encoding for plasmid partitioning were found (*parAB*). The functional annotation of the putative plasmid resulted in mostly hypothetical proteins, although annotations were assigned for a DotL-like protein, which has been shown in previous studies to be part of the Dot/Icm

system involved in conjugative plasmid mobilization (Buscher *et al.*, 2005), and a zeta toxin protein domain. Zeta toxin is thought to be part of an toxin-antitoxin system to select for plasmid inheritance through post-segregational termination of cells that have lost the plasmid (Meinhart *et al.*, 2003). Additional plasmid-encoded proteins include a type IV pilus assembly ATPase (*pilB*) shown to promote bacteriophage infection, virulence, and natural transformation (Berry *et al.*, 2014), DNA double-strand break repair Rad50, single-stranded DNA exonuclease RecJ, single-stranded DNA binding protein, DNA topoisomerase III, and multiple integrase/recombinases. Plasmid-encoded multidrug efflux pumps were identified but shared <40% sequence similarity and <30 bit score with database proteins, so function could not be inferred. Multidrug efflux pumps have are linked with in the intrinsic and acquired antibiotic resistance of bacterial pathogens, and have been shown to be involved in detoxification of intracellular metabolites, bacterial virulence, cell homeostasis and intercellular signal trafficking (Li *et al.*, 2016).

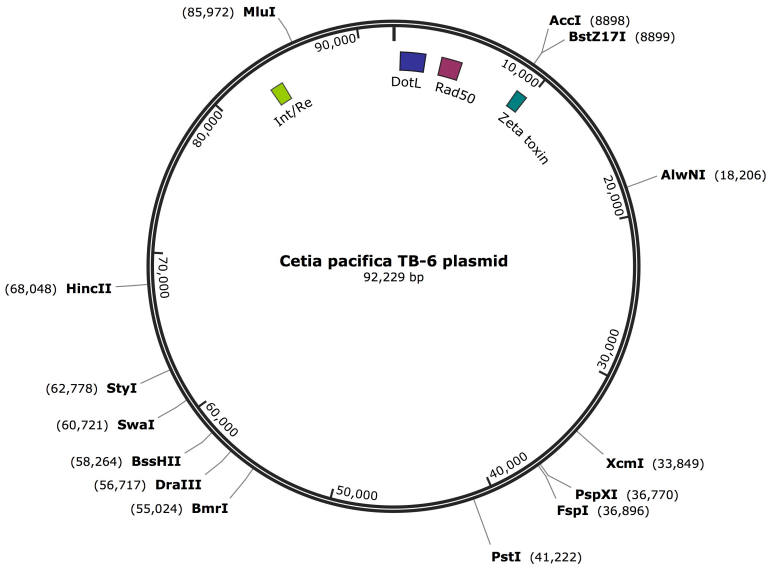

Fig. 4.3 Plasmid of *Cetia pacifica*

CRISPR-Cas System and Putative Phage Signatures

The *Nautiliaceae* genera *Cetia*, *Caminibacter*, and *Lebetimonas* encode for a type-I CRISPR-Cas system. This is composed of a CRISPR repeat RNA endoribonuclease Cas6 for pre-crRNA processing, Cas5h for crRNA and target binding, Cas3 for target cleavage, and, Cas2 and/or Cas4 for spacer insertion and regulation (**Fig 4.7**). Five CRISPR spacers were identified in the genome of *Cetia pacifica*, eight were identified in the genome of *Caminibacte*r sp. TB-1, and two were identified in the genome of *Lebetimonas natsushimae* (**Table 4.1**). Sequences between genera showed low similarity and evidence for cross infection could not be supported, although as previous studies have reported, a conserved spacer was identified in several *Lebetimonas* strains. A

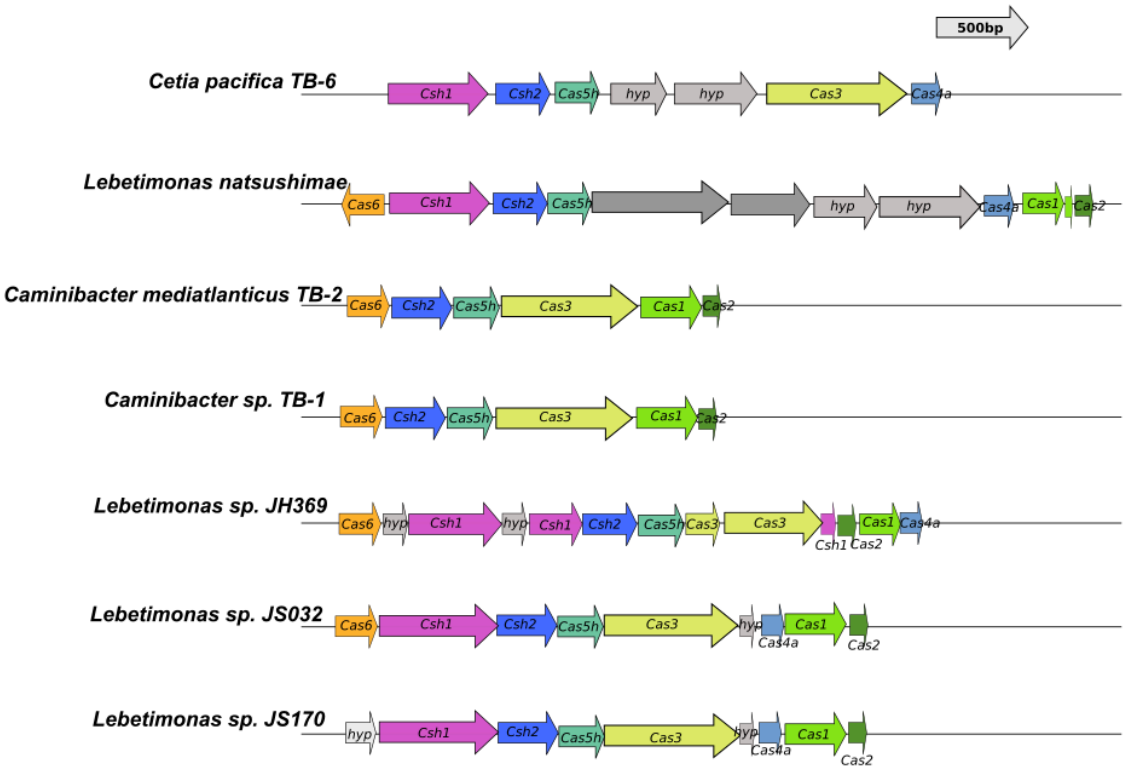

Fig. 4.4 Synteny of the Cas proteins found in the *Nautiliaceae* members

highly-conserved (76-83% sequence similarity) putative phage repressor protein was annotated in all of the *Nautiliaceae* genomes. Phage repressor proteins have been shown to serve as transcriptional repressors that enable bacteriophages to establish and maintain latency within the host cell (Paul, 2008). The ubiquity and high sequence homology within the *Nautiliaceae* family suggests a lysogeny-hosted lifestyle with host-specific infections. One incomplete prophage was annotated in *Cetia pacifica* (8 proteins), and an intact prophage was annotated in *Nautilia* PV-1 (37 proteins). Proteins for the ramp complex were also annotated in *Cetia pacifica* (Cmr23456*)*.

Alginate biosynthesis

Cetia pacifica and *Caminibacter* spp. encode for a putative alginate biosynthesis pathway including GDP-mannose 6-dehydrogenase (*algD*) and poly beta-D-mannuronate C5 epimerase precursor (*algG*) for the synthesis of the two uronic acid building blocks, alginate biosynthesis proteins (*alg8*) and (*alg44*), outer membrane protein (*algE*), and alginate lyase (*algL*), an enzyme required for the both the synthesis and breakdown of alginate which is hypothesized to be mechanistically necessary to break out of biofilms containing alginate (Wong *et al.*, 2000) (**Fig 4.3**). AlgK, AlgX, AlgI, AlgJ and AlgF were not annotated perhaps due to low homology with known *Pseudomonas* and *Azotobacter* proteins. The same gene cluster was annotated in the genome of deep-sea epsilonproteobacterium *Nitratiruptor* sp. SB155-2 during a characterization study that verified the functional activity of the annotated alginate lyase (Inoue *et al.*, 2016).

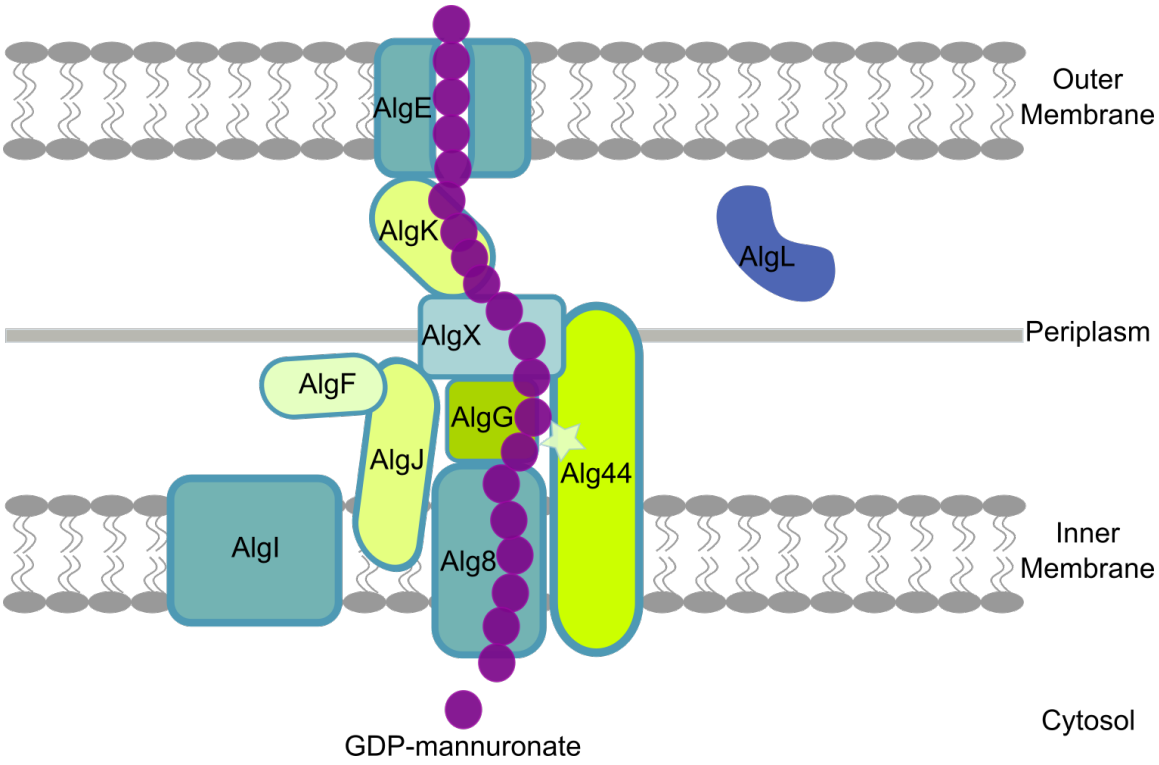

Fig. 4.5 Proposed model of the putative multi-enzyme complex involved in alginate polymerization, modification and export. The star represents the effector molecule bis-(3-5)-cyclic dimeric guanosine monophosphate (c-di-GMP)

Alginate biosynthesis and secretion has proven to act as a protective barrier against host immune defenses and antibiotic activity. *Pseudomonas aeruginosa* infections within cystic fibrosis patients are exacerbated by the overproduction of alginate in the host lungs (Maleki *et al.*, 2016). Treatment efforts for cystic fibrosis have led to clinical interest in the bacterial mechanism behind alginate production. Alginates are synthesized by brown seaweeds, and the only bacteria known to produce alginate are *Pseudomonas* and *Azotobacter* species.

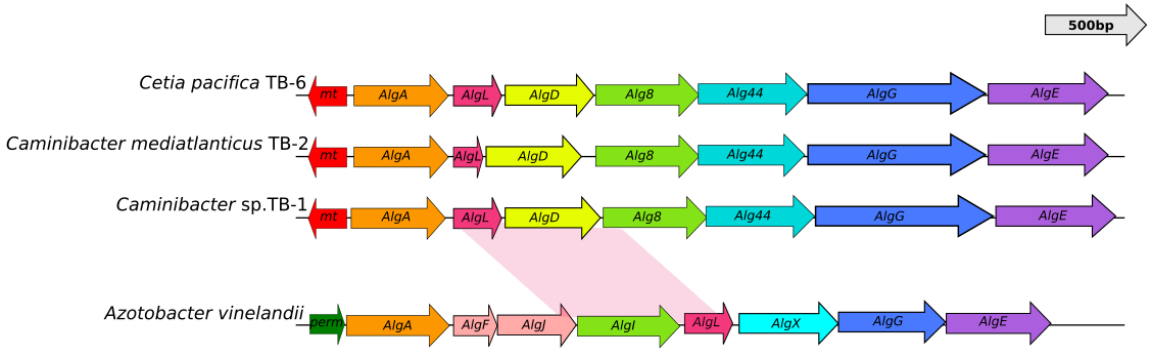

Fig. 4.6 Synteny of the putative alginate biosynthesis gene cluster between *Nautiliaceae* members and verified alginate-producing bacterium *Azotobacter vinelandii*.

While genes involved in alginate anabolism were only detected in *Cetia* and *Caminibacter* species, alginate lyase was found in ten of the twelve genomes, which suggests that alginate production and degradation are relevant metabolic strategies at deep-sea vents perhaps likely to enhance adherence to surfaces near venting fluids and to shield from adverse conditions typical of deep-sea hydrothermal vents. Further testing is needed to determine if the alginate biosynthesis pathway is functional, which could represent a new reservoir of heat-stable alginate for commercial and clinical interests.

Chapter 5

Conclusions and Future Work

This body of work began with the goal to broaden the knowledge of microbial ecology at deep-sea hydrothermal vents. Deep-sea hydrothermal vent communities are part of a productive, highly dynamic, extreme ecosystem. Their very existence is intimately linked to microbial activity, from the early conditioning of post-eruptive vent sites to the long-established symbiosis of gut microbiota in the trophosome of a tubeworm. Because microorganisms interact at a systems-level in many aspects of deep-sea vent life, the assessment of microbial diversity and distribution should also be evaluated as a whole system as well, and this includes the association of microbes with vent macrofauna. Chapter two of this thesis uses this approach to evaluate microbial biogeography across a broad range of biogeochemical conditions classified according to the multidimensional concept of "bioregime". This study is novel in that 1) it provided a comprehensive, systematic survey of diversity across varying conditions to paint a broad picture of diversity, and 2) RNA was used as the starting material for the survey, to identify representatives of the actively transcribing members of the community. Together, this allowed for the reconstruction of metabolically relevant microbial distribution and abundance across a mosaic of habitats that together form the deep-sea vent landscape.

Sulfurovum and *Sulfurimonas* are widespread Epsilonproteobacteria at deep-sea vents, and are detected frequently in microbial colonization devices. This study determined that there are specific taxa of both groups unique to newly-formed and mature biofilms, which may reflect different metabolic capabilities better suited for early or late stages of colonization. *Sulfurovum* species were thought to be the predominant pioneer

colonizing species in microbial biofilms, but results from this study show that under elevated venting conditions, *Sulfurimonas* clades predominate instead. Evidence for *Sulfurovum* and *Sulfurimonas* was found in the metatranscriptomic data for both ribosomal and functional transcripts, which further cements their ecological significance as active, abundant players at deep-sea vents. Investigation into the metabolic versatility of both genera is sorely needed to further resolve their ecological role in the vent environment.

The characterization of vent isolates is fundamental to understanding the metabolism and physiology of microorganisms through culture-dependent laboratory-based studies that test for phenotypes that may be expressed under *in situ* conditions. Additionally, remote accessibility and cultivation difficulty are major factors in the underrepresentation of deep-sea vent microorganisms currently in culture. Therefore, in order to widen our breadth of knowledge in regards to microbial activity at hydrothermal vents, we must continue culturing efforts and physiology studies of deep-sea vent microorganisms. The second chapter of this thesis contributes to this with the characterization of a novel isolate from the East Pacific Rise, Epsilonproteobacteria *Cetia pacifica* strain TB-6. *Cetia* is a member of the *Nautiliaceae*, an ecologically relevant family of thermophilic, chemoautotrophic, and sometimes, chemoorganotrophic bacteria exclusively found at deep-sea hydrothermal vents. Although detected in low abundance in diffuse flow vents, the *Nautiliaceae* are consistently found in biofilm samples and in higher abundance with high temperature habitats (*e.g.*, the walls of actively venting polymetallic sulfides), and it is proposed that they may play a role as pioneer colonization during biofilm formation. *Cetia* and several *Nautilia* species show the ability to oxidize

formate to sustain growth. Recent studies have noted the ubiquity of formate dehydrogenase within the Epsilonproteobacteria and it appears that formate metabolism is relatively widespread in the predominant taxa at deep-sea vents. Further investigation is warranted to constrain the diversity, distribution, and ecology of formate-utilizing bacteria in an investigation of alternative C1 metabolism that may predominate at deep-sea hydrothermal vents.

The addition of organic carbon often shows adverse effects on pure-culture studies of the *Nautiliaceae*. *Cetia* was inhibited by the amendment of several different organics to the growth medium. This inhibition by organics is a common phenomenon among many deep-sea vent autotrophs, and begs the question of why. Future studies may benefit from analyzing the relationship between the addition of organics and the detection of intracellular signaling for growth suspension, which may play a role in successional colonization patterns at deep-sea vents.

The physiology of hydrothermal vent isolates tested in the laboratory is often selected for during the primary enrichment of the organisms (*e.g.,* hydrogen-oxidizers are selected by supplementing culture medium with H_2 gas), and can lead to a dogmatic view of microbial metabolism. Genomic data can provide a starting point for formulation of hypotheses regarding the metabolism and physiology of microorganisms. Chapter four of this thesis compares the genome of *Cetia pacifica* with eleven other members of the *Nautiliaceae* to reconstruct the core metabolic features of the group, and also to determine unique, accessory genes indicative of adaptive metabolic capacities. Through this analysis, several core functions conserved to most members of the *Nautiliaceae* were found, including a suite of hydrogenase genes, conserved mechanisms for motility, and

the presence of a plasmid (of many unknown functions) in *Cetia pacifica*. Evidence for biosynthesis of alginate, a thick, heat-stable polymer often associated with the phenotype of chronic infections of *Pseudomonas*, was found in the genomes of *Cetia pacifica* and *Caminibacter* species. Also common in brown algae, this pathway has been identified and experimentally verified in only two other bacterial genera, *Pseudomonas* and *Azotobacter*. If the cellular machinery is functional, alginate biosynthesis could provide a tremendous benefit for the long-term adhesion to surfaces experiencing fluid sheer, and a competitive advantage during reversion to the planktonic lifestyle relative to species lacking the enzymes for alginate decomposition. Future studies are needed to verify functionality of the pathway in vent isolates and detect alginate in their biofilm matrix.

Appendix 1

Carbon cycling at deep-sea hydrothermal vents: investigating the microbial bottleneck of carbon fixation by species predominating chemosynthetic biofilms.

Introduction

It is estimated that hydrothermal vent communities supply up to 25% of carbon to the benthic zone of the ocean, and the global contribution of chemosynthetic primary production at deep sea vents is projected to be 10^{13}g biomass per year, approximately 0.02% of primary production in the ocean (McCollom *et al.*, 1997). Primary production at deep-sea hydrothermal vent sites is reliant on the conversion of CO_2 into microbial biomass via chemosynthesis, a process that is often performed by microbial consortia bound in biofilms that coat the vent edifices. While the amount of chemical energy potentially available for autotrophic metabolism has been studied, direct measurements of carbon content in microbial biofilms have not been performed. Additionally, the rates of carbon fixation within chemoautotrophic communities, retention time bound in biofilms, and export into the water column are components of the deep-sea carbon cycle that not been examined.

Methods

The availability of organic carbon at deep-sea vents is largely constrained by the bottleneck of fixation by chemolithoautotrophic organisms. CO_2 fixation experiments were performed as previously described (Wirsen *et al.*, 2002). In short, to estimate the rate of carbon fixation in such chemosynthetic communities, representatives from dominant taxa found in chemosynthetic biofilms were grown under optimal conditions

and spiked with $NaH^{14}CO_3$ during mid-exponential growth. Culture density and radioactivity were measured over time to determine the rate of carbon incorporation into biomass. Aliquots from several time points during exponential growth were analyzed using a scintillation counter to quantify radiation per cell, which in conjunction with cell counts, allowed for the determination of CO_2 fixed per cell over time. Each representative was selected according to its environmental relevance, its capability to fix carbon dioxide, and its thermal optimum for growth (temperature niche).

Members of the *Desulfurobacteriaceae* (phylum *Aquificae*) constitute a significant portion of the microbial community at deep-sea vents (~2% in samples > 40°C, Vetriani *et al*., unpublished data, but likely higher in high temperature habitats). These microbes are key players in the rapid conversion of carbon dioxide, most often coupled to hydrogen oxidation . *Thermovibrio ammonificans* and *Phorcysia thermohydrogeniphila* (*Desulfurobacteriaceae*) are characterized isolates used to represent the extremely thermophilic subset of biofilm constituents with ~75°C growth optima (Perez-Rodriguez *et al.*, 2012; Vetriani *et al.*, 2004). Previous studies found that uncultured *Nautiliaceae* species constitute 29% of a biofilm sample experiencing moderately hot temperatures (~50°C). *Caminibacter mediatlanticus* (Voordeckers *et al*., 2005) was used as a thermophilic representative of this group (55°C optimum growth temperature). *Sulfurimonas* and *Sulfurovum* species dominate newly-formed biofilms experiencing sulfidic conditions at deep-sea and shallow water hydrothermal vents, and can account for most of the microbial population in these environments. *Sulfurimonas paralvinellae* (Takai *et al.*, 2006), and *Sulfurovum riftiae* (Giovannelli et al, 2016) two Epsilonproteobacteria isolated from deep-sea hydrothermal vents, were used as

representatives of this group (30°C optimum growth temperature). *Arcobacter* species constitute 4-13% of the microbial population in newly-formed biofilms, however, carbon fixation rates for Candidatus *Arcobacter sulfidicus* have been previously determined (Wirsen *et al.*, 2002) and were used for comparative purposes for this study. The peak rate of carbon fixation was determined to be 0.077nmol of C ml^{-1} min^{-1} (**Fig A1.1**).

Results and Discussion

Fixation rates measured in pure-cultures were comparable to *in situ* measurements in a vent microbial community carried out by a collaborating lab (**Table A1.1**). A pattern of higher fixation rates was observed in thermophilic species (**Fig. A1.2**). However, further experimentation including additional isolates is needed.

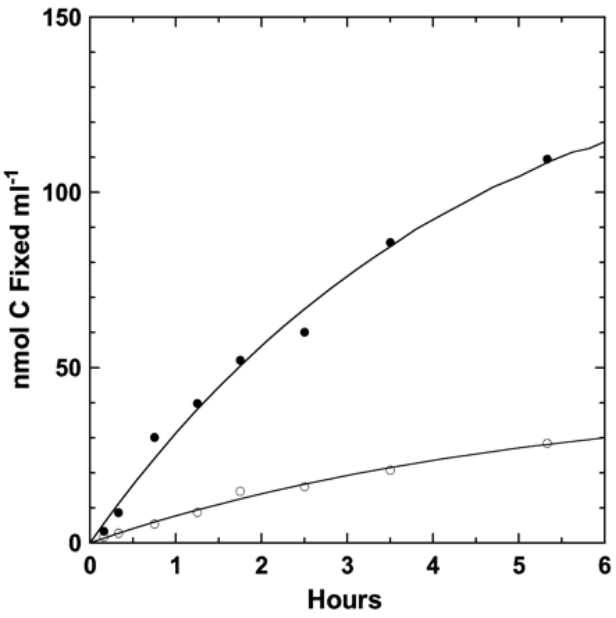

Fig A1.1 Carbon dioxide fixation by Candidatus *Arcobacter sulfidicus*. Reactor-grown filaments with associated cells were compared with filament-free seawater obtained from the reactor and containing cells dissociated from the filamentous matrix (Wirsen *et al.*, 2002).

Cellular Carbon Production	
Organism	**mM C/m3/day**
Thermovibrio ammonificans	3.02
Phorcysia thermohydrogeniphila	5.69
Caminibacter mediatlanticus	8.2
In situ measurement (NanoSIMS)	>0-10
In situ measurement (C-IRMS)	>0-15

Table A1.1 Rates of cellular carbon fixation by vent isolates (determined in this study) and *in situ* rates measured by a collaborating laboratory (unpublished)

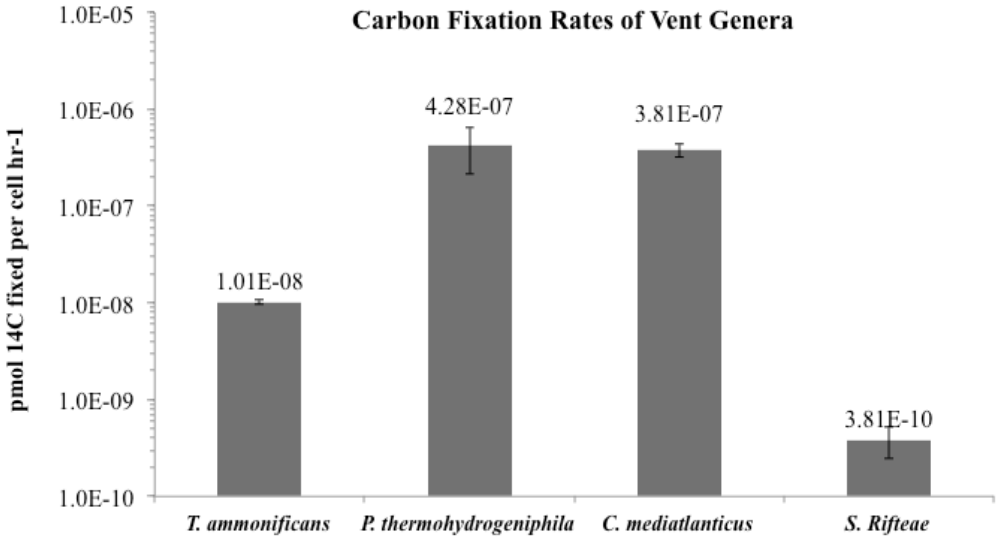

Fig. A1.2 Rates of carbon fixation of vent genera *Thermovibrio ammonificans*, *Phorcysia thermohydrogeniphila*, *Caminibacter mediatlanticus*, and *Sulfurovum riftiae*

Appendix 2

ROS Detoxification in Pure-Culture and Environmental Biofilms:

Production of Reactive Oxygen Species at Deep-Sea Geothermal Environments

Biofilms formed in extreme environments offer protection from environmental perturbations, among the most harmful of these being oxidative stress. Oxidative stress is a ubiquitous process that stems from the formation of reactive oxygen species (ROS). These species are generated by the incomplete reduction of oxygen, and the auto-oxidation of thiols and flavins (Scandalios, 2002). Reactive oxygen species include singlet oxygen, superoxide radicals (O_2^-), hydrogen peroxide (H_2O_2), and hydroxyl radicals ($HO\cdot$). These species can damage membrane lipids, induce peptide bond breaks, depolymerize nucleic acids, and oxidize sulfhydryl groups, polysaccharide molecules, and polyunsaturated fatty acids (Brioukhanov *et al.*, 2007). Each radical can be characterized by its potential for cellular damage. The potency of superoxides lies in their

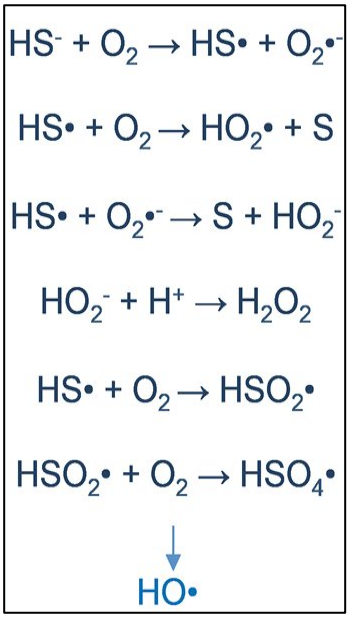

Fig. A2.1 Chemical reactions describing the formation of reactive species

ability to readily diffuse across the membrane at a slow rate, as well as their capability of spontaneous disproportionation, resulting in the formation of hydrogen peroxide and singlet oxygen (Brioukhanov *et al.*, 2007). Hydrogen peroxide is characterized by considerable diffusion capacity due to its uncharged state (Rocha *et al.*, 1996). Once inside the cell, Fenton chemistry evolves, and hydrogen peroxide reacts with transition metals, resulting in the formation of hydroxyl radicals (Peskin *et al.*, 2000). Among the reactive species, the hydroxyl radical has the highest potential for biological damage owing to its reactivity and indiscretion when attacking components of the cell in a diffusion-controlled manner (Lesser, 2006). Each reactive oxygen species has the potential to retard cellular mechanisms, and exposure may result in cell death.

Strictly anaerobic microbes at deep-sea hydrothermal vents are regularly exposed to reactive oxygen species, which are present in high abundance in areas of fluid-seawater mixing. Generation occurs when hydrogen sulfide emitted in the vent fluid reacts with oxygen in the seawater to create oxygen- and sulfur- centered radicals (**Fig A2.1**). Sulfide oxidation produces O_2^-, which can be subsequently dismutated, leading to the production of hydrogen peroxide (Lesser, 2006). There is also evidence that, although disequilibrium exists between hydrogen, oxygen and water present at the oxic-anoxic interface of mixing zones, hydrogen oxidation is inhibited as temperature decreases. This leads to the accumulation of excess hydrogen in solution, which promotes a metastable hydrogen peroxide intermediate in the redox reaction producing water (Foustoukos *et al.*, 2011).

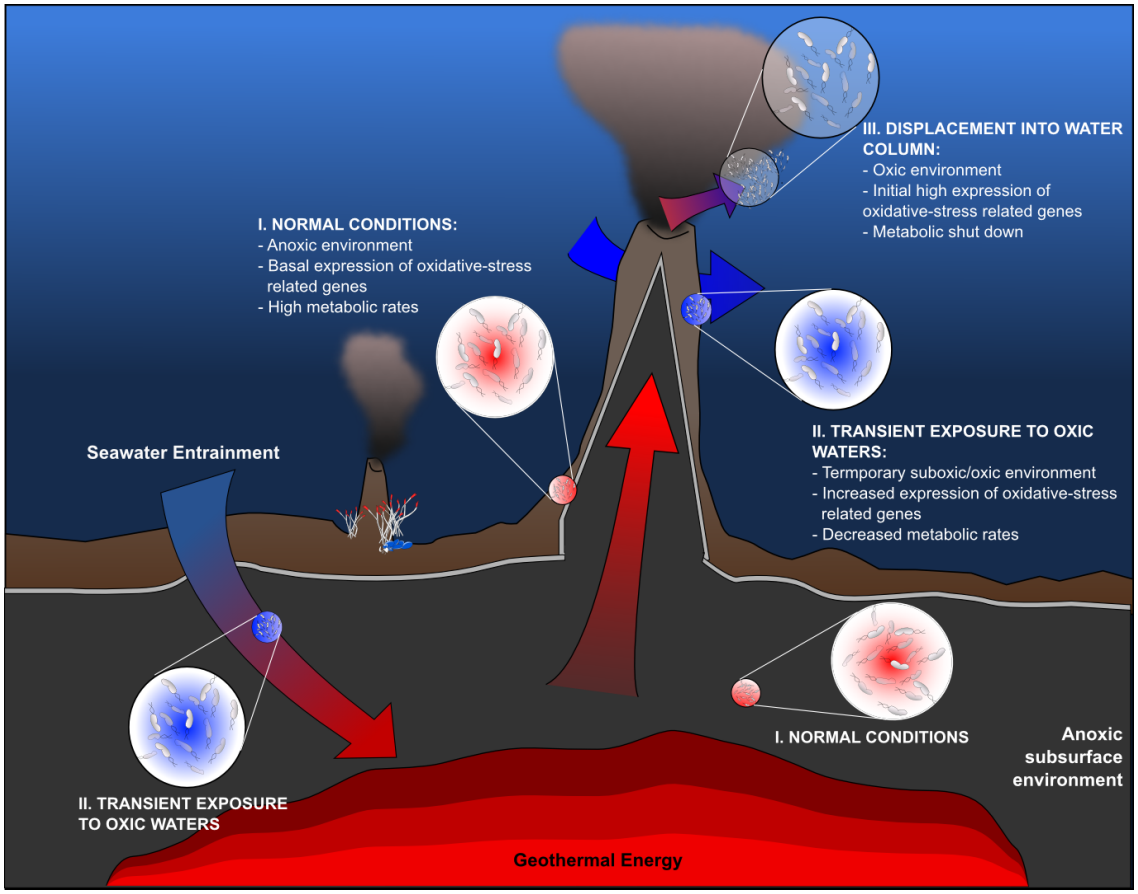

Fig. A2.2. Diagram of a deep-sea hydrothermal vent ecosystem outlining the predicted physiologic state of microbes during (I) normal conditions, (II) transient exposure to seawater, and (III) long-term displacement into the water column (Figure courtesy of Dr. Donato Giovannelli)

This process occurs in the plumes, as well as in the subsurface surrounding the vent site, which functions as a conduit of exchange for fluids, temperature flux, chemical species, and biological materials. Microbial populations experience an influx of nutrients and oxidized chemical species from the seawater, while they are also exposed to reduced compounds and elevated temperature from diffuse-flow fluids (**Fig. A2.2**). At the plume emission field and hydrothermal subsurface, the microbial community must rely on adaptive mechanisms such as conversion to a sessile lifestyle to avoid exposure to radicals.

Results and Discussion

During exposure to oxygen in the atmosphere, *Thermovibrio ammonificans* appeared to generate bubbles over time (~25min) at the gas-liquid interface, as seen in the photograph (**Fig. A2.3**) Cell viability after exposure to ROS was variable, but a consistent pattern of decreased viability was observed in assays performed > 4°C (**Fig. A2.4**). Transcripts for catalase, peroxidase, and superoxide reductase were detected in RNA

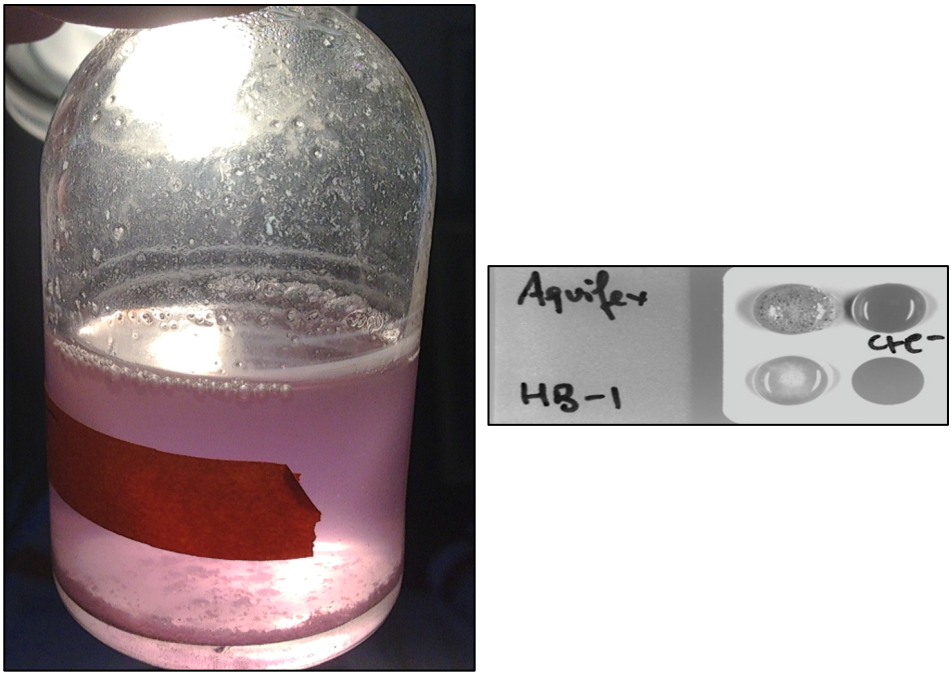

Fig. A2.3 Gas production by *Thermovibrio ammonificans* strain HB-1 after exposure to dioxygen in the atmosphere (left) and weak production of gas after the addition of hydrogen peroxide to cell pellets (right).

extracted after exposure at all three temperature regimes, which could be a result of transcript expression at high-temperature and preservation at low temperature or constitutive expression. Catalase activity tested on crude cell extracts showed a weak pattern of increased expression under mesophilic growth conditions (~25-45°C) with high variability between experimental replicates (**Fig A2.5**).

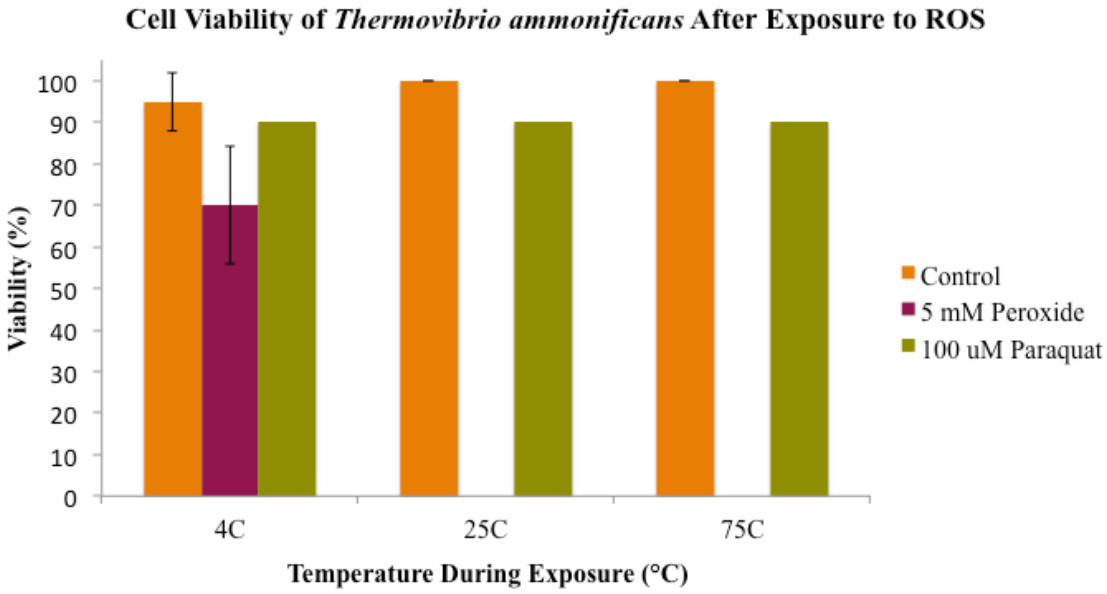

Fig. A2.4 Cell viability of *Thermovibrio ammonificans* after exposure to ROS at 4°C, 25°C, and 75°C

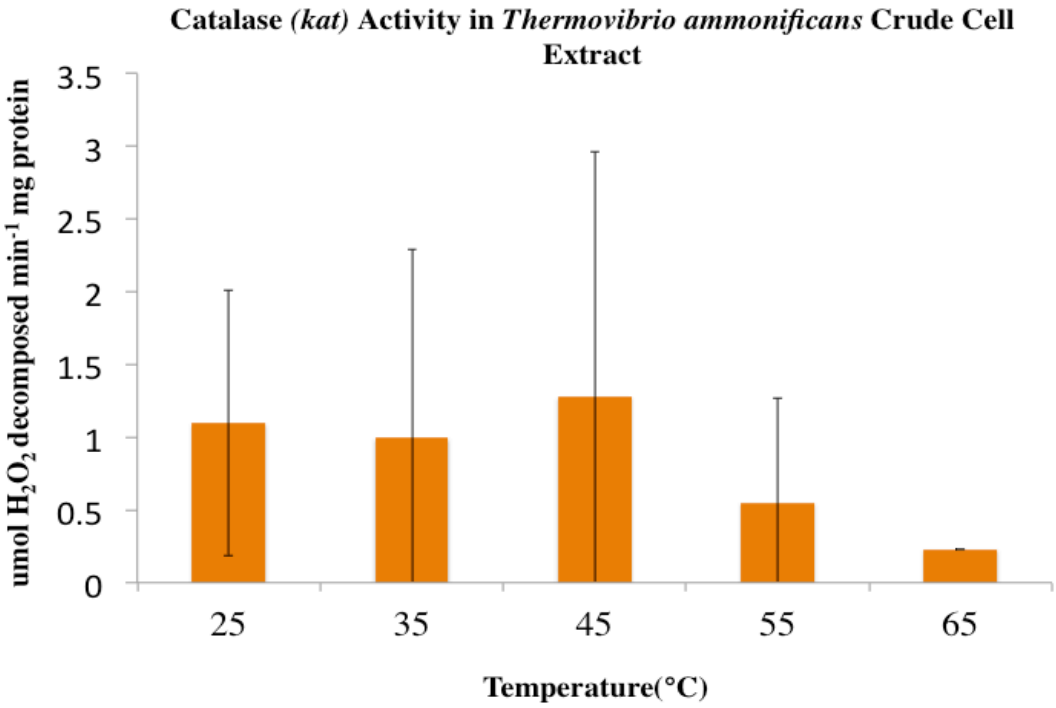

Fig. A2.5 Catalase (*kat*) activity detected in crude cell extracts from *Thermovibrio ammonificans*

References

Alain, K., Querellou, J., Lesongeur, F., Pignet, P., Crassous, P., Raguénès, G., Cueff, V., and Cambon-Bonavita, M. (2002). *Caminibacter hydrogeniphilus* gen. nov., sp. nov., a novel thermophilic, hydrogen-oxidizing bacterium isolated from an East Pacific Rise hydrothermal vent. International journal of systematic and evolutionary microbiology *52*, 1317-1323.

Alain, K., Zbinden, M., Le Bris, N., Lesongeur, F., Quérellou, J., Gaill, F., and Cambon‐Bonavita, M.A. (2004). Early steps in microbial colonization processes at deep‐sea hydrothermal vents. Environmental microbiology *6*, 227-241.

Altschul, S.F., Gish, W., Miller, W., Myers, E.W., and Lipman, D.J. (1990). Basic local alignment search tool. Journal of molecular biology *215*, 403-410.

Anantharaman, K., Breier, J.A., Sheik, C.S., and Dick, G.J. (2013). Evidence for hydrogen oxidation and metabolic plasticity in widespread deep-sea sulfur-oxidizing bacteria. Proceedings of the National Academy of Sciences *110*, 330-335.

Arndt, D., Grant, J., Marcu, A., Sajed, T., Pon, A., Liang, Y., and Wishart, D. (2016). PHASTER: a better, faster version of the PHAST phage search tool. Nucleic acids research *44*, W16-W21.

Assié, A., Borowski, C., van der Heijden, K., Raggi, L., Geier, B., Leisch, N., Schimak, M.P., Dubilier, N., and Petersen, J.M. (2016). A specific and widespread association between deep‐sea *Bathymodiolus* mussels and a novel family of Epsilonproteobacteria. Environmental microbiology reports *8*, 805-813.

Bankevich, A., Nurk, S., Antipov, D., Gurevich, A.A., Dvorkin, M., Kulikov, A.S., Lesin, V.M., Nikolenko, S.I., Pham, S., and Prjibelski, A.D. (2012). SPAdes: a new genome assembly algorithm and its applications to single-cell sequencing. Journal of computational biology *19*, 455-477.

Beaulieu, S. (2010). InterRidge global database of active submarine hydrothermal vent fields: prepared for InterRidge, Version 2.0. Interridge.

Berry, J.-L., and Pelicic, V. (2014). Exceptionally widespread nanomachines composed of type IV pilins: the prokaryotic Swiss Army knives. FEMS microbiology reviews *39*, 134-154.

Bolger, A., Lohse, M., and Usadel, B. (2014). Trimmomatic: a flexible trimmer for Illumina sequence data. Bioinformatics *30*, 2114-2120.

Brioukhanov, A.L., and Netrusov, A.I. (2007). Aerotolerance of strictly anaerobic microorganisms and factors of defense against oxidative stress: a review. Applied Biochemistry and Microbiology *43*, 567-582.

Buscher, B.A., Conover, G.M., Miller, J.L., Vogel, S.A., Meyers, S.N., Isberg, R.R., and Vogel, J.P. (2005). The DotL protein, a member of the TraG-coupling protein family, is essential for viability of *Legionella pneumophila* strain Lp02. Journal of bacteriology *187*, 2927-2938.

Calloni, G., Chen, T., Schermann, S.M., Chang, H.-c., Genevaux, P., Agostini, F., Tartaglia, G.G., Hayer-Hartl, M., and Hartl, F.U. (2012). DnaK functions as a central hub in the *E. coli* chaperone network. Cell reports *1*, 251-264.

Campbell, B.J., and Cary, S.C. (2001). Characterization of a novel spirochete associated with the hydrothermal vent polychaete annelid, *Alvinella pompejana*. Applied and environmental microbiology *67*, 110-117.

Campbell, B.J., and Cary, S.C. (2004). Abundance of reverse tricarboxylic acid cycle genes in free-living microorganisms at deep-sea hydrothermal vents. Applied and environmental microbiology *70*, 6282-6289.

Campbell, B.J., Engel, A.S., Porter, M.L., and Takai, K. (2006). The versatile epsilonproteobacteria: key players in sulphidic habitats. Nature Reviews Microbiology *4*, 458-468.

Campbell, B.J., Stein, J.L., and Cary, S.C. (2003). Evidence of chemolithoautotrophy in the bacterial community associated with *Alvinella pompejana*, a hydrothermal vent polychaete. Applied and environmental microbiology *69*, 5070-5078.

Caporaso, J.G., Kuczynski, J., Stombaugh, J., Bittinger, K., Bushman, F.D., Costello, E.K., Fierer, N., Pena, A.G., Goodrich, J.K., and Gordon, J.I. (2010). QIIME allows analysis of high-throughput community sequencing data. Nature methods *7*, 335-336.

Caporaso, J.G., Lauber, C.L., Walters, W.A., Berg-Lyons, D., Lozupone, C.A., Turnbaugh, P.J., Fierer, N., and Knight, R. (2011). Global patterns of 16S rRNA diversity at a depth of millions of sequences per sample. Proceedings of the National Academy of Sciences *108*, 4516-4522.

Cary, S.C., Cottrell, M.T., Stein, J.L., Camacho, F., and Desbruyeres, D. (1997). Molecular identification and localization of filamentous symbiotic bacteria associated with the hydrothermal vent annelid *Alvinella pompejana*. Applied and environmental microbiology *63*, 1124-1130.

Cavanaugh, C.M., Gardiner, S.L., Jones, M.L., Jannasch, H.W., and Waterbury, J.B. (1981). Prokaryotic cells in the hydrothermal vent tube worm *Riftia pachyptila* Jones: possible chemoautotrophic symbionts. Science *213*, 340-342.

Chao, A. (1984). Nonparametric estimation of the number of classes in a population. Scandinavian Journal of Statistics *11*, 265-270.

Chao, A., and Yang, M.C.K. (1993). Stopping rules and estimation for recapture debugging with unequal failure rates. Biometrika *80*, 193-201.

Childress, J.J., and Fisher, C.R. (1992). The biology of hydrothermal vent animals: physiology, biochemistry, and autotrophic symbioses. Oceanogr Mar Biol Annu Rev *30*, 337-441.

Clarke, K.R. (1993). Non-parametric multivariate analyses of changes in community structure. Australian Journal of Ecology *18*, 117-143.

Contreira-Pereira, L., Yücel, M., Omanovic, D., Brulport, J.-P., and Le Bris, N. (2013). Compact autonomous voltammetric sensor for sulfide monitoring in deep sea vent habitats. Deep Sea Research Part I: Oceanographic Research Papers *80*, 47-57.

Cosentino, S., Larsen, M.V., Aarestrup, F.M., and Lund, O. (2013). PathogenFinder-distinguishing friend from foe using bacterial whole genome sequence data. PloS one *8*, e77302.

Delcher, A.L., Kasif, S., Fleischmann, R.D., Peterson, J., White, O., and Salzberg, S.L. (1999). Alignment of whole genomes. Nucleic acids research *27*, 2369-2376.

Demšar, J., Curk, T., Erjavec, A., Gorup, Č., Hočevar, T., Milutinovič, M., Možina, M., Polajnar, M., Toplak, M., and Starič, A. (2013). Orange: data mining toolbox in Python. The Journal of Machine Learning Research *14*, 2349-2353.

Desbruyères, D., Chevaldonné, P., Alayse, A.M., Jollivet, D., Lallier, F.H., Jouin-Toulmond, C., Zal, F., Sarradin, P.M., Cosson, R., and Caprais, J.C. (1998). Biology and ecology of the "Pompeii worm"(*Alvinella pompejana* Desbruyères and Laubier), a normal dweller of an extreme deep-sea environment: a synthesis of current knowledge and recent developments. Deep Sea Research Part II: Topical Studies in Oceanography *45*, 383-422.

Dick, G.J., Anantharaman, K., Baker, B.J., Li, M., Reed, D.C., and Sheik, C.S. (2013). The microbiology of deep-sea hydrothermal vent plumes: ecological and biogeographic linkages to seafloor and water column habitats. Front Microbiol *4*, 124.

Distel, D.L., Lane, D.J., Olsen, G.J., Giovannoni, S.J., Pace, B., Pace, N.R., Stahl, D.A., and Felbeck, H. (1988). Sulfur-oxidizing bacterial endosymbionts: analysis of phylogeny and specificity by 16S rRNA sequences. Journal of Bacteriology *170*, 2506-2510.

Felbeck, H. (1981). Chemoautotrophic potential of the hydrothermal vent tube worm, *Riftia pachyptila* Jones (Vestimentifera). Science *213*, 336-338.

Fisher, C.R., Takai, K., and Le Bris, N. (2007). Hydrothermal vent ecosystems. Oceanography *20*, 14-23.

Forterre, P. (2002). A hot story from comparative genomics: reverse gyrase is the only hyperthermophile-specific protein. Trends in Genetics *18*, 236-237.

Foustoukos, D.I., Houghton, J.L., Seyfried Jr, W.E., Sievert, S.M., and Cody, G.D. (2011). Kinetics of H2–O2–H2O redox equilibria and formation of metastable H2O2

under low temperature hydrothermal conditions. Geochimica et Cosmochimica Acta *75*, 1594-1607.

Fox, E., Kuo, J., Tilling, L., and Ulrich, C. (1994). User's manual: Sigma stat: statistical software for windows. Germany, Jandel.

Gaill, F., Desbruyères, D., and Prieur, D. (1987). Bacterial communities associated with "Pompei worms" from the East Pacific rise hydrothermal vents: SEM, TEM observations. Microbial Ecology *13*, 129-139.

Galkin, S.V. (2016). Structure of hydrothermal vent communities, Vol 50 (Springer International Publishing AG Switzerland).

Gardebrecht, A., Markert, S., Sievert, S.M., Felbeck, H., Thürmer, A., Albrecht, D., Wollherr, A., Kabisch, J., Le Bris, N., and Lehmann, R. (2012). Physiological homogeneity among the endosymbionts of *Riftia pachyptila* and *Tevnia jerichonana* revealed by proteogenomics. The ISME journal *6*, 766-776.

Gihring, T.M., Green, S.J., and Schadt, C.W. (2012). Massively parallel rRNA gene sequencing exacerbates the potential for biased community diversity comparisons due to variable library sizes. Environmental Microbiology *14*, 285-290.

Giuffrè, A., Borisov, V.B., Arese, M., Sarti, P., and Forte, E. (2014). Cytochrome bd oxidase and bacterial tolerance to oxidative and nitrosative stress. Biochimica et Biophysica Acta (BBA)-Bioenergetics *1837*, 1178-1187.

Gollner, S., Govenar, B., Fisher, C.R., and Bright, M. (2015). Size matters at deep-sea hydrothermal vents: different diversity and habitat fidelity patterns of meio- and macrofauna. Marine ecology progress series *520*, 57-66.

Grissa, I., Vergnaud, G., and Pourcel, C. (2007). CRISPRFinder: a web tool to identify clustered regularly interspaced short palindromic repeats. Nucleic acids research *35*, W52-W57.

Grissa, I., Vergnaud, G., and Pourcel, C. (2008). CRISPRcompar: a website to compare clustered regularly interspaced short palindromic repeats. Nucleic acids research *36*, W145-W148.

Grosche, A., Sekaran, H., Pérez-Rodríguez, I., Starovoytov, V., and Vetriani, C. (2015). *Cetia pacifica* gen. nov., sp. nov., a chemolithoautotrophic, thermophilic, nitrate-ammonifying bacterium from a deep-sea hydrothermal vent. International journal of systematic and evolutionary microbiology *65*, 1144-1150.

Grzymski, J.J., Murray, A.E., Campbell, B.J., Kaplarevic, M., Gao, G.R., Lee, C., Daniel, R., Ghadiri, A., Feldman, R.A., and Cary, S.C. (2008). Metagenome analysis of an extreme microbial symbiosis reveals eurythermal adaptation and metabolic flexibility. Proceedings of the National Academy of Sciences *105*, 17516-17521.

Gulmann, L.K., Beaulieu, S.E., Shank, T.M., Ding, K., Seyfried, W.E., and Sievert, S.M. (2015). Bacterial diversity and successional patterns during biofilm formation on freshly exposed basalt surfaces at diffuse-flow deep-sea vents. Frontiers in microbiology *6*.

Gupta, S.K., Padmanabhan, B.R., Diene, S.M., Lopez-Rojas, R., Kempf, M., Landraud, L., and Rolain, J.-M. (2014). ARG-ANNOT, a new bioinformatic tool to discover antibiotic resistance genes in bacterial genomes. Antimicrobial agents and chemotherapy *58*, 212-220.

Gurevich, A., Saveliev, V., Vyahhi, N., and Tesler, G. (2013). QUAST: quality assessment tool for genome assemblies. Bioinformatics *29*, 1072-1075.

Haddad, A., Camacho, F., Durand, P., and Cary, S.C. (1995). Phylogenetic characterization of the epibiotic bacteria associated with the hydrothermal vent polychaete *Alvinella pompejana*. Applied and Environmental Microbiology *61*, 1679-1687.

Han, Y., and Perner, M. (2014). The role of hydrogen for *Sulfurimonas denitrificans*' metabolism. PloS one *9*, e106218.

Han, Y., and Perner, M. (2015). The globally widespread genus *Sulfurimonas*: versatile energy metabolisms and adaptations to redox clines. Frontiers in microbiology *6*.

Hessler, R.R., Smithey Jr, W.M., and Keller, C.H. (1985). Spatial and temporal variation of giant clams, tube worms and mussels at deep-sea hydrothermal vents. Bulletin of the biological society of Washington, 411-428.

Huber, J.A., Butterfield, D.A., and Baross, J.A. (2003). Bacterial diversity in a subseafloor habitat following a deep-sea volcanic eruption. FEMS Microbiology Ecology *43*, 393-409.

Huber, J.A., Welch, D.B.M., Morrison, H.G., Huse, S.M., Neal, P.R., Butterfield, D.A., and Sogin, M.L. (2007). Microbial population structures in the deep marine biosphere. science *318*, 97-100.

Iizuka, T., Tokura, M., Jojima, Y., Hiraishi, A., Yamanaka, S., and Fudou, R. (2006). Enrichment and phylogenetic analysis of moderately thermophilic myxobacteria from hot springs in Japan. Microbes and Environments *21*, 189-199.

Inagaki, F., Takai, K., Kobayashi, H., Nealson, K.H., and Horikoshi, K. (2003). *Sulfurimonas autotrophica* gen. nov., sp. nov., a novel sulfur-oxidizing epsilonproteobacterium isolated from hydrothermal sediments in the Mid-Okinawa Trough. International Journal of Systematic and Evolutionary Microbiology *53*, 1801-1805.

Inoue, A., Anraku, M., Nakagawa, S., and Ojima, T. (2016). Discovery of a novel alginate lyase from *Nitratiruptor* sp. SB155-2 thriving at deep-sea hydrothermal vents

and identification of the residues responsible for its heat stability. Journal of Biological Chemistry *291*, 15551-15563.

Ives, A., and Carpenter, S. (2007). Stability and diversity of ecosystems. Science *317*, 58-62.

Janausch, I., Zientz, E., Tran, Q., Kröger, A., and Unden, G. (2002). C4-dicarboxylate carriers and sensors in bacteria. Biochimica et Biophysica Acta (BBA)-Bioenergetics *1553*, 39-56.

Jannasch, H.W. (1985). Review lecture: The chemosynthetic support of life and the microbial diversity at deep-sea hydrothermal vents. Proceedings of the Royal Society of London B: Biological Sciences *225*, 277-297.

Jannasch, H.W., and Wirsen, C.O. (1981). Morphological survey of microbial mats near deep-sea thermal vents. Applied and Environmental Microbiology *41*, 528-538.

Jia, B., Raphenya, A.R., Alcock, B., Waglechner, N., Guo, P., Tsang, K.K., Lago, B.A., Dave, B.M., Pereira, S., and Sharma, A.N. (2016). CARD 2017: expansion and model-centric curation of the comprehensive antibiotic resistance database. Nucleic acids research, gkw1004.

Johnson, K.S., Childress, J.J., Hessler, R.R., Sakamoto-Arnold, C.M., and Beehler, C.L. (1988). Chemical and biological interactions in the Rose Garden hydrothermal vent field, Galapagos spreading center. Deep Sea Research Part A Oceanographic Research Papers *35*, 1723-1744.

Kikuchi, A., and Asai, K. (1984). Reverse gyrase—a topoisomerase which introduces positive superhelical turns into DNA. Nature *309*, 677.

Koboldt, D.C., Chen, K., Wylie, T., Larson, D.E., McLellan, M.D., Mardis, E.R., Weinstock, G.M., Wilson, R.K., and Ding, L. (2009). VarScan: variant detection in massively parallel sequencing of individual and pooled samples. Bioinformatics *25*, 2283-2285.

Krafft, T., Gross, R., and Kröger, A. (1995). The function of *Wolinella succinogenes psr* genes in electron transport with polysulphide as the terminal electron acceptor. The FEBS Journal *230*, 601-606.

Kunin, V., Engelbrektson, A., Ochman, H., and Hugenholtz, P. (2010). Wrinkles in the rare biosphere: pyrosequencing errors can lead to artificial inflation of diversity estimates. Environmental microbiology *12*, 118-123.

Langille, M.G., and Brinkman, F.S. (2009). IslandViewer: an integrated interface for computational identification and visualization of genomic islands. Bioinformatics *25*, 664-665.

Lenihan, H.S., Mills, S.W., Mullineaux, L.S., Peterson, C.H., Fisher, C.R., and Micheli, F. (2008). Biotic interactions at hydrothermal vents: recruitment inhibition by the mussel *Bathymodiolus thermophilus*. Deep Sea Research Part I: Oceanographic Research Papers *55*, 1707-1717.

Lesser, M.P. (2006). Oxidative stress in marine environments: biochemistry and physiological ecology. Annual review of physiology *68*, 253-278.

Li, H., and Durbin, R. (2009a). Fast and accurate short read alignment with Burrows–Wheeler transform. Bioinformatics *25*, 1754-1760.

Li, H., Handsaker, B., Wysoker, A., Fennell, T., Ruan, J., Homer, N., Marth, G., Abecasis, G., and Durbin, R. (2009b). The sequence alignment/map format and SAMtools. Bioinformatics *25*, 2078-2079.

Li, X.-Z., and Mehrotra, M. (2016). Role of plasmid-encoded drug efflux pumps in antimicrobial resistance. In Efflux-Mediated Antimicrobial Resistance in Bacteria: Mechanisms, Regulation and Clinical Implications, X.-Z. Li, C.A. Elkins, and H.I. Zgurskaya, eds. (Cham: Springer International Publishing), pp. 595-623.

López‐García, P., Gaill, F., and Moreira, D. (2002). Wide bacterial diversity associated with tubes of the vent worm *Riftia pachyptila*. Environmental Microbiology *4*, 204-215.

Lozupone, C., and Knight, R. (2005). UniFrac: a new phylogenetic method for comparing microbial communities. Applied and Environmental Microbiology *71*, 8228-8235.

Lutz, R.A., Shank, T.M., Luther III, G.W., Vetriani, C., Tolstoy, M., Nuzzio, D.B., Moore, T.S., Waldhauser, F., Crespo-Medina, M., and Chatziefthimiou, A.D. (2008). Interrelationships between vent fluid chemistry, temperature, seismic activity, and biological community structure at a mussel-dominated, deep-sea hydrothermal vent along the East Pacific Rise. Journal of Shellfish Research *27*, 177-190.

Maleki, S., Almaas, E., Zotchev, S., Valla, S., and Ertesvåg, H. (2016). Alginate biosynthesis factories in *Pseudomonas fluorescens*: localization and correlation with alginate production level. Applied and environmental microbiology *82*, 1227-1236.

McCollom, T.M., and Shock, E.L. (1997). Geochemical constraints on chemolithoautotrophic metabolism by microorganisms in seafloor hydrothermal systems. Geochimica et cosmochimica acta *61*, 4375-4391.

Meier, D.V., Pjevac, P., Bach, W., Hourdez, S., Girguis, P.R., Vidoudez, C., Amann, R., and Meyerdierks, A. (2017). Niche partitioning of diverse sulfur-oxidizing bacteria at hydrothermal vents. The Isme Journal *11*, 1545.

Meinhart, A., Alonso, J.C., Sträter, N., and Saenger, W. (2003). Crystal structure of the plasmid maintenance system ε/ζ: Functional mechanism of toxin ζ and inactivation by ε2ζ2 complex formation. Proceedings of the National Academy of Sciences *100*, 1661-1666.

Meyer, J.L., and Huber, J.A. (2014). Strain-level genomic variation in natural populations of *Lebetimonas* from an erupting deep-sea volcano. The ISME journal *8*, 867.

Mino, S., Nakagawa, S., Makita, H., Toki, T., Miyazaki, J., Sievert, S.M., Polz, M.F., Inagaki, F., Godfroy, A., and Kato, S. (2017). Endemicity of the cosmopolitan mesophilic chemolithoautotroph *Sulfurimonas* at deep-sea hydrothermal vents. The ISME journal.

Miroshnichenko, M., Kostrikina, N., l'Haridon, S., Jeanthon, C., Hippe, H., Stackebrandt, E., and Bonch-Osmolovskaya, E. (2002). *Nautilia lithotrophica* gen. nov., sp. nov., a thermophilic sulfur-reducing epsilonproteobacterium isolated from a deep-sea hydrothermal vent. International journal of systematic and evolutionary microbiology *52*, 1299-1304.

Nakagawa, S., and Takai, K. (2008). Deep‐sea vent chemoautotrophs: diversity, biochemistry and ecological significance. FEMS microbiology ecology *65*, 1-14.

Nakagawa, S., and Takai, K. (2014). The family *Nautiliaceae*: the genera *Caminibacter*, *Lebetimonas*, and *Nautilia*. In The Prokaryotes (Springer), pp. 393-399.

Nakagawa, S., Takai, K., Inagaki, F., Chiba, H., Ishibashi, J.-i., Kataoka, S., Hirayama, H., Nunoura, T., Horikoshi, K., and Sako, Y. (2005a). Variability in microbial community and venting chemistry in a sediment-hosted backarc hydrothermal system: impacts of subseafloor phase-separation. FEMS microbiology ecology *54*, 141-155.

Nakagawa, S., Takai, K., Inagaki, F., Hirayama, H., Nunoura, T., Horikoshi, K., and Sako, Y. (2005b). Distribution, phylogenetic diversity and physiological characteristics of epsilonproteobacteria in a deep‐sea hydrothermal field. Environmental Microbiology *7*, 1619-1632.

Nakagawa, S., Takai, K., Inagaki, F., Horikoshi, K., and Sako, Y. (2005c). *Nitratiruptor tergarcus* gen. nov., sp. nov. and *Nitratifractor salsuginis* gen. nov., sp. nov., nitrate-reducing chemolithoautotrophs of the epsilonproteobacteria isolated from a deep-sea hydrothermal system in the Mid-Okinawa Trough. International journal of systematic and evolutionary microbiology *55*, 925-933.

Nichols, C.A., Guezennec, J., and Bowman, J.P. (2005). Bacterial exopolysaccharides from extreme marine environments with special consideration of the southern ocean, sea ice, and deep-sea hydrothermal vents: a review. Marine biotechnology *7*, 253-271.

O'Toole, G., Kaplan, H.B., and Kolter, R. (2000). Biofilm formation as microbial development. Annual Reviews in Microbiology *54*, 49-79.

O'Brien, C.E., Giovannelli, D., Govenar, B., Luther, G.W., Lutz, R.A., Shank, T.M., and Vetriani, C. (2015). Microbial biofilms associated with fluid chemistry and megafaunal colonization at post-eruptive deep-sea hydrothermal vents. Deep Sea Research Part II: Topical Studies in Oceanography *121*, 31-40.

Oksanen, J. (2011). Vegan: community ecology package. R package version 2.0-2. http://CRAN R-project org/package= vegan.

Pal, C., Bengtsson-Palme, J., Rensing, C., Kristiansson, E., and Larsson, D.J. (2013). BacMet: antibacterial biocide and metal resistance genes database. Nucleic acids research *42*, D737-D743.

Parks, D.H., Imelfort, M., Skennerton, C.T., Hugenholtz, P., and Tyson, G.W. (2015). CheckM: assessing the quality of microbial genomes recovered from isolates, single cells, and metagenomes. Genome research *25*, 1043-1055.

Paul, J.H. (2008). Prophages in marine bacteria: dangerous molecular time bombs or the key to survival in the seas? The ISME journal *2*, 579.

Pérez-Rodríguez, I., Bolognini, M., Ricci, J., Bini, E., and Vetriani, C. (2015). From deep-sea volcanoes to human pathogens: a conserved quorum-sensing signal in Epsilonproteobacteria. The ISME journal *9*, 1222.

Perez-Rodriguez, I., Grosche, A., Massenburg, L., Starovoytov, V., Lutz, R.A., and Vetriani, C. (2012). Phorcysia thermohydrogeniphila gen. nov., sp. nov., a thermophilic, chemolithoautotrophic, nitrate-ammonifying bacterium from a deep-sea hydrothermal vent. Int J Syst Evol Microbiol *62*, 2388-2394.

Peskin, A.V., and Winterbourn, C.C. (2000). A microtiter plate assay for superoxide dismutase using a water-soluble tetrazolium salt (WST-1). Clinica Chimica Acta *293*, 157-166.

Polz, M.F., and Cavanaugh, C.M. (1995). Dominance of one bacterial phylotype at a Mid-Atlantic Ridge hydrothermal vent site. Proceedings of the National Academy of Sciences *92*, 7232-7236.

Ponsard, J., Cambon-Bonavita, M.A., Zbinden, M., Lepoint, G., Joassin, A., Corbari, L., Shillito, B., Durand, L., Cueff-Gauchard, V., and Compere, P. (2013). Inorganic carbon fixation by chemosynthetic ectosymbionts and nutritional transfers to the hydrothermal vent host-shrimp *Rimicaris exoculata*. ISME J *7*, 96-109.

Pruesse, E., Quast, C., Knittel, K., Fuchs, B.M., Ludwig, W., Peplies, J., and Glöckner, F.O. (2007). SILVA: a comprehensive online resource for quality checked and aligned ribosomal RNA sequence data compatible with ARB. Nucleic acids research *35*, 7188-7196.

Pysz, M.A., Conners, S.B., Montero, C.I., Shockley, K.R., Johnson, M.R., Ward, D.E., and Kelly, R.M. (2004). Transcriptional analysis of biofilm formation processes in the anaerobic, hyperthermophilic bacterium Thermotoga maritima. Applied and environmental microbiology *70*, 6098-6112.

Quinlan, A.R., and Hall, I.M. (2010). BEDTools: a flexible suite of utilities for comparing genomic features. Bioinformatics *26*, 841-842.

Raguénès, G.H.C., Peres, A., Ruimy, R., Pignet, P., Christen, R., Loaec, M., Rougeaux, H., Barbier, G., and Guezennec, J.G. (1997). *Alteromonas infernus* sp. nov., a new polysaccharide‐producing bacterium isolated from a deep‐sea hydrothermal vent. Journal of Applied Microbiology *82*, 422-430.

Ramirez-Llodra, E., Shank, T.M., and German, C.R. (2007). Biodiversity and biogeography of hydrothermal vent species: thirty years of discovery and investigations. Oceanography *20*, 30-41.

Rocha, E.P., Cornet, E., and Michel, B. (2005). Comparative and evolutionary analysis of the bacterial homologous recombination systems. PLoS genetics *1*, e15.

Rocha, E.R., Selby, T., Coleman, J.P., and Smith, C.J. (1996). Oxidative stress response in an anaerobe, Bacteroides fragilis: a role for catalase in protection against hydrogen peroxide. Journal of bacteriology *178*, 6895-6903.

Rodriguez-R, L.M., and Konstantinidis, K.T. (2016). The enveomics collection: a toolbox for specialized analyses of microbial genomes and metagenomes. PeerJ Preprints.

Russo, R., and Silver, P. (1996). Cordillera formation, mantle dynamics, and the Wilson cycle. Geology *24*, 511-514.

Salman-Carvalho, V., Fadeev, E., Joye, S.B., and Teske, A. (2016). How clonal is clonal? Genome plasticity across multicellular segments of a "*Candidatus* Marithrix sp." filament from sulfidic, briny seafloor sediments in the Gulf of Mexico. Frontiers in Microbiology *7*, 1173.

Scandalios, J.G. (2002). Oxidative stress responses--what have genome-scale studies taught us? Genome Biol *3*, REVIEWS1019.

Schluter, D. (2000). The ecology of adaptive radiation (OUP Oxford).

Schoenhofen, I.C., McNally, D.J., Vinogradov, E., Whitfield, D., Young, N.M., Dick, S., Wakarchuk, W.W., Brisson, J.-R., and Logan, S.M. (2006). Functional characterization of dehydratase/aminotransferase pairs from *Helicobacter* and *Campylobacter* enzymes distinguishing the pseudaminic acid and bacillosamine biosynthetic pathways. Journal of Biological Chemistry *281*, 723-732.

Seemann, T. (2014). Prokka: rapid prokaryotic genome annotation. Bioinformatics *30*, 2068-2069.

Shank, T., Fornari, D., Von Damm, K., Lilley, M., Haymon, R., and Lutz, R. (1998). Temporal and spatial patterns of biological community development at nascent deep-sea hydrothermal vents (9 50′ N, East Pacific Rise). Deep Sea Research Part II: Topical Studies in Oceanography *45*, 465-515.

Shannon, C.E. (1948). A mathematical theory of communication. The Bell System Technical Journal *27*, 379-423.

Sievert, S., Scott, K., Klotz, M., Chain, P., Hauser, L., Hemp, J., Hügler, M., Land, M., Lapidus, A., and Larimer, F. (2008). Genome of the epsilonproteobacterial chemolithoautotroph *Sulfurimonas denitrificans*. Applied and environmental microbiology *74*, 1145-1156.

Sievert, S.M., and Vetriani, C. (2012). Chemoautotrophy at deep-sea vents: past, present, and future. Oceanography *25*, 218-233.

Simpson, E.H. (1949). Measurement of diversity. Nature *163*, 688.

Soderlund, C., Nelson, W., Shoemaker, A., and Paterson, A. (2006). SyMAP: A system for discovering and viewing syntenic regions of FPC maps. Genome research *16*, 1159-1168.

Sunamura, M., Higashi, Y., Miyako, C., Ishibashi, J.-i., and Maruyama, A. (2004). Two bacteria phylotypes are predominant in the Suiyo Seamount hydrothermal plume. Applied and Environmental Microbiology *70*, 1190-1198.

Sylvan, J., Toner, B., and Edwards, K.J. (2012). Life and death of deep-sea vents: bacterial diversity and ecosystem succession on inactive hydrothermal sulfides. MBio *3*, e00279-00211.

Takai, K., Hirayama, H., Nakagawa, T., Suzuki, Y., Nealson, K., and Horikoshi, K. (2005). *Lebetimonas acidiphila* gen. nov., sp. nov., a novel thermophilic, acidophilic, hydrogen-oxidizing chemolithoautotroph within the Epsilonproteobacteria, isolated from a deep-sea hydrothermal fumarole in the Mariana Arc. International journal of systematic and evolutionary microbiology *55*, 183-189.

Takai, K., Suzuki, M., Nakagawa, S., Miyazaki, M., Suzuki, Y., Inagaki, F., and Horikoshi, K. (2006). Sulfurimonas paralvinellae sp. nov., a novel mesophilic, hydrogen- and sulfur-oxidizing chemolithoautotroph within the Epsilonproteobacteria isolated from a deep-sea hydrothermal vent polychaete nest, reclassification of Thiomicrospira denitrificans as Sulfurimonas denitrificans comb. nov. and emended description of the genus Sulfurimonas. International Journal of Systematic and Evolutionary Microbiology *56*, 1725-1733.

Tatusova, T., DiCuccio, M., Badretdin, A., Chetvernin, V., Nawrocki, E., Zaslavsky, L., Lomsadze, A., Pruitt, K., Borodovsky, M., and Ostell, J. (2016). NCBI prokaryotic genome annotation pipeline. Nucleic acids research *44*, 6614-6624.

Team, R.C. (2015). R: A language and environment for statistical computing. Vienna: R foundation for statistical computing. Vienna: R Foundation for Statistical Computing.

Teske, A., and Salman, V. (2014). The Family *Beggiatoaceae*. In The Prokaryotes: Gammaproteobacteria, E. Rosenberg, E.F. DeLong, S. Lory, E. Stackebrandt, and F. Thompson, eds. (Berlin, Heidelberg: Springer Berlin Heidelberg), pp. 93-134.

Tivey, M.K. (2007). Generation of seafloor hydrothermal vent fluids and associated mineral deposits. Oceanography *20*, 50-65.

Tunnicliffe, V. (1988). Biogeography and evolution of hydrothermal-vent fauna in the eastern Pacific Ocean. Proceedings of the Royal Society of London B: Biological Sciences *233*, 347-366.

Van Dover, C. (2000). The ecology of deep-sea hydrothermal vents (Princeton University Press).

Vetriani, C., Speck, M., Ellor, S., Lutz, R., and Starovoytov, V. (2004). *Thermovibrio ammonificans* sp. nov., a thermophilic, chemolithotrophic, nitrate-ammonifying bacterium from deep-sea hydrothermal vents. International journal of systematic and evolutionary microbiology *54*, 175-181.

Vetriani, C., Voordeckers, J., Crespo-Medina, M., O'brien, C.E., Giovannelli, D., and Lutz, R. (2014). Deep-sea hydrothermal vent Epsilonproteobacteria encode a conserved and widespread nitrate reduction pathway (Nap). The ISME journal *8*, 1510.

Voordeckers, J., Do, M., Hügler, M., Ko, V., Sievert, S., and Vetriani, C. (2008). Culture dependent and independent analyses of 16S rRNA and ATP citrate lyase genes: a comparison of microbial communities from different black smoker chimneys on the Mid-Atlantic Ridge. Extremophiles *12*, 627-640.

Waite, D., Vanwonterghem, I., Rinke, C., Parks, D., Zhang, Y., Takai, K., Sievert, S., Simon, J., Campbell, B., Hanson, T.*, et al.* (2017). Comparative genomic analysis of the class Epsilonproteobacteria and proposed reclassification to Epsilonbacteraeota (phyl. nov.). Frontiers in Microbiology *8*.

Watnick, P., and Kolter, R. (2000). Biofilm, city of microbes. Journal of bacteriology *182*, 2675-2679.

Wick, R., Judd, L., Gorrie, C., and Holt, K. (2017). Unicycler: resolving bacterial genome assemblies from short and long sequencing reads. PLoS computational biology *13*, e1005595.

Wickham, H. (2009). Elegant graphics for data analysis. In ggplot2: Elegant Graphics for Data Analysis (New York, NY: Springer New York), pp. 1-7.

Wilson, J.T. (1963). Continental drift. Scientific American *208*, 86-103.

Wirsen, C.O., Sievert, S.M., Cavanaugh, C.M., Molyneaux, S.J., Ahmad, A., Taylor, L.T., DeLong, E.F., and Taylor, C.D. (2002). Characterization of an autotrophic sulfide-oxidizing marine Arcobacter sp. that produces filamentous sulfur. Applied and Environmental Microbiology *68*, 316-325.

Wong, T.Y., Preston, L., and Schiller, N. (2000). Alginate lyase: review of major sources and enzyme characteristics, structure-function analysis, biological roles, and applications. Annual Reviews in Microbiology *54*, 289-340.

Wood, D., and Salzberg, S. (2014). Kraken: ultrafast metagenomic sequence classification using exact alignments. Genome biology *15*, R46.

Zahirovic, S., Matthews, K., Flament, N., Müller, R.D., Hill, K., Seton, M., and Gurnis, M. (2016). Tectonic evolution and deep mantle structure of the eastern Tethys since the latest Jurassic. Earth-Science Reviews *162*, 293-337.

Zankari, E., Hasman, H., Cosentino, S., Vestergaard, M., Rasmussen, S., Lund, O., Aarestrup, F.M., and Larsen, M.V. (2012). Identification of acquired antimicrobial resistance genes. Journal of antimicrobial chemotherapy *67*, 2640-2644.

Zhou, Y., Liang, Y., Lynch, K., Dennis, J., and Wishart, D. (2011). PHAST: a fast phage search tool. Nucleic acids research *39*, W347-W352.